



# **Redesigned Shark Tagging**

**MQP**

## **Authors**

Amelia Harvey  
Aram Soultanian  
Brooke Dawson  
Hannah Gallagher  
Lilly Nardelli

## **Professors**

Professor Wodin-Schwartz  
Professor Savilonis

**May 6, 2021**

*A Major Qualifying Project submitted to the Faculty of Worcester Polytechnic Institute in partial fulfillment of the requirements for the degree of Bachelor of Science in Engineering Sciences.*

*This report represents the work of one or more undergraduate students submitted to the faculty as evidence of completion of a degree requirement. WPI routinely publishes these reports on the web without editorial or peer review.*

## Table of Contents

Acknowledgements.....	xi
Abstract.....	xii
1 Introduction .....	1
2 Literature Review and Background .....	3
2.1 Importance of Great White Sharks .....	3
2.2 Shark Anatomy .....	3
2.2.1 Skin Properties .....	3
2.2.2 Dorsal Fin.....	5
2.2.3 Swimming Mechanics.....	6
2.3 Shark Movements.....	7
2.3.1 Movement influences and Swimming Behavior .....	7
2.4 Shark Interactions with Prey and Humans.....	8
2.4.1 Interaction with Prey .....	8
2.4.2 Patterns in Attacks on Humans.....	8
2.5 Various Types of Shark Tagging and Tracking.....	9
2.5.1 History.....	9
2.5.2 Acoustic Tags.....	10
2.5.3 Satellite and Archival Tags.....	11
2.5.4 Post Tagging Release Stress.....	12
2.6 Previous Mechanisms for Tagging Sharks .....	12
2.6.1 Crittercam Design .....	12
2.6.2 Metal Clamp and Tagging System with Spikes .....	13
2.6.3 Iteration of Metal Clamp and Tagging System with Friction Pads.....	15
2.7 Injury Prevention .....	17

3	Project Strategy.....	19
3.1	Client Statement.....	19
3.2	Design Requirements (technical).....	19
3.3	Design Requirements (standards).....	20
3.3.1	Marine Standards.....	20
3.3.2	Software and Manufacturing Standards.....	20
3.4	Revised Client’s Statement.....	21
3.5	Management Approach.....	21
4	Pole Design Process.....	22
4.1	Needs Analysis.....	22
4.2	Design Matrix.....	22
4.3	Pole Alternative Designs.....	24
4.3.1	Grabbing Pole.....	24
4.3.2	Electromagnet Pole.....	25
4.3.3	Flex Release Pole.....	28
4.4	Final Pole Design Stages.....	29
4.4.1	Hydrofoil.....	29
4.4.2	Hydrofoil and Bike Brake.....	32
4.4.3	Clamp Opener.....	39
4.4.4	Manufacturing of the Final Design.....	46
5	Design Verification.....	49
5.1	Deflection Calculations for Pole.....	49
5.2	Force Gauge Measurements.....	52
5.2.1	Clamp Opening Force.....	52
5.3	Sensitivity and Angles of Release Mechanism.....	55

5.4	Buoyancy and Water-tight Testing.....	56
5.5	Stress Analysis.....	56
5.5.1	Compressive Stress Calculations.....	56
5.5.2	ANSYS Software Analysis of Stresses.....	57
5.6	Full System Tests.....	60
6	Final Design and Validation.....	63
6.1	Economics.....	64
6.2	Environmental Impact.....	64
6.3	Societal Influence.....	64
6.4	Political Ramifications.....	65
6.5	Ethical Concerns.....	65
6.6	Health and Safety Issues.....	65
6.7	Manufacturability.....	66
6.8	Sustainability.....	66
7	Discussion.....	68
8	Conclusions and Recommendations.....	69
9	Works Cited.....	71

## List of Figures

Figure 1 : Sharktivity app visual map (Blue represents confirmed shark sightings, purple & yellow represent pings from different sharks and orange is an unconfirmed shark sighting) .....	1
Figure 2 : Scanning electron microscope (top) and confocal laser scanning microscope (bottom) images of dermal denticles of the great white shark in four areas of the body [5].	4
Figure 3 : Diagram of the attack angle (alpha) of dermal denticles of the great white shark [6].....	5
Figure 4 : Anatomy of the midsection of a great white shark, including the orientation of the three layers of cartilaginous fibers [7] .....	5
Figure 5 : The fins of a great white shark [14].....	6
Figure 6 : Petersen disc tag on a warmouth [25].....	9
Figure 7 : Rototags once used for shark tagging [26] .....	9
Figure 8 : Dart tag [26].....	10
Figure 9 : Acoustic tag on great white shark in the front with PSAT in the back [28] .....	11
Figure 10 : Smart Position or Temperature Transmitting Tag (SPOT) Tag [29] .....	11
Figure 11 : Crittercam Clamp [33].....	12
Figure 12 : Clamp system design consisting of (a) and (b) micro-bubble housing, in which a VHS transmitter, logger, and acoustic transmitter are enclosed. The magnesium sleeve (k) and the GTR with cotter-pin and monofilament (g) are methods of detachment [34].....	14
Figure 13 : Current CATS Cam Clamp [35].....	15
Figure 14 : Dr. Skomal tagging a great white shark off the coast of Cape Cod .....	16
Figure 15 : The bones of the wrist [39] .....	17
Figure 16 : Dorsal/palmar flexion and radial/ulnar deviation of the wrist [43] .....	18
Figure 17 : ANSI standards format example [47] .....	20
Figure 18 : Pinch and release mechanism pole. A is un-squeezed, pinched position, B is squeezed, released position.....	24
Figure 19 : Second iteration of the grabbing pole. Top: Closed, un-squeezed position, Bottom: open, squeezed position.....	25
Figure 20 : Overall design of the electromagnet pole .....	26

Figure 21 : Close up of the electromagnet attached to the pole.....	26
Figure 22 : Example of an electromagnet.....	27
Figure 23 : Telescoping pole design .....	28
Figure 24 : Clamp adapter piece for flex release pole (clamp open position in red; clamp closed position in orange) .....	29
Figure 25 : Clamp adapter connected to crossbar and pole .....	29
Figure 26 : Dimensions and shape of hydrofoil [53] .....	30
Figure 27 : Hydrofoil and bike brake iteration 1 .....	33
Figure 28 : Hydrofoil and bike brake iteration 2 .....	34
Figure 29 : Hydrofoil and bike brake iteration 3 .....	35
Figure 30 : Hydrofoil and bike brake female pole pieces .....	36
One additional clip piece was added to this iteration of the design to secure the bike brake to the female pole fitting. This clip will fit snugly around the cylindrical geometry of the pole fitting and will utilize a circular hose clamp to secure its position. The existing geometry of the bike brake will then be inserted into the M6 hole and secured with a hex nut .....	36
Figure 31 : Hydrofoil and bike brake fourth iteration.....	37
Figure 32 : Drawings of bolts for rotating wing piece .....	38
Figure 33 : Hydrofoil and bike brake final design (left and middle) and manufactured product (right) .....	38
Figure 34 : Mechanism of bar clamp.....	39
Figure 35 : Clamp opener iteration 1 .....	40
Figure 36 : Clamp opener iteration 2 .....	41
Figure 37 : Clamp opener iteration 3 .....	42
Figure 38 : Clamp opener final iteration.....	43
Figure 39 : Manufactured clamp opener with offset arm.....	43
Figure 40 : Offset arm wedged against object, preventing clamp from closing completely. 44	
Figure 41 : Final clamp opener version after testing .....	45
Figure 42 : Final manufactured assembly .....	45
Figure 43 : Slide shaft finished sub-assembly.....	46
Figure 44 : Grip piece (left) and offset arm (right) .....	47

Figure 45 : Initial trigger operation one (left), actual first trigger operation (middle), final trigger piece (right).....	47
Figure 46 : Abrasive fluid jet cutting locking plate .....	48
Figure 47 : Free body diagram of pole in water. In blue: known forces, in red: unknown reaction forces and moment.....	49
Figure 48 : Simplified model of pole as a deflected beam in water. In blue: known forces, in red: unknown reaction forces and moment .....	50
Figure 49 : Free body diagram of pole in air. In blue: known forces, in red: unknown reaction forces and moment.....	50
Figure 50 : Simplified model of pole as a deflected beam in air. In blue: known forces, in red: unknown reaction forces and moment .....	51
Figure 51 : Top: Set up for the clamp opening force test. Bottom: Graphic for a clearer visual of the set up for the clamp opening force test .....	53
Figure 52 : Opening force over angle open (in radians) for the gauge at Top: 4 cm from 90, Middle: 6 cm from 90, Bottom: 20 cm from 90 .....	54
Figure 53 : Release mechanism testing for sensitivity and angles (left) and in pool (right)	55
Figure 54 : Hydrofoil watertight test with PLA endcaps .....	56
Figure 55 : Free body diagram of the clamp opener with compressive forces applied by the clamp.....	57
Figure 56 : Results of total deformation ANSYS analysis .....	58
Figure 57 : Results of ANSYS convergence analysis .....	58
Figure 58 : Testing of clamp opener deformation in PLA plastic material.....	59
Figure 59 : Results of von Mises stress analysis in ANSYS (top); stresses on pin (bottom).	60
Figure 60 : Image of pool testing set up where we held the device stationary in the water	61
Figure 61 : Image of pool testing where we moved the whole system through the water by walking along the pool deck .....	61
Figure 62 : Image from pool testing with the clamp loaded into the clamp opener, taken before testing the release mechanism in water .....	62
Figure 63 : Final tagging apparatus design.....	63

## List of Tables

Table 1 : Customer Requirements and Importance Scores for Pole .....	22
Table 2 : Material properties and weight of Dr. Skomal's pole. ....	51
Table 3 : Resultant forces and deflection of Dr. Skomal's pole under our assumed loads....	52

## Authorship and Contributions

	Amelia	Aram	Brooke	Hannah	Lilly
Abstract			X		
Ch. 1-INTRODUCTION	X	X	X		
Ch. 2-LITERATURE REVIEW AND BACKGROUND	X	X	X	X	X
2.1 Importance of Great White Sharks			X		
2.2 Shark Anatomy	X				
2.2.1 Skin Properties	X				
2.2.2 Dorsal Fin	X				
2.2.3 Swimming Mechanics				X	
2.3 Shark Movements				X	
2.3.1 Movement Influences and Swimming Behavior				X	
2.4 Shark Interactions with Prey and Humans					X
2.4.1 Interactions with Prey					X
2.4.2 Patterns in Attacks on Humans					X
2.5 Various Types of Shark Tagging and Tracking			X		X
2.5.1 History			X		
2.5.2 Acoustic Tags			X		
2.5.3 Satellite and Archival Tags			X		
2.5.4 Post Tagging Release Stress					X
2.6 Previous Mechanisms for Tagging Sharks		X	X		
2.6.1 Crittercam Design		X			
2.6.2 Metal Clamp and Tagging System with Spikes			X		
2.6.3 Iteration of Metal Clamp and Tagging System with Friction Pads		X			
2.7 Injury Prevention	X				
Ch. 3-PROJECT STRATEGY	X	X	X	X	X
3.1 Client Statement				X	
3.2 Design Requirements (technical)	X	X	X	X	X
3.3 Design Requirements (standards)				X	
3.4 Revised Client's Statement				X	
3.5 Management Approach				X	
Ch.4 -POLE DESIGN PROCESS	X	X	X	X	X
4.1 Needs Analysis	X				
4.2 Design Matrix	X		X		
4.3 Pole Alternative Designs	X	X	X	X	
4.3.1 Grabbing Pole	X				
4.3.2 Electromagnetic Pole			X	X	
4.3.3 Flex Release Pole		X	X		
4.4 Final Pole Design Stages		X	X		X
4.4.1 Hydrofoil			X		
4.4.2 Hydrofoil and Bike Brake					X
4.4.3 Clamp Opener	X	X	X		
4.4.4 Manufacturing of the Final Design		X			X

Ch. 5-DESIGN VERIFICATION	X		X		
5.1 Deflection Calculations for Pole	X				
5.2 Force Gauge Measurements	X				
5.2.1 Clamp Opening Force	X				
5.3 Sensitivity and Angles of Release Mechanism			X		
5.4 Buoyancy and Water-tight Testing			X		
5.5 Stress Analysis	X		X		
5.5.1 Compressive Stress Calculations	X				
5.5.2 ANSYS Software Analysis of Stresses			X		
5.6 Full System Tests			X		
Ch. 6-FINAL DESIGN AND VALIDATION	X		X		
6.1 Economics			X		
6.2 Environmental Impact			X		
6.3 Societal Influence			X		
6.4 Political Ramifications			X		
6.5 Ethical Concerns			X		
6.6 Health and Safety Issues	X				
6.7 Manufacturability			X		
6.8 Sustainability			X		
Ch. 7-DISCUSSION	X		X		
Ch. 8-CONCLUSIONS AND RECOMMENDATIONS	X		X		
APPENDICES	X	X	X	X	X
CAD Modeling		X			X
Calculations	X		X		
Budget				X	
Manufacturing		X		X	X
Primary Editors	X		X		

## **Acknowledgements**

We would like to thank our advisors, Prof. Sarah Wodin-Schwartz and Prof. Brian Savilonis, for their continued support, commitment, and advice which contributed to the success of this project. We also would like to extend a special thank you to Dr. Greg Skomal and MA Division of Fisheries for sponsoring this project and giving us the opportunity to work on such a unique design challenge. The team would like to thank Dr. Erica Stults for her rapid prototyping expertise and James Loiselle for his manufacturing expertise and willingness to teach us about machining processes. We also would like to extend our thanks to Paul Leinard from AM 3D & CNC Fabrication LLC for his assistance with engineering drawings and for machining some of our complex parts. Lastly, we would like to thank our family and friends for their encouragement throughout this project experience.

## **Abstract**

Acoustic and satellite tags have mapped the migration patterns and predatory habits of great white sharks, resulting in a safer beach environment for humans. However, the CATS Cam system is a new tagging technology which measures accelerometer, water temperature, and depth data while providing video from a shark's eye view. This project partnered with MA Division of Fisheries and senior fisheries biologist, Dr. Greg Skomal, to create a tagging pole to attach this system to the dorsal fin of a great white. Iterations of this pole design included ideation, calculations, CAD drafting, initial fabrication with 3D printed plastics, and finally manufacturing with machining equipment before testing the full system in an open body of water. It was not possible to test the device directly on a shark in the ocean due to the academic year not aligning with shark season. The results of testing showed that the device effectively released the tag system onto a foam dorsal fin in still water without causing injury or significant strain on the user. This project paves the way for further data collection on great whites, leading to more awareness and predictability of shark locations for safer beachgoing experience.

# 1 Introduction

This project is in partnership with the MA Division of Marine Fisheries and Dr. Greg Skomal, a senior fisheries biologist at the MA Division of Fisheries and Wildlife (MassWildlife) and head of the Massachusetts Shark Research Program. Dr. Skomal has been tagging sharks off the coast of Cape Cod and other regions of the world for decades. The Atlantic White Shark Conservancy (AWSC) with the help of Dr. Skomal and his team have developed an app called “Sharktivity” that combines human-input shark sightings with an array of receiver buoys to alert to coastal Cape Cod towns and its citizens of potential danger. The app serves as a visual database, as seen in Figure 1, where users can view a map with various icons that represent where the great white sharks are located during a given time frame. Data from the “Sharktivity” app combined with video and tracking data leads to a more informed awareness of shark behavior. Dr. Skomal hopes to better understand how and when sharks hunt to allow beachgoers to safely share the waters with this apex predator.



*Figure 1: Sharktivity app visual map (Blue represents confirmed shark sightings, purple & yellow represent pings from different sharks and orange is an unconfirmed shark sighting)*

Researchers currently track great white sharks by attaching the CATS (Customized Animal Tracking Solutions) Cam tag to the dorsal fin of the shark with a clamp attached to a pole. To attach the clamp to the shark, ideally, the researcher should be able to stand on the pulpit of the boat and tag the shark from behind as it swims forward. This operation has proven difficult due to the aggressive nature of the great white shark and the equipment’s design. Design limitations include the short pole length and the required 90° angle between

the shark and researcher during application. These specifications make the tagging process difficult, unsafe, and inefficient from the boat's pulpit.

Our project used a multistage approach to develop a better-suited tagging apparatus in accordance with the CATS Cam tag. The final design gives Dr. Skomal a new method of tagging great whites from the pulpit of a boat, allowing him and his team to further their research about the species and their predatory patterns. The overall goal of this project is to design and manufacture a tagging device to attach a clamp and sensor system to great whites for the progression of shark research.

## **2 Literature Review and Background**

### **2.1 Importance of Great White Sharks**

Great whites are considered apex predators, or the top predators, of the sea; therefore, they are necessary to maintain the health of the marine ecosystem [1]. If these sharks did not exist as the apex predators, the dynamics of the marine food web would be interrupted [1]. As such, the prey species of great whites, typically seals, goes unchecked. This disruption of the food chain can have detrimental effects all the way down to the lowest organisms of the chain.

Great white sharks are now considered a vulnerable species due to humans hunting them for their jaws, teeth, and fins, as well as for sport [2]. Great whites are especially susceptible to overfishing since they are a slow growing species and produce few young [2]. Yet, they are an adaptable species, easily changing habitats when food sources run low. The significance of great white sharks to the marine ecosystem is evident in how they uphold balance in the food web and their ability to adapt to changing environments. With these factors, it is even more critical to understand great white sharks and work towards protecting their species in conservation efforts.

### **2.2 Shark Anatomy**

#### *2.2.1 Skin Properties*

A shark's skin is divided into three layers: the epidermis on top, the dermis, and the underlying flesh [3]. The epidermis is the location of the dermal denticles, or scales of the shark [4] (see Figure 2). The dermis is divided into the upper and lower stratum compactum which are made of cartilaginous fibrils. The structural organization of shark skin allows it to resist the internal pressure created by muscle contraction [3].

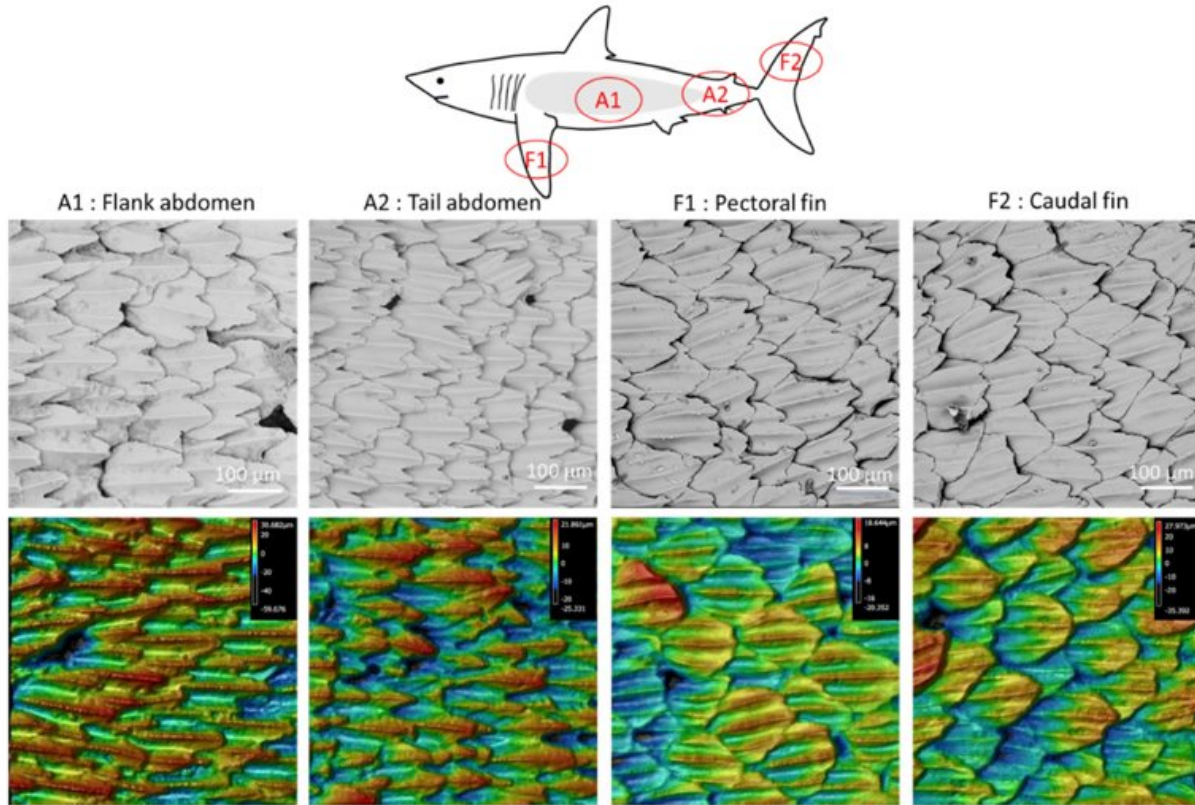


*Figure 2: Scanning electron microscope (top) and confocal laser scanning microscope (bottom) images of dermal denticles of the great white shark in four areas of the body [5]*

Dermal denticles are interlocked concave grooves that reduce the amount of drag that a shark experiences as it swims [4]. Dermal denticles reduce shear stress and momentum transfer at the skin surface by keeping water vortices above riblet tips and reducing cross-stream velocity fluctuations in riblet valleys. Keeping vortices above tips also reduces the surface area exposed to high velocity flow. Dermal denticles also reduce vortex ejection and outer layer turbulence by impeding the translation of streamwise vortices. Surface shear stress is also reduced by modifying the velocity distribution [4]. Dermal denticles are at an angle  $\alpha$  from the surface of the skin. This is also called the attack angle, ranging from 10-30°, which serves to reduce turbulence intensity (Figure 3). The attack angle produces pressure on the skin of the shark; however, the reduction of the turbulence intensity more than offsets the generated pressure force from the angle of the scales [6].

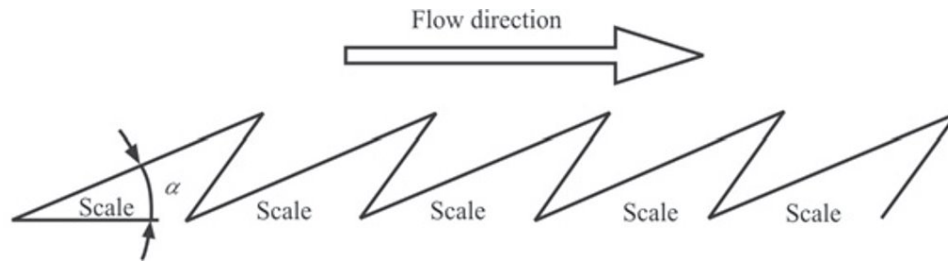


Figure 3: Diagram of the attack angle ( $\alpha$ ) of dermal denticles of the great white shark [6]

### 2.2.2 Dorsal Fin

The dorsal fin of great whites acts as a “dynamic stabilizer.” The cartilaginous fibers in the dermis of the dorsal fin are tightly packed at high angles (over  $60^\circ$ ) and are strained. The orientation of these fibers facilitates the transfer of tension from the body of the shark. Additionally, during fast swimming, hydrostatic pressure causes the fin to stiffen which resists roll [7]. Figure 4 shows the three layers of cartilaginous fibers in the great white dorsal fin. Tags are typically placed on the dorsal fin of a shark because they send location data when the dorsal fin breaches the water [8]. A study on satellite linked tags found that when the tag sat higher on the dorsal fin, the location data was more accurate [9].

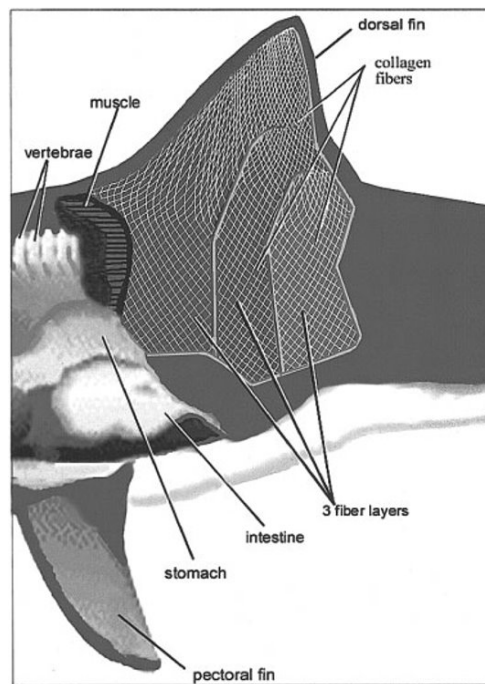


Figure 4: Anatomy of the midsection of a great white shark, including the orientation of the three layers of cartilaginous fibers [7]

### 2.2.3 Swimming Mechanics

Hydrodynamics play an important role in the buoyancy and swimming mechanics of great white sharks. In one study, researchers discuss the hydrodynamic components of a shark's anatomy, specifically the role of the heterocercal tail, the pectoral fins, and the body as a lifting surface [10]. Unlike other marine life, sharks do not possess a swim bladder and cannot control their buoyancy using this common anatomical feature. Instead, sharks utilize different methods to counter their negative buoyancy. Some sharks have been observed to swallow air at the surface to increase their buoyancy [11]. Great white sharks also have livers that contain lipids, and because oil weighs less than water, this increases their neutral buoyancy. However, most sharks have an overall density higher than the surrounding water and therefore, are negatively buoyant.

To counteract their negatively buoyant bodies, sharks utilize their fins to generate lift and prevent sinking in the water column. As seen in Figure 5, a shark possesses several paired and unpaired fins, notably the caudal fin, dorsal fins, and pectoral fins [12]. Of the shark's fins, the caudal fin and the paired pectoral fins are thought to be the most important fins for providing lift [11]. The caudal fin, or heterocercal tail, is nearly symmetrical for the great white sharks. Researchers believe that the anterior lift is necessary to balance the lift produced by the heterocercal tail, resulting in a torque about the center of mass, which can be generated by the body or the pectoral fins [13].

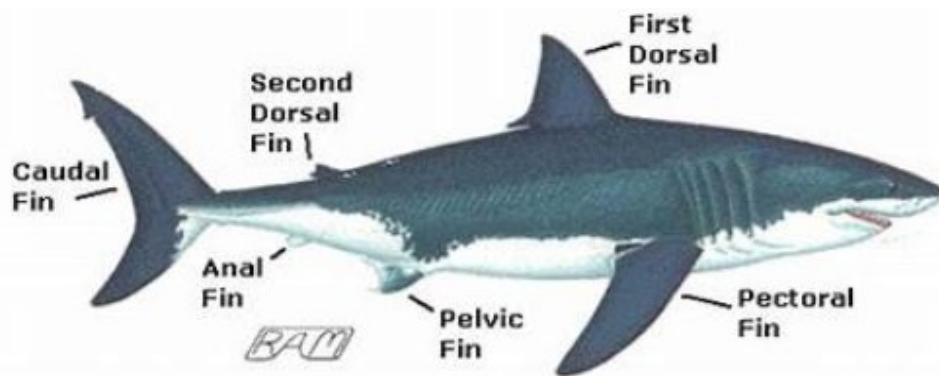


Figure 5: The fins of a great white shark [14]

The primary source of lift comes from their pectoral fin. The fins' resemblance to aircraft wings results from their similar function. The pectoral fins are thought to act as hydrofoils, and they are the dominating factor in countering this torque created by the heterocercal fin [15]. The pectoral fins originate in front of the shark's center of gravity and have a hydrofoil-like cross-section. When sharks swim through the water, they use their pectoral fins in such a way that they generate lift. The shape and angle of their pectoral fins cause the water below the fin to flow downward. Due to the Coanda effect, it also causes water flowing above it to follow its curve and deflect downward. Ultimately, the downward deflection of water forces the fin upward, resulting in lift [16].

## **2.3 Shark Movements**

### *2.3.1 Movement influences and Swimming Behavior*

Satellite tags have made it possible for researchers to gain a better understanding of the swimming behaviors and movement patterns of white sharks around the world. Studies suggest that white sharks prefer water in the range of 13-23° C, spending 85% of their time in this range. However, depending upon whether they are spending time off the continental shelf at mesopelagic depths, they may experience a much wider range of temperatures between 1.6 and 30.4° C [17].

Data from some studies suggests that white sharks spend most of the time in one place when food sources are available, but when the resources deplete, they make rapid and directed movements away from such areas, likely looking for other prey sources [17]. As these sharks move between habitats searching for prey, they exhibit distinctly different swimming behavior, suggesting they alter their hunting strategies for increased success [18]. White sharks have also been shown to exhibit deep-diving behavior, which has been linked to feeding and reproduction [17].

### *2.3.2 Migration patterns*

Sharks often exhibit different behavior based on age and size. Most white sharks spend a significant portion of their time on the continental shelf off the coast in water depths less than 100 m [18]. Movements into oceanic waters beyond the shelf edge are far more common in sub-adult and adult sharks of both sexes and with increasing size. Studies have shown that 45% of sub-adult and adult sharks spend some fraction of each year in water beyond the continental shelf [17]. Smaller individuals are more restricted to coastal and shelf habitats, and as they grow, they venture more towards pelagic and offshore movements. Similar behavior has been observed in white sharks tagged in the Eastern North Atlantic, North Pacific, South Africa, Australia, and off New Zealand.

Great white sharks are frequently centered in temperate coastal waters with an abundance of fish and marine mammals. These waters mainly include the coast of the northeastern and western United States, Chile, northern Japan, southern Australia, New Zealand, southern Africa, and the Mediterranean [19]. Little is known about the migration patterns of sharks; however, recent studies have shown that great white sharks can range across vast stretches of the open ocean. A study in California revealed that one male shark tagged along the central California coast migrated thousands of miles to Hawaii. Previously, it was believed that sharks remained close to shore; however, the invention of satellite tags (which will be described in detail in “Various Types of Shark Tagging and Tracking”) in the early 2000’s, made it possible to monitor long-distance migration which allowed researchers to better understand the migration patterns of great whites [20].

## **2.4 Shark Interactions with Prey and Humans**

### *2.4.1 Interaction with Prey*

The primary constituents of the white shark's diet are pinnipeds, which include seals, sea lions, and walruses. Dead whales are another important food source for great whites [21]. A study over the course of an eight-year period at Seal Island, South Africa observed the conditions under which sharks were most likely to attack seals. The study found that attacks occurred primarily during northerly winds, at high tide, within 400 m of land, over a depth range of 5–31 m, with significantly more occurring at depths of 26–30 m, and at low light levels [22]. White sharks have a metabolic rate of around 0.2 Kcal/kg/hr and only use a very small expenditure of energy for swimming (0.05Kcal/kg/h to swim at 3.2 km/h) [21]. This means that an adult white shark only needs to feed approximately once every 15 days.

The US Marine Mammal Protection Act has led to an increase in the population of the gray seal (*Halichoerus gryus*) population especially in the Gulf of Maine to Cape Cod and other coastal areas in the United States. The act protects these pinnipeds from hunting and reckless killing. The rebound in the seal population has led to white sharks becoming more abundant in these areas [17]. Understanding great white sharks' interactions with prey can help keep humans more aware of shark patterns and activity that they should avoid.

### *2.4.2 Patterns in Attacks on Humans*

A study was conducted of all white shark attacks on humans around the world. From this study, researchers discovered many similarities between shark interaction with prey and attack behavior on humans [23]. The study looked at all conditions and factors that were present during the time of attack, including location, water temperature, amount of light, water conditions (clear or murky), what the person was doing, what they were wearing, and how many other individuals were present at the time of attack. Around 15.2% of great white shark attacks on humans resulted in fatality [23]. This observation leads researchers to believe that when a great white shark attacks a human, the shark is under the impression that the human is a pinniped. The study showed that in 56.8% of attacks, the shark only took one bite and then swam away [23]. This demonstrates the bite and spit theory: when a shark bites and realizes the prey is not what it was looking for, the shark releases it, and swims away. This theory is further confirmed by how most attacks occurred with people wearing the color black, similar to the dark colorization of marine animals. Sharks primarily hunt pinnipeds, and humans (especially in a kayak or on a surfboard) present an image that approximates that of a pinniped in size, shape, color, and behavior such that predatory behavior is triggered. Additionally, white sharks generally attack solitary marine mammals, and in 84.8% of attacks, the target was isolated [23].

## 2.5 Various Types of Shark Tagging and Tracking

### 2.5.1 History

Shark tagging in its earliest form began with a large-scale tagging program in the 1940s with Petersen disc tags (Figure 6) and internal Nesbit tags [24]. Researchers attached the Petersen disc tags with titanium wire through a hole in the dorsal fin. Since these tags were thought to have high shedding rates, the program implemented Nesbit tags, which were inserted internally into the coelomic cavity of the shark using a scalpel. While the internal tags lasted longer in the sharks, these tags could only be retrieved through gutting and processing, unless another external tag was attached to the shark as well. This led to the trial of Rototags, or plastic cattle ear tags, in the 1960s as seen in Figure 7 [24]. The cattle tags also had good retention, but they required punching a hole through the shark's dorsal fin. Additionally, these tags dug into the fins of the sharks, causing irritation as their fins thickened.

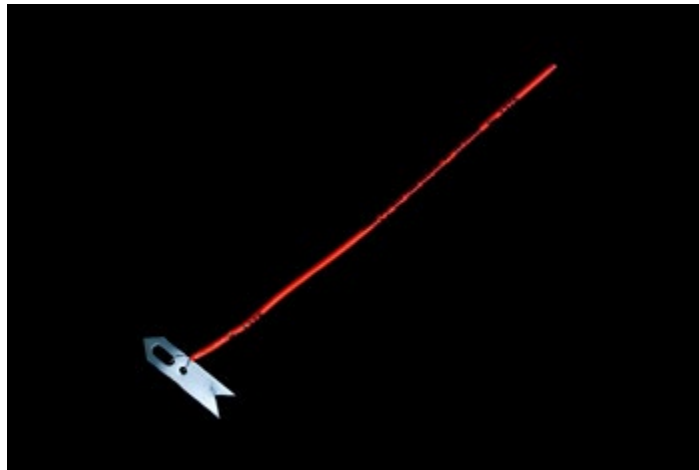


Figure 6: Petersen disc tag on a warmouth [25]



Figure 7: Rototags once used for shark tagging [26]

Around the same time as the cattle tags, new fish tagging programs began that allowed for tagging without having to bring the marine animal into the boat [24]. The first tag of this type was the 'M' dart tag, shown in Figure 8, which used a needle at the tip of a pole to inject the tag under the first dorsal fin. Dart tags did not have very good retention but led to less harm to the shark upon removal. Shortly after, in 1965, electronic tags, similar those still used today, originated with the first acoustic tagged shark [24]. After the implementation of acoustic tags, satellite and archival tags were used. These three primary electronic tag types have expanded into various new tagging technologies and are all still used today.



*Figure 8: Dart tag [26]*

### 2.5.2 Acoustic Tags

Acoustic shark tags interact with an underwater receiver using specific frequency and transmitting patterns to the receiver [27]. Acoustic tags, as shown in Figure 9, exist in two forms: acoustic pingers and passive acoustic monitoring. An acoustic pinger actively tracks the animal which it is attached to; researchers typically follow the animal using a hydrophone and receiver to gain information. Some versions of these tags include sensors which can measure the depth, water temperature, and swimming speed [27]. Passive acoustic monitoring tags are better suited for long-term tracking studies as long as months or even years. Passive acoustic tags use the same technology with transmitters and receivers as the pingers, but they use ultrasonic transmitters which are implanted into the animal for better retention. Each shark tag has a unique identification code which pings the receiver and records the data and time every time the shark swims within approximately one kilometer.



*Figure 9: Acoustic tag on great white shark in the front with PSAT in the back [28]*

### 2.5.3 Satellite and Archival Tags

Similar to acoustic tags, satellite shark tags also send signals to a receiver, but they send a signal every time the shark's dorsal fin breaks the water's surface and comes in contact with the air [29]. Since these are external tags, the researcher must hold the shark to the side of the boat to apply them. A satellite tag tracks the shark until its battery dies, but it is more susceptible to damage and early shedding due to its external attachment [29].

Some examples of satellite tags include the Smart Position or Temperature Transmitting Tag (SPOT), as depicted in Figure 10 and the Pop-up Satellite Archival Tag (PSAT) [30]. The SPOT is usually applied to the dorsal fin and transmit signals to the Argos satellite array, giving a wide range of geo-location accuracies [30]. The PSAT is attached to the shark and carries all data within the device itself. The tag releases from the animal after a certain period and then is collected by the researcher.

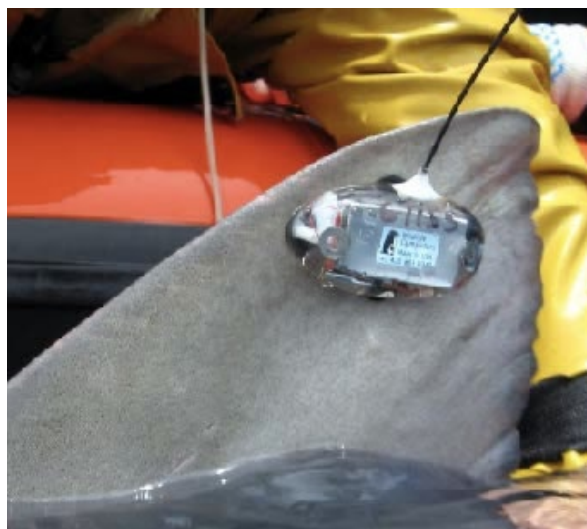


*Figure 10: Smart Position or Temperature Transmitting Tag (SPOT) Tag [29]*

#### 2.5.4 Post Tagging Release Stress

The effects of shark tagging procedures may alter the behavior, growth, and or reproduction of sharks. For this reason, shark stress responses to tagging events is an area of active research in the field. According to blood chemistry assessments conducted by J.P Hoolian, physiological stress responses to tagging events included elevated levels of electrolytes, enzymes, blood metabolites, and hematocrit values in the shark. These physiological changes may lead to changes in the shark's behavior. Blood acidosis and high blood lactate levels were also reported for tuna, sharks, and billfish subjected to capture and handling. Behavioral changes are also often exacerbated by physical bodily injury from fishing gear, as well as acclimatization to the tag being attached [31]. While these physical and physiological responses are present immediately after release, they diminish significantly over time. It is important to consider post tagging release stress effects on shark behavior, especially, when conducting short term studies, because irregular post release behavior may be present for a significant portion of the study, introducing bias into the data, and therefore producing unreliable results. Future studies have the potential to provide information to increase survivorship when practicing catch and release of marine animals [32].

## 2.6 Previous Mechanisms for Tagging Sharks

### 2.6.1 Crittercam Design

Invented by National Geographic marine biologist Greg Marshall in 1987, the Crittercam records sensor data, audio, and video of great white sharks and other animals in their natural habitat without the interference of humans. The Crittercam attaches to the dorsal fin of the great white shark [33].

The Crittercam pole and clamp are far more complicated than the alternative metal coil spring designs used in similar taggings. The Crittercam uses a conventional spring and hinge to keep the clamp open until forced closed [33]. To secure the Crittercam clamp to the dorsal fin, a zip tie seen on the left on the in Figure 11, is looped at the end of the clamp arms and is tightened and cut in one motion by the application device shown below on the right [33].



Figure 11: Crittercam Clamp [33]

Large curved abrasive friction pads eliminate any movement once the zip tie is secured. The seven-foot-long pole uses four attachment points to grip the Crittercam as it is slipped on so that the zip tie is behind the dorsal fin. The pole is attached to a SCUBA tank which powers the pole's zip tie tightening and cutting mechanism. With the push of a trigger, the pole uses pneumatics to tighten, trim and release the Crittercam securely to the shark in approximately one second. The application pole and clamp use 17 highly specialized custom machined components in addition to off-the-shelf parts. The Crittercam housing is also custom machined with the option of aluminum for expected depths up to 1000 m or titanium for depths up to 2000 m [33].

Instead of relying solely on passive galvanic corrosion to release the tag from the shark, the Crittercam uses an electronically controlled burn wire. This allows the tag to be released with a high level of accuracy, certainty, and consistency. Once the signal to release is sent from the onboard computer within Crittercam, a small amount of current is passed through a wire which rapidly corrodes. Once the reaction is complete, the spring clamping system releases, and the connected tag and Crittercam float to the surface together for retrieval. If the burn wire malfunctions, a backup Galvanic-Timed-Release (GTR) link is used to release the zip tie relieving the clamping pressure, detaching the Crittercam and clamp. One of the advantages of the Crittercam clamp design over the others is that it stays attached to the Crittercam and floats to the surface to be recovered and reused. The only nonreusable parts of the Crittercam clamp are the burn wire, backup GTR, and zip tie compared to far less eco-friendly designs which lose the entire clamp [33].

The Crittercam pole and clamp mechanism sounds promising but still does not allow Dr. Skomal to implement the device in the field. This pole would require Dr. Skomal to be perpendicular to the shark instead of trailing behind. Additionally, the Crittercam pole is approximately half the length of the pole Dr. Skomal currently uses to insert dart tags from the pulpit of a boat. Chum and fish heads on a rope were also used to position the shark in the right spot for the clamp to be attached. Two other issues arise with the Crittercam pole and clamp design: cost and complexity. The cost of the custom machined parts and pneumatic application pole that requires a SCUBA tank goes beyond this project's budget and makes this system out of reach for Dr. Skomal's intended application [33].

### *2.6.2 Metal Clamp and Tagging System with Spikes*

Gleiss et al. explored a new mechanism to attach data-loggers to large sharks. The clamp and tag package design as presented in Figure 12 was intended to attach to sharks with a stable base (primarily on the dorsal fin) such as whale sharks, white sharks, and basking sharks, without restricting their movement [34]. The tag package used in this study was compiled of a multiple channel logger, a two-stage coded VHF transmitter, and a continuous medium power-output acoustic transmitter [34]. The entire tag was housed in a micro-bubble and epoxy resin case with positive buoyancy [34]. This tagging device was

connected to one elongated arm of the clamp, which was connected to a second arm with a torsion spring. Titanium sleeves covered the two arms of the clamp which each had two 1.5 cm welded spikes for firm attachment to the fin.

One clamp arm had a small segment removed and replaced with a magnesium sleeve. The magnesium acted as a mechanism for clamp detachment from the fin because it corrodes after approximately three weeks in seawater. The two mechanisms for detaching the tag housing from the clamp included a bolt connected to the spring using GTR for automatic release after GTR corrosion, and a cotter-pin connected to a short line of monofilament which ended in a loop connected to GTR for manual release [34].

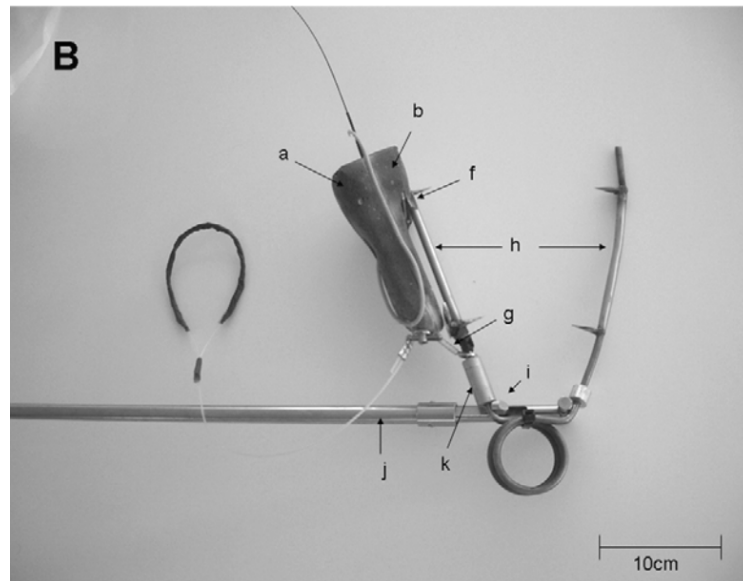


*Figure 12: Clamp system design consisting of (a) and (b) micro-bubble housing, in which a VHS transmitter, logger, and acoustic transmitter are enclosed. The magnesium sleeve (k) and the GTR with cotter-pin and monofilament (g) are methods of detachment [34]*

A snorkeler attached the clamp and tag housing to various whale sharks with a customized tagging-gun, including a 1.5 m shaft, handle and trigger with a safety pin, and a spring release system. The tagging-gun held the spring of the clamp open in tension, long enough to ensure proper placement on the second dorsal fin of the shark [34].

The clamp alone weighed 137 g in air with a density of approximately 4.9kg/L, whereas the micro-bubble housing and tagging technology combined weighed 224 g in air with a density of approximately 1kg/L. The total weight of the system on the shark was 361 g in air and 109 g in seawater [34].

The response of the whale sharks to this tagging system varied. Only one shark had no reaction, while a majority displayed a passive dive underwater following the attachment, and some showed obvious signs of disturbance as exhibited through beating

their tails and diving underneath the water [34]. While the spikes of the clamp left noticeable indentations in the sharks' fins, no sharks showed signs of bleeding. One potential cause for concern with this design is its impact on hydrodynamic drag. The associated drag due to the clamp moving through the water may lead to slow tearing of the fin with superficial tissue damage [34]. Therefore, a reduction in hydrodynamic drag on the tagging system can greatly lessen the risk of possible damage to the sharks.

### 2.6.3 Iteration of Metal Clamp and Tagging System with Friction Pads

Researchers in South Africa revised the welded spike clamp design from 2009 discussed above. Their improved clamping mechanism employs many of the same design principles from Gleiss et al. but differentiates itself by replacing the potentially harmful sharp spikes with four abrasive friction pads. Unlike the spikes which puncture the skin and flesh of the shark, the abrasive friction pads utilize the roughness of the shark's dermal denticles to create enough friction with the aid of a strong clamping force of 196 N to hold the tag on the shark [35]. This new clamp system shown in Figure 13, was designed to work directly with the CATS Cam and Diary tagging devices. The CATS Cam and CATS Diary tags record real time data from an array of onboard sensors in addition to recording live video, allowing researchers to observe sharks in a new way.

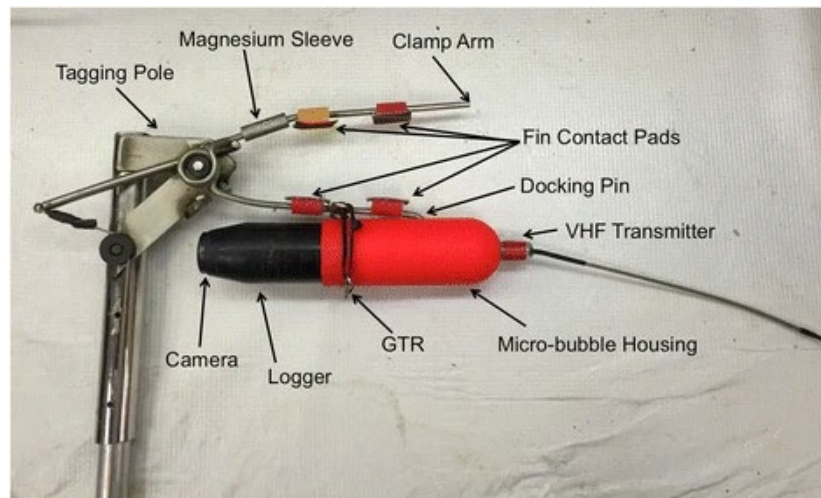


Figure 13: Current CATS Cam Clamp [35]

The clamp connects to the CATS devices with a docking pin located at one end of the clamp which seats into the CATS devices' micro-bubble exterior housing without locking, allowing the clamp to disconnect at the desired release time. The docking pin does not lock to allow the clamp to disconnect from the device at the desired release time [35]. The size of the GTR which is attached to a zip tie that joins the clamp and tag together, determines how long the tag stays on the clamp. Once the GTR corrodes, releasing the zip tie, the clamp naturally unseats itself from the device, allowing the device to float to the surface for retrieval [35]. After the tag releases, the clamp continues to stay clamped to the dorsal fin

of the shark. Welded between the metal spring coil and the arm with friction pads is a magnesium sleeve, designed to corrode a safe period after the GTR and relinquishing the spring force holding the clamp arm to the dorsal fin [35]. Once the two halves of the clamp release from the shark, they sink and are not retrieved. The magnesium sleeve acts as a safety in case the tag does not naturally release from the clamp. Slight modification to the location of the magnesium sleeve was required after tests showed the clamps remained attached to the shark even after the sleeve corroded away. One test resulted in the clamp staying on until researchers were able to knock it off, showing visual abrasions at a later encounter approximately five weeks later [35]. The researchers addressed this by moving the magnesium closer to the torsion spring to ensure the clamp fell off the dorsal fin in subsequent tagging events.

Gleiss et al. were able to test their design by hand attaching the spiked clamp to the dorsal fin of a harmless whale shark [34]. For Chapple et al., using a free-swimming attachment method identical to Gleiss et al. would threaten the life of the researchers [35]. Chapple et al. instead opted to create a one-meter clamp attachment device which opened the clamp wide enough for the dorsal fin and when released, allowed the clamp to instantly secure itself to the shark.

The Chapple et al. design is ineffective for Dr. Skomal's applications primarily since he intends to attach his tagging device while trailing the shark instead of tagging beside it. Chapple et al. designed their application pole device to rely on manipulating the shark with chum to the ideal location, within one meter to the side of the boat [35]. Dr. Skomal has decided to avoid using chum and fish to bring the sharks to him and instead opts to locate the sharks by spotter plane and chase after them on a boat.



*Figure 14: Dr. Skomal tagging a great white shark off the coast of Cape Cod*

As shown in Figure 14, sharks are spotted in clear shallow water close to shore where the dark silhouette of the shark contrasts the light sandy bottom instead of blending in with the dark blue depths offshore. Not only are these sharks close to shore, but the

sharks are often cruising directly off heavily trafficked summer tourist beaches with swimmers. Using chum and fish to attract nearby sharks to heavily populated beaches is unsafe and is the reason why Dr. Skomal chooses not to use these methods that are popular elsewhere in the world.

## 2.7 Injury Prevention

When designing the clamp and pole system, it is important to consider preventing injuries to its user, including injury to the wrist, arm, and hand.

Common types of wrist injury relevant to our design are scaphoid waist fracture, triangular fibrocartilage complex (TFCC) injury, and hook of hamate fractures. Figure 15 below shows the carpal bones in the wrist. A scaphoid waist fracture is the most common wrist injury. Scaphoid waist fractures can occur in a pronated, radially deviated hand or when the hand is in the extended position [36]. Scaphoid waist fractures in the extended position occur because of an increased force concentration on the scaphoid. The force concentration on the scaphoid fossa is 52% in the neutral position and 62% in the extended position [37]. The TFCC acts as an articular and load bearing surface between the radius and the carpal bones. Injuries to the TFCC can occur when the wrist is in hyperextension and pronation or when it is ulnar deviated and axially loaded (the extended position)[36]. Decreasing ulnar variance decreases the risk of injury to the TFCC because it reduces radio-scaphoid peak pressures [38]. Direct blows from a pole, or repeated lesser impacts can cause a hook of hamate fracture. Hook of hamate fractures are common in golfers as a result of hitting the earth with a club [36].

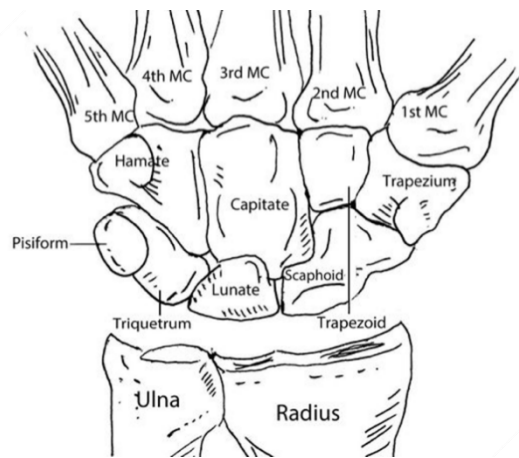


*Figure 15: The bones of the wrist [39]*

Most carpal injuries occur when the wrist is axially loaded in either compression or extension. Stress concentration on carpal bones leads to fracture. These stress concentrations occur from either instantaneous large loads or repetitive smaller loads [40]. The functional position has the wrist in slight ulnar deviation and extension with the distal and proximal interphalangeal joints in flexion; this position, when compared to a neutral

position, results in lower stress concentrations on the scaphoid fossa but higher stress concentrations on the lunate fossa. Stress concentration on the lunate fossa is the leading cause of bone necrosis [41]. Stress concentration patterns on the distal radius and scaphoid are similar to intra-articular fracture patterns [40].

Cartilage injuries occur when a load is above the maximum allowable at the articulation surface. Cartilage in a joint decreases the peak load experienced by the bones in the joint by increasing the load distribution. An increased load increases the contact area between joints via cartilage. However, the contact area remains constant after a maximum loading because the cartilage is already maximally loaded. In the carpal row, the wrist bones, the maximum load is 46 lbs. [42].

Possible relevant injuries to the hand and fingers include closed annular pulley ruptures and metacarpal phalangeal fractures. Closed annular pulley ruptures are common in mountain climbers because they result from large tensile loads on the fingers. A high load on the flexor tendon system causes ruptures in the “pulley system” of the tendons in the fingers. Metacarpal and phalangeal fractures account for about 10% of all fractures at the emergency room. Metacarpals are the bones within the hand that connect to the fingers (phalanges). Metacarpal phalangeal fractures result from blows, crushing, or hard falls [36].

The optimal position to prevent injuries to both the scaphoid, carpal bones, and TFCC is to place the wrist in slight radial deviation and palmar flexion. Figure 16 below shows dorsal/palmar flexion and radial/ulnar deviation of a wrist.

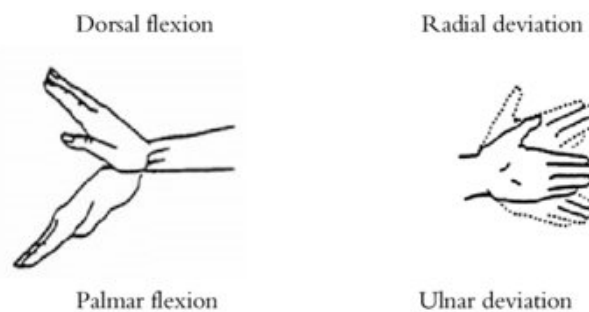


*Figure 16: Dorsal/palmar flexion and radial/ulnar deviation of the wrist [43]*

The research conducted in this section influences our approach to the project strategy and provides insight into shark anatomy, past tagging systems, and human safety to inform our designs.

### **3 Project Strategy**

#### **3.1 Client Statement**

The client, Dr. Greg Skomal, stated that he wanted a tagging system (clamp and pole) that would allow researchers to easily tag great white sharks from the pulpit of a boat with minimal risk to the user. This project was to be completed in the time frame of an academic year with a given budget of \$1000 USD from the sponsor and \$1000 from the Mechanical Engineering Department at WPI.

#### **3.2 Design Requirements (technical)**

The design objectives are categorized into those for the tagging system, the pole, and the overall system. The primary objective for the tagging and pole system is to minimize potential failure during the tagging process. Potential failure could be characterized as premature or incomplete deployment of the tag system, losing control of the pole, or an inability to attach the tag to the shark. The separate objectives for the tagging system and the pole are listed below.

Tagging System Objectives:

- The tagging system needs to firmly attach to the shark without falling off and remain properly oriented for the CATS Cam.
  - The tagging system cannot cause any permanent damage to the dorsal fin of the shark.
- The tagging system should be retrievable after release, and the majority of its components should be reusable.
- The tagging system should be easily manufactured.

Pole Objectives:

- The pole should effectively deploy the tag with minimal effort on the user's part.
  - The pole should be able to attach the tagging system while the user is travelling behind the shark from the pulpit of the boat.
  - The pole should not require the user to strain physically to attach the tagging system to the shark.
- The pole needs to withstand the potential drag forces and forces generated by the movement of the shark and the boat.
- The pole should be reusable.

Additionally, the preliminary design constraints for the overall system include:

- The whole system should be created within the given budget of 1,000 USD.
- The whole system needs to be created and tested by the end of the third quarter of the academic year.
- The system material needs to withstand degradation in a salt-water environment.

- The maximum deflection of the pole should be less than 0.5 in.

### 3.3 Design Requirements (standards)

#### 3.3.1 Marine Standards

Chumming is the practice of luring marine animals by placing chum, a form of bait that consists of fish bones, parts and blood that attracts marine life [44]. Chumming is illegal in some parts of the world due to the danger it presents in associating feeding with the presence of humans. The rules vary by region but are commonly enforced to reduce the following: bacteria in waterways, excessive bait fishing, littering and diseases introduced by bait fish. Chumming is commonly prohibited in public fishing bridges or piers, drinking water lakes, beaches and many national parks and preserves [45].

There are certain places throughout the United States where chumming is illegal; however, Massachusetts is not one of them. In 2015, new regulations were enacted to prohibit purposely attracting great white sharks in state waters without a permit. The regulation is aimed to stop anyone without a proper license from attracting sharks to people or their vessels through chumming water [46]. There are no specific Occupational Safety and Health Administration (OSHA) regulations that specify the protocol of shark chumming, marine animal tagging, or pole handling.

#### 3.3.2 Software and Manufacturing Standards

To model this design in Solidworks and develop final engineering drawings, the standards of the American National Standards Institute (ANSI) were followed. The standard for ANSI is represented in Figure 17.

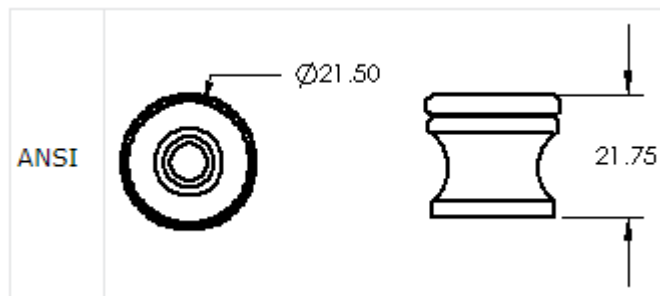


Figure 17: ANSI standards format example [47]

A strict set of standards were followed in the machining of this project in the Washburn Laboratory, the machine shop at Worcester Polytechnic Institute (WPI). All OSHA standards and specific WPI machine guides were also followed. The machines that were used consisted of the HaasSL10 Lathe and the Haas Mini Mill. The regulations

applicable to machine shops are found in the OSHA Safety and Health Standards 29 CFR (1910). These standards require conditions or practices necessary to protect the worker utilizing said machine[48]. The OSHA standard 29 CFR 1910 contains various regulations, including but not limited to:

- Occupational Health and Environmental Controls (Ventilation, Noise, Radiation)
- Personal Protective Equipment (Eye and Face Protection, Respiratory Protection, etc.)
- General Environmental Protection (Sanitation)
- Machinery and Machine Guarding (Mechanical Power Presses, Abrasive Wheels, etc.)
- Hand and Portable Powered Tools
- Welding, Cutting, and Brazing
- Electrical

The safety protocols for the specific machines used in the machine shop were obtained from the Washburn Laboratory website. The *CNC Quick Guide for Haas Mills* by Torbjorn Bergstrom (to operate the CNC Haas Mills), and the *Lathe Operator's Manual* by Haas Automation Inc. (to operate the HaasSL10 Lathe) were referenced.

### **3.4 Revised Client's Statement**

The project scope shifted from designing the entire tagging system (clamp and pole) to only creating a pole. This allowed for a more detailed and focused design of the pole that worked with the given dimensions and design of Dr. Skomal's current clamp.

### **3.5 Management Approach**

Each term we set goals and tasks to ensure we would be able to develop a final prototype for Dr. Skomal at the completion of our project. Due to the limitations of COVID, we worked into the final academic term to complete our project. Appendix A outlines our approach to our MQP project on a term-by-term basis

## 4 Pole Design Process

### 4.1 Needs Analysis

The pole will be used to deploy the clamp and tag from the pulpit of the boat; therefore, any release mechanism on the pole needs to be accessible from 10-16 feet away. The potential for premature release of the clamp during the tagging process, or incomplete tagging of the shark, should be minimal. Additional considerations include the unpredictable nature of the shark's movements while being tagged; to account for this, the pole needs to be maneuverable by the user. The most important design feature of the pole includes accounting for the user's safety by ensuring the load of the tag and pole cannot injure the user.

### 4.2 Design Matrix

The design options for the pole were weighed in a design matrix. Based on Dr. Skomal's needs for the pole, the customer requirements were summarized in Table 1. The requirements have importance levels ranging from 0.1 (least important) to 1 (most important). Weights were determined based on Dr. Skomal's input and through research on existing pole tagging systems. The full design matrices can be found in Appendix B and Appendix C.

*Table 1: Customer Requirements and Importance Scores for Pole*

Customer Requirements	Weight/Importance (0-1)
Easy to Use	1
Low Potential for Failure due to Design	1
Safe for user	1
Adaptable approach angle	0.8
Durable	0.8
Lightweight	0.8
Low Cost	0.7
Simple in Complexity	0.5
Reproducibility	0.3

The pole is "*easy to use*" if the user can easily manipulate it into the correct position to deploy the tag. It is crucial that the pole only require minimal user effort in a fast-moving environment with many variables (ocean waves, moving shark, moving boat, wind, etc.). The pole's "*ease of use*" scored a one because it is the primary device that controls the clamp attachment to the shark.

The "*low potential for failure*" requirement includes two components which decide whether the system has failed. Failure is characterized as the pole malfunctioning before the clamp is deployed. Premature detachment also indicates failure; this occurs if the clamp

falls off before the shark is tagged. This requirement also scored the highest with a score of one as functionality and success of the system are the primary goal of any design.

“*Safe for user*” indicates that the pole design will not injure the user in the tagging process. This received the high score of one because it is of utmost importance that the design is ergonomic and does not allow for any potential injury when properly used.

The pole has an “*adaptable approach angle*” if it allows for various angles around the shark to attach the clamp. The angles for the pole depend on the required clamp attachment angle. This requirement received a score of 0.8 due to an emphasis on safety for the user, which can be impacted by challenging approach angles. Additionally, the “*adaptable approach angle*” is important for quick and concise tagging in fast-paced environments.

A “*durable*” pole will not break or fall apart during the attachment process and will last for multiple uses through the shark season. “*Durability*” scored 0.8 for the pole because the pole is only used for a short period at a time and does not have to withstand long periods of force and drag from the water.

A “*lightweight*” pole depends on material selection and maximum deflection; furthermore, it contributes to how easy the pole is to use. The pole must be lightweight so that the user can control it in moving water with associated drag forces without experiencing injury. This requirement scored 0.8 since it plays a role in the safety of the design for the shark and more importantly, the user. It also contributes to how easy the system is to use and the total cost (depending on materials).

The “*low-cost*” requirement for the prototyping process was set at 1,000 USD per the sponsor agreement. This requirement received an importance of 0.7 since it is relatively important that the project is capable of being produced under budget, but it is not as important a factor in deciding designs as the functionality requirements.

A pole that is “*simple in complexity*” has a minimal number of parts and utilizes relatively simplistic mechanisms in the design. A score of 0.5 was given for this requirement since simplistic designs are often easier to use, and having fewer parts leads to a lower probability of failure.

“*Reproducibility*” includes the pole being easily remanufactured without many customized parts. Having too many parts which are unable to be remade without customization will make it difficult and expensive for Dr. Skomal to produce multiple tagging and pole systems for his research. This received a score of 0.3 because it is a good consideration for the designs, but it is not necessary for the success and functionality of the overall system.

This design matrix was used throughout the entire design process to assess various designs and iterations. The scores from the design matrix informed decisions about designs and identified certain design aspects that could be combined for a more optimal final design.

### 4.3 Pole Alternative Designs

#### 4.3.1 Grabbing Pole

The grabbing pole design holds the CATS Cam clamp during clamp application and then release it once the clamp is in place. The pole can be made to be any length, with an outer hollow pole and an inner hollow pole. The handle would be at 70 degrees to ensure the wrist is in a position of slight palmar flexion and radial deviation, which prevents possible wrist injuries. The handle is composed of two pieces, a top and a bottom that are hinged together at the non-pole end. Figure 18A below shows the pole in the un-squeezed handle and pinched rods position, and Figure 18B shows the squeezed handle and open rods position.

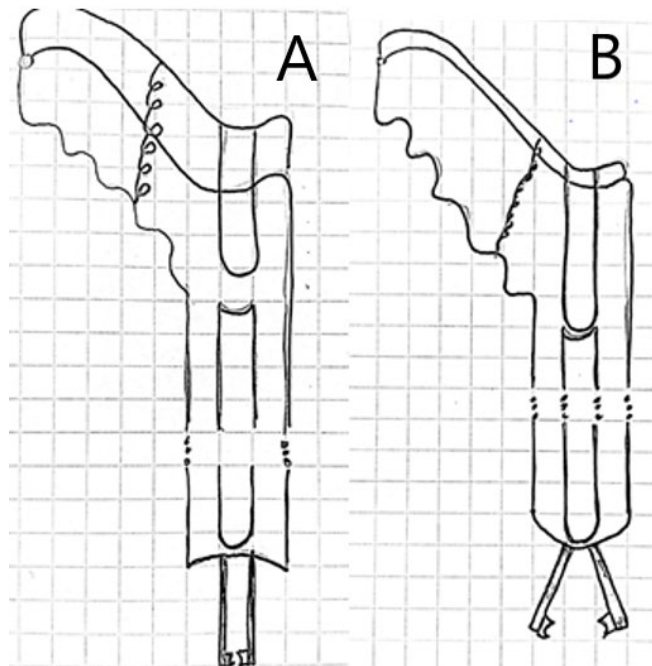


*Figure 18: Pinch and release mechanism pole. A is un-squeezed, pinched position, B is squeezed, released position*

This pole design was inspired by the Critter Catcher, which was used to test the ability of this design to hold an object heavier than a bug. This test showed that the elastic circle would expand when an object over 20 g was placed in the vertical spines. For this project's design, in the un-squeezed handle position, the rods would open with the clamp in

it. As a result, this pole could not hold the tagging system long enough to ensure the tag was placed on the shark.

The second iteration of the grabbing pole includes a “locking” mechanism to prevent the pole from releasing the tagging system prematurely. The handle in this iteration remains the same as the previous iteration, as do the external and internal pole structure. This iteration changed the articulation with the tagging system. In this design, the pinching rods attach to the internal rod and the walls of the external rod with two pin joints each. When the user squeezes the handle, the internal rod is pushed down, in turn pushing out the pinching rods (see Figure 19).

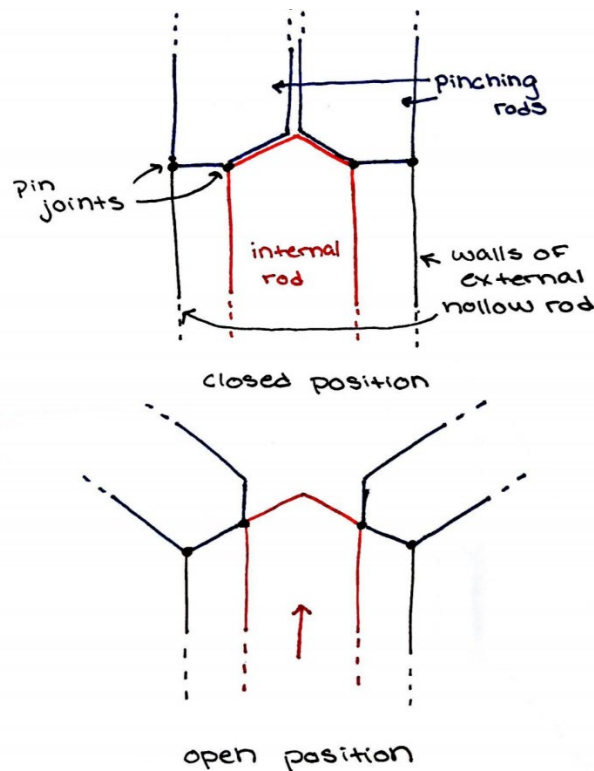


*Figure 19: Second iteration of the grabbing pole. Top: Closed, un-squeezed position, Bottom: open, squeezed position*

This design scored poorly on the design matrix (11.2/18.3) (see Appendix B) because it can only be used in tagging when it is perpendicular to the shark. One challenge with perpendicular tagging is that the pole would have to hold the tag on the side rather than directly facing forward. For this reason, it would be impossible to angle the rod in such a way to ensure that the internal/external rod mechanism would work properly.

#### 4.3.2 Electromagnet Pole

Another preliminary pole design was the electromagnet pole. An electromagnet would mount to the opposite end of the pole from the user’s hands. This electromagnet will

serve as the connection or “glue” between the clamp and the pole. As seen in Figure 20 and Figure 21, the design consists of mounting the electromagnet to the end of a hollow pole. Another magnet on the clamp would attract to the electromagnet on the pole. Various clamp designs will work with this electromagnet pole system.

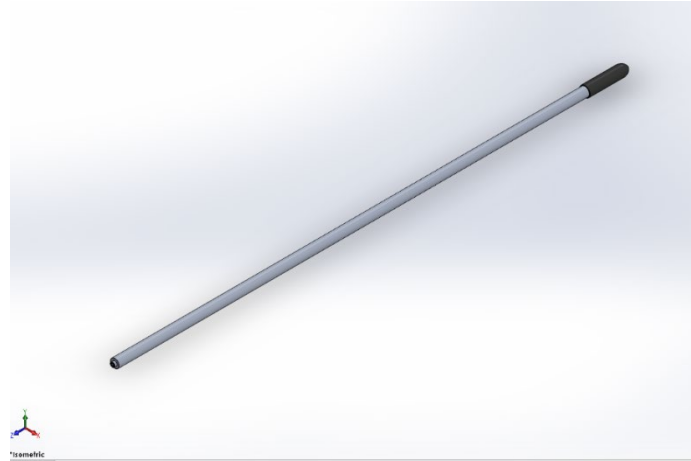


*Figure 20: Overall design of the electromagnet pole*

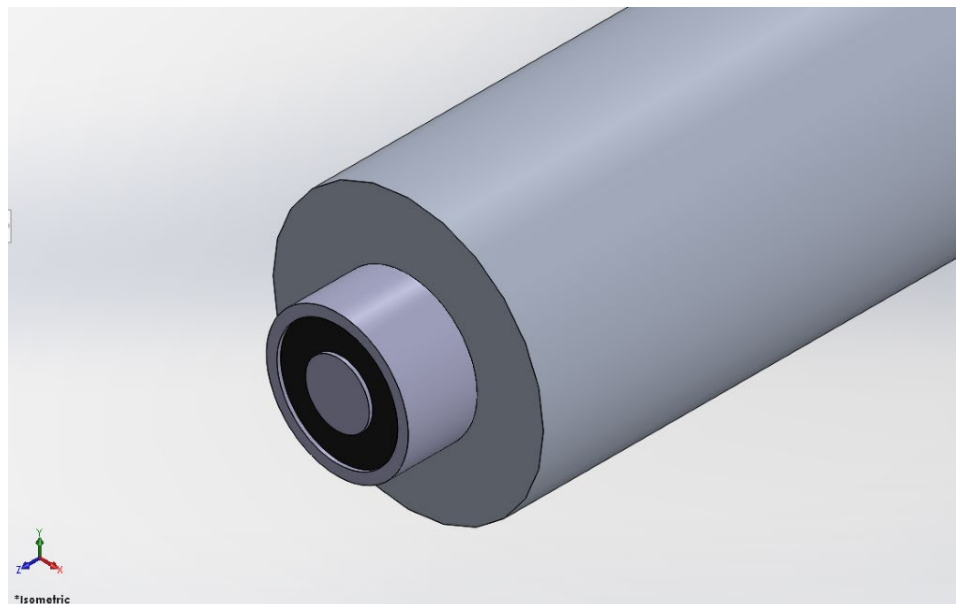


*Figure 21: Close up of the electromagnet attached to the pole*

An electromagnet, as seen in Figure 22, is a type of magnet where the magnetic field is produced by an electric current [49]. The main advantage of using an electromagnet in the design is that the user can easily turn the magnetic field on and off by controlling the current. Electromagnets require a power source that can send current to the electromagnet which means that the pole needs to be connected to a battery, either within the pole or to a power source on the boat. Depending on the power source, the battery and any external

cables required to activate the electromagnet would be safely secured inside the pole. For an external power source, the source would be securely bolted to the boat to ensure the system is as safe as possible.

Electromagnets have varying holding forces ranging from 22 to 490 lb. The holding force represents five times the weight that the magnet can lift; therefore, dividing holding force by five gives an approximate estimate of that weight [50]. For example, an electromagnet with a 22 lb holding force can only lift a maximum of 4 lb, and a 490 lb holding force can lift a maximum of roughly 100 lb [50]. To be able to withstand the forces of the shark and the ocean, initially the pole design included the electromagnet with the highest holding force of 490 lb, but the heaviness of the electromagnet itself (5 lb) would contribute greatly to the force that the user feels on the other end of the pole. An alternative with a 190 lb holding force weighed slightly less than one pound with a diameter of 2.37 in [51]. This electromagnet required a voltage of 6 V and a current of 0.92 Amperes.

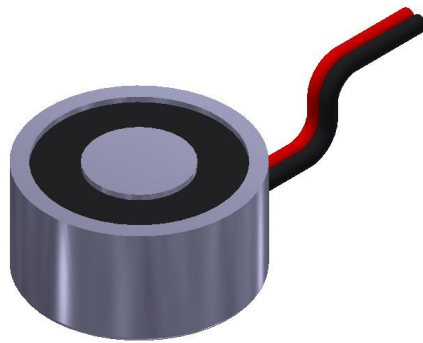


*Figure 22: Example of an electromagnet*

A long telescoping rod, as seen in Figure 23, with an overall length of approximately 16 ft was an option for the pole design. This would allow the user to collapse the pole to a shorter length when it is not being used. The materials for the telescoping pole consisted of carbon fiber and aluminum. There were two primary concerns for the electromagnet design with a telescoping pole. First, the forces from the water and the shark could potentially collapse the pole back in on itself, preventing it from attaching the clamp at the proper pole length. Second, the wires of the electromagnet would have to fit within the hollow pole, but its collapsible nature could tangle the wires or allow water to seep in, which could prevent the current from holding the clamp to the pole until attachment is complete.

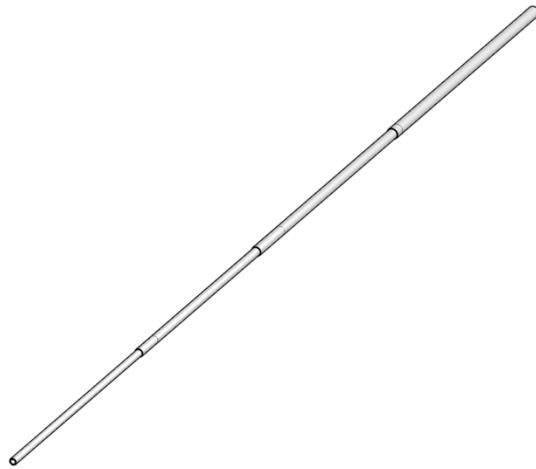


*Figure 23: Telescoping pole design*

From the design matrix, the electromagnet scored 15.2/18.3 (see Appendix B). While the electromagnet pole scored well in how easy it is to use, its adaptable approach angle, and durability, weight and concerns with electrical insulation contributed to the group moving forward with a different pole design. Many of the electromagnets researched also required either a motor or solenoid driver for kick-back protection so that the electromagnet does not potentially explode, as an electromagnet coil is very close to being a short circuit [50]. Additionally, due to the electrical nature of the electromagnet system, it would be essential to waterproof the pole to prevent water damage and possible harm to the user or shark [50]. This pole design is significantly more expensive overall with the electromagnet components, wiring, sealant materials, and a power source, in addition to the cost of the pole itself.

#### *4.3.3 Flex Release Pole*

The flex release pole design is a simple design intended to work with the soft-lock clamp from Appendix D. This pole can be adapted to a better angle (90 degrees with the dorsal fin) without the user and the pole itself having to be perpendicular to the shark when attaching the clamp. The concept is to have a triangular shaped plate which holds the clamp in its fully open and lock position from the outside and fits well around the clamp as shown in Figure 24. The clamp holder is designed to flex slightly when the clamp is in its widest position before the clamp is tapped against the shark's fin and fully collapses inwards to close. Then the force of the spring which closes the clamp will pull the clamp arms from the slots on the triangular holder, and the pole attachment will no longer fit the closed clamp. At this point, the user can simply pull the pole away from the shark, as the clamp will be secured in place and the pole will no longer be connected.

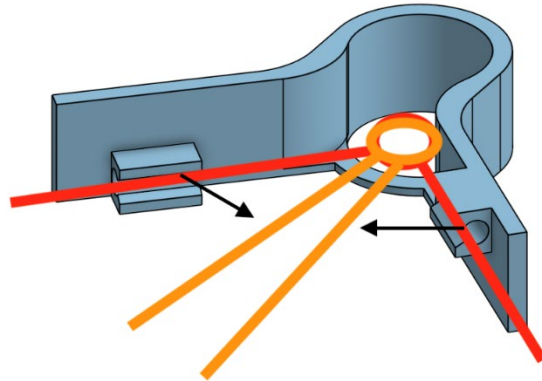


*Figure 24: Clamp adapter piece for flex release pole (clamp open position in red; clamp closed position in orange)*

A 24-inch crossbar connects the flex clamp release to the pole as seen in Figure 25. This allows the clamp and pole to be parallel with each other and the shark yet offset by 24 in, allowing the pole to hook around the front of the shark's fin while the user trails from behind. The adjustable telescopic pole would be attached to the far end of the bar, opposite the clamp.

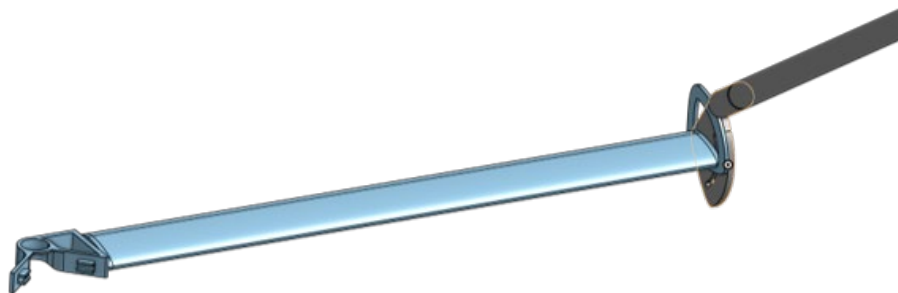


*Figure 25: Clamp adapter connected to crossbar and pole*

This pole scored the highest in the design matrix; however, the prototype was not able to flex outward enough without snapping. Additionally, the slots for the clamp arms broke very easily when fitting the clamp in place.

#### **4.4 Final Pole Design Stages**

##### *4.4.1 Hydrofoil*

One consideration for the crossbar of the pole design was to implement a hydrofoil into the pole design to provide an upward force, to help counteract the weight and drag forces on the pole and assist the user in the tagging process. A hydrofoil is a wing which provides lift, usually for applications in water [52]. Through preliminary calculations for a

hydrofoil with a chord dimension of 1.63 in and a span of 24 in as shown in Figure 26, we found the lift, drag, aspect ratio, and Reynold's number on this hydrofoil, with specific initial parameters.

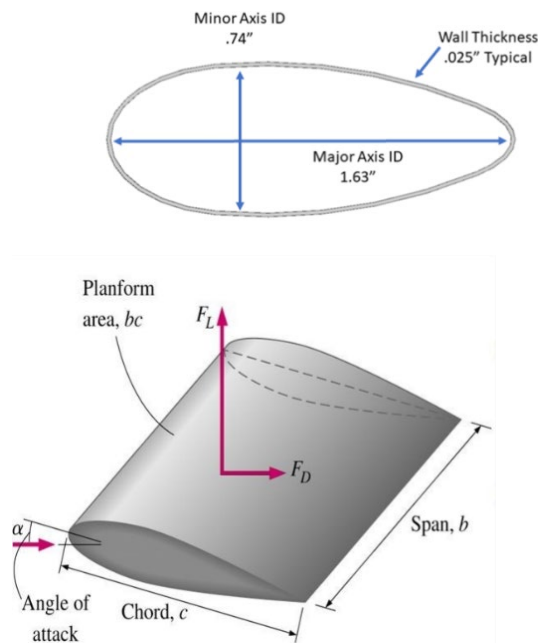


Figure 26: Dimensions and shape of hydrofoil [53]

The Reynold's number of the foil was found assuming the foil will be moving through water at 3.5 m/s (7.8 mph). Reynold's number is a dimensionless number which gives an indication of where the flow of the fluid is laminar or turbulent using velocity, kinematic viscosity of the liquid, and a measure of length [52]. A Reynold's number greater than 100,000 usually indicates turbulent flow; therefore, since the Re was 88,000, the flow is likely to be laminar.

To find the lift and drag, lift and drag coefficients found experimentally at different angles of attack were used [54]. The hydrofoil lift and drag calculations are based on an 8-degree angle of attack, using 0.61 as the coefficient of lift,  $C_L$ , and 0.04 as the coefficient of drag,  $C_D$  [54]. The final calculations for lift and drag produced values of 96 N and 6 N, respectively. From these values, the lift-to-drag ratio is approximately 15. The aspect ratio (AR) of the hydrofoil is found by squaring the span (24 in) and dividing by the planform area, which is the area of the foil from a top-down view (chord times span). The AR of this specific foil to be 14.7. The greater the AR, the less induced drag the foil will experience in the fluid it travels through [52]. The AR also affects the lift-to-drag ratio, since induced drag takes place at the tip of the wing [52]. The equations and calculations are shown below:

## Reynold's Number:

Kinematic viscosity of water @ 0°C:  $\nu = 1.643 * 10^{-6} m^2/s$

$$Re = \frac{\rho v c}{\mu} = \frac{v c}{\nu} = \frac{(3.5)(0.0414)}{1.643 * 10^{-6}} = \mathbf{88,000}$$

## Lift and Drag Equations and Variables:

$C_L = \text{Lift coefficient}$

$C_D = \text{Drag coefficient}$

$\rho = \text{density of saltwater} = 1,023 \text{ kg/m}^3$

$A = \text{planform area} = b * c = 0.0252 \text{ m}^2$

$v = \text{velocity} = 3.5 \text{ m/s (7.8 mph)}$

$$\text{Lift} = 0.61 * \frac{1}{2} \left( \frac{1023 \text{ kg}}{\text{m}^3} \right) \left( 3.5 \frac{\text{m}}{\text{s}} \right)^2 (0.0252 \text{ m}^2) = \mathbf{96 \text{ N (22 lbf)}}$$

$$\text{Drag} = 0.04 * \frac{1}{2} \left( \frac{1023 \text{ kg}}{\text{m}^3} \right) \left( 3.5 \frac{\text{m}}{\text{s}} \right)^2 (0.0252 \text{ m}^2) = \mathbf{6 \text{ N (1.3 lbf)}}$$

$$\text{Lift-to-Drag Ratio: } \frac{L}{D} = \mathbf{15.2}$$

$$\text{Aspect Ratio: } AR = \frac{b^2}{A} = \mathbf{14.7}$$

From these calculations, it appeared that this hydrofoil would be a good addition to the pole design, as it provides a lift and reduced drag compared to a rectangular crossbar, but these calculations did not consider the effect of the pole and the pole adapter on the two sides of the hydrofoil, which could impact the balance, lift, and drag of the foil in the water. Since the clamp must be attached underwater where the shark's dorsal fin is located, having a foil that provides too much lift may make it more difficult for the user to push the entire clamp and pole system far enough under water to complete the tag attachment. Eliminating the angle of attack will reduce the lift while maintaining a very low drag on the hydrofoil itself.

Endcaps for the hydrofoil will allow for a more adaptable pole once in the water. These end caps would allow for a rod through the length of the foil to attach the clamp adapter and pole to either end of the foil. The hydrofoil will freely rotate about this rod such that it can self-stabilize to a 0-degree angle of attack once placed in the water. Free rotation eliminates the need for the user to set the foil to a specific angle prior to placement

in the water, since water conditions and speeds are often unpredictable. While the hydrofoil freely rotates around the center rod, it is important that the clamp adapter and pole are in fixed positions for the easiest application of the clamp to the shark.

#### *4.4.2 Hydrofoil and Bike Brake*

There are a few drawbacks of using a rod through the hydrofoil as the crossbar. First, the end caps of the hydrofoil would need to be watertight as to not allow water into the foil. The air trapped inside the hydrofoil produces a counterclockwise moment in the opposite direction to the clamp opener. Also, if the hydrofoil fills with water, its mass will increase, making it difficult for the operator to lift the pole and hydrofoil into the air. Additionally, the seal between the rod and endcaps would still need to allow the hydrofoil to rotate about the rod, which would likely be difficult to accomplish while keeping the seal watertight.

After identifying these disadvantages, a new system was developed that would attach to the outside of the hydrofoil endcaps. The design utilizes a bike brake to allow the user to hold the hydrofoil in its desired position (0-degree angle of attack) once it is placed in the water and leveled based on the user's position relative to the shark being tagged. The design allows for the hydrofoil to level itself at any approach angle from zero (directly behind the shark or level with the water) to 90 (directly above the shark) degrees. The bike brake is attached at the bottom of the pole and has a cable that runs up the pole to a handle at the top, which when squeezed, clamps the bike brake and holds the hydrofoil in place. This design was developed through various iterations outlined below.

##### *4.4.2.1 Hydrofoil and Bike Brake: Iteration 1*

The first iteration of the hydrofoil and bike brake design consists of only four parts: the hydrofoil, the hydrofoil endcap, the female pole fitting, and the bike brake (not shown in Figure 27 but would be attached where the plates meet). One drawback is that the location of the bike brake would prohibit the hydrofoil from rotating a full 90 degrees because it would obstruct its path. Additionally, the female pole fitting has only one plate (gray) which might allow for unwanted rotation about the x-axis. This rotation could potentially create significant 'wobble', effectively adding friction to the pin in the slot, not allowing free rotation of the hydrofoil.

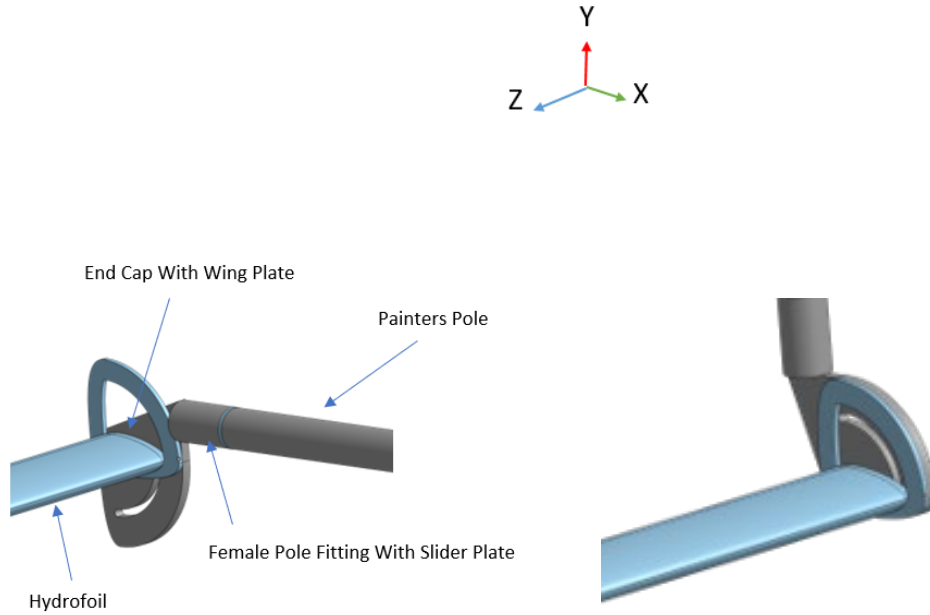


*Figure 27: Hydrofoil and bike brake iteration 1*

#### 4.4.2.2 Hydrofoil and Bike Brake: Iteration 2

The female pole fitting (as seen in dark blue in Figure 28) was altered to have two plates rather than one, addressing two previous concerns. First, the added plate would decrease rotation that may occur around the x-axis by adding a second point of contact for the pins on the hydrofoil endplate and wing (dark gray). Additionally, the second plate allowed for relocation of the bike brake. Moving the bike brake to clamp onto the outside plates of the pole, eliminated the concern of the brake obstructing the hydrofoil's motion.

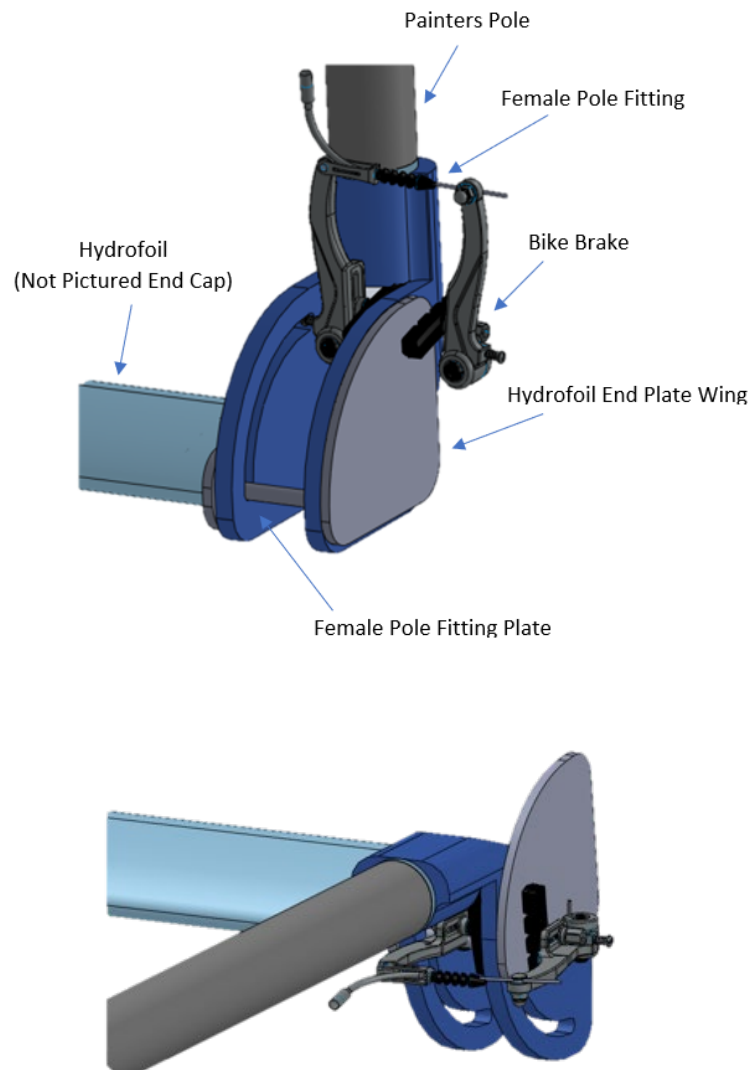


*Figure 28: Hydrofoil and bike brake iteration 2*

The main concern with this design included the potential for high amounts of friction between the hydrofoil endplate wing (dark gray), and the female pole fitting plate (dark blue), as well as within the pin joint and the pin and slot joint. This version also required further adjustments to ensure manufacturability of the overall system.

#### 4.4.2.3 Hydrofoil and Bike Brake: Iteration 3

This iteration consists of two ball bearings, two M5 35 mm binding barrel and screws, the hydrofoil and hydrofoil endplate, the female pole fitting (which is manufactured in three pieces and assembled with four M3 10 mm screws), the endplate wing, and the bike brake.

Bearings in the pin joint of the female pole fitting side plates reduce the friction, allowing the hydrofoil to rotate more easily. A geometric change to the endplate wing

aided in reducing the friction by ensuring the two pieces only make contact at the top where the bike brake will clamp them together. Additionally, edges were added around the holes in the hydrofoil endcap in order to reduce the friction between the endplate and the left side plate of the female pole fitting.

Additional geometric alterations include the addition of a small plate on the left side plate of the female pole fitting to allow for a more secure attachment of the bike brake by giving it a spot to rest on. Backings were also added to the holes for the bearing to prevent them from falling out. Lastly, a platform was added to the right-side plate of the female pole fitting in order to reduce the distance that the bike brake would have to be closed to adequately clamp onto the wing.

To improve the overall manufacturability of this design, two main changes were made. First, the hydrofoil endplate and wing would be manufactured in two pieces and connected using binding barrel and screws. Second, rather than attempting to manufacture the complex shape of the female pole fitting in one piece, it was separated into three components to be assembled using M3 screws, tabs along the edges, and slots to hold it together as additional support. The design of this new female pole piece assembly also allowed for better structural integrity than the previous design because it included supports between the two sides plates.

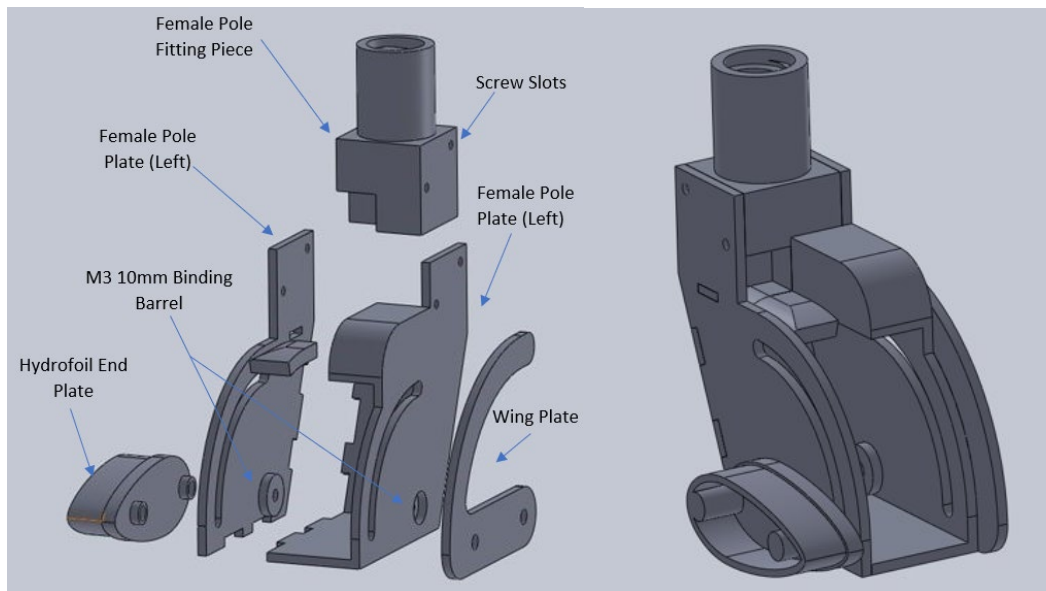
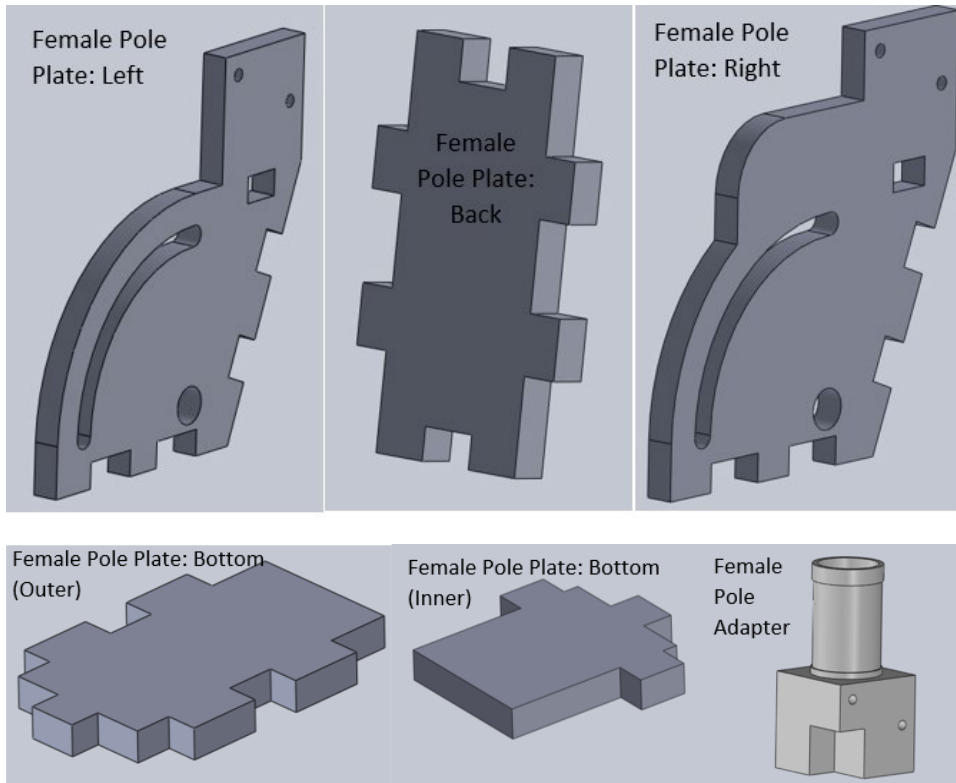


Figure 29: Hydrofoil and bike brake iteration 3

#### 4.4.2.4 Hydrofoil and Bike Brake: Iteration 4

The optimal way to machine this design was to utilize abrasive fluid jet machining, and thus each piece had to be redesigned to be completely flat. For this reason, any existing geometries that would create raised surfaces were removed, and their functions

performed by other design aspects. The female pole fitting is made from six separate pieces that can be assembled using tabs, slots, and four M3 screws. Each of the pieces for the female pole fitting can be found in Figure 30.



*Figure 30: Hydrofoil and bike brake female pole pieces*

One additional clip piece was added to this iteration of the design to secure the bike brake to the female pole fitting. This clip will fit snugly around the cylindrical geometry of the pole fitting and will utilize a circular hose clamp to secure its position. The existing geometry of the bike brake will then be inserted into the M6 hole and secured with a hex nut.

This design still utilizes two ball bearings (11mm OD x 4mm ID x 3mm thick) in the same location as previously mentioned and two 45 mm binding barrels and screws (M4 and M5). The binding barrels were switched from 35mm due to the increased thickness of the wing and female pole fitting pieces.

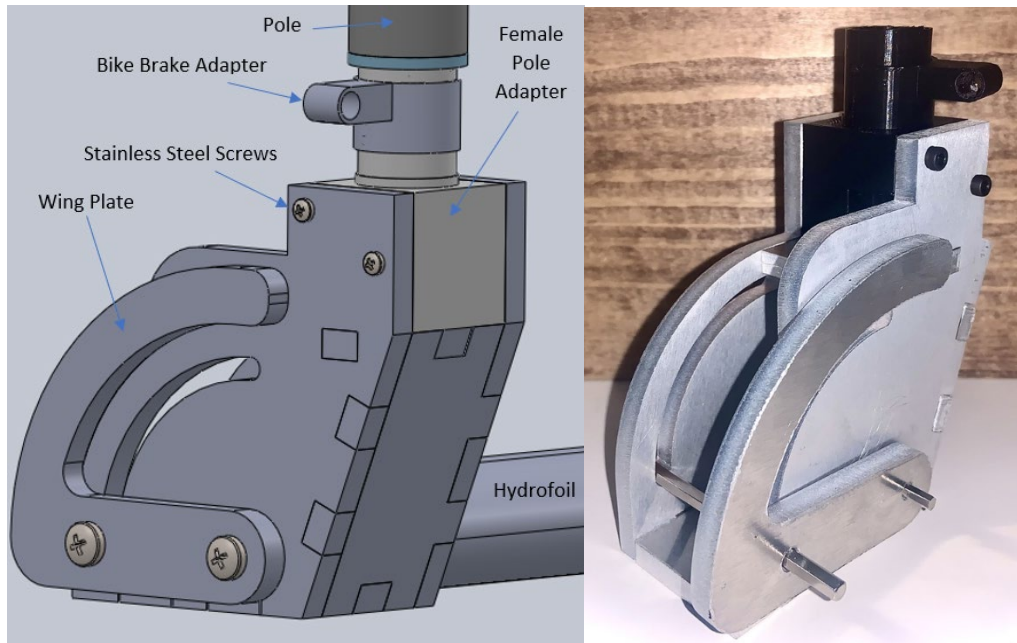


*Figure 31: Hydrofoil and bike brake fourth iteration*

#### 4.4.2.5 Hydrofoil and Bike Brake: Final Iteration

The most significant alteration to this design is that the bike brake will be mounted directly in the center with the brake pads on the outsides of the plates, much like an actual bike brake would sit in relation to a bike wheel. This was done to create a more secure attachment of the brake. Additionally, this reduced the distance the bike brake would need to close in order to properly clamp onto the device as it now more closely replicating the motion it was intended to perform on a bike. To make this possible, the entire design needed to be made thinner in order to fit completely between the bike brake pads. The bike brake connection piece is no longer separate from the female pole fitting and is now a simple through hole underneath the threaded portion of the female pole fitting. The left and right sides of this design are also now identical so the bike brake can clamp on both sides.

Several changes were also made with the intention of reducing the overall weight of the design. First, the side pieces, wing piece, backpiece, and bottom piece were reduced from  $\frac{1}{4}$  in aluminum to  $\frac{1}{8}$  in aluminum, and the top piece was removed altogether (as the bike brake no longer needs a place to rest in the middle of the device). Additionally, weight savings were achieved though reducing the amount of material used by adding cutouts in the back, bottom, and side pieces. These cutouts will also aid in reducing the overall drag of the device when in water, as water will now be able to flow through more easily.

The last changes that were made include small changes to the hardware being used to assemble the device. First, bushings rather than bearings are used in the final design.

The inner diameter of the bushings, and the overall width of this design changed, resulting in the diameter and length of the through bolts changing as well. The stainless steel bolts (see Figure 32) thread into the end cap of the hydrofoil. The final design and manufactured product are shown in Figure 33.

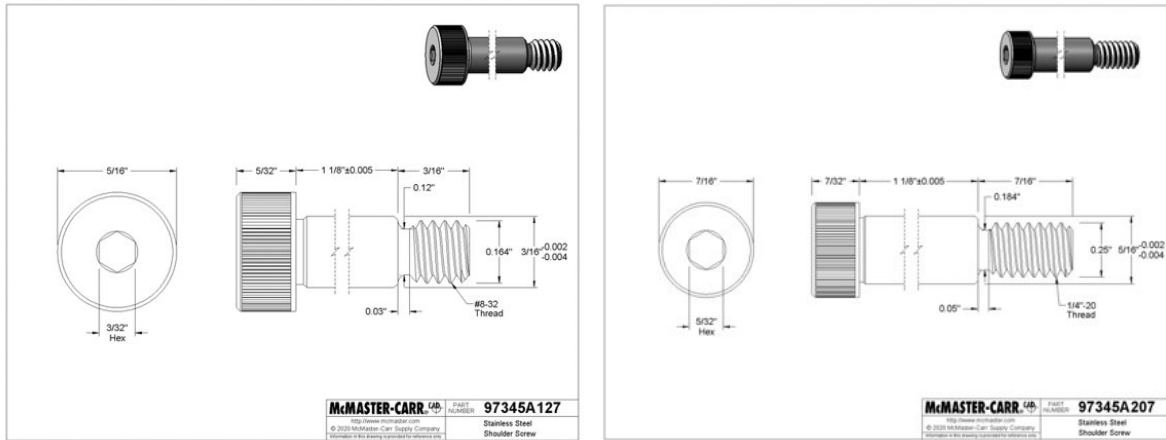


Figure 32: Drawings of bolts for rotating wing piece

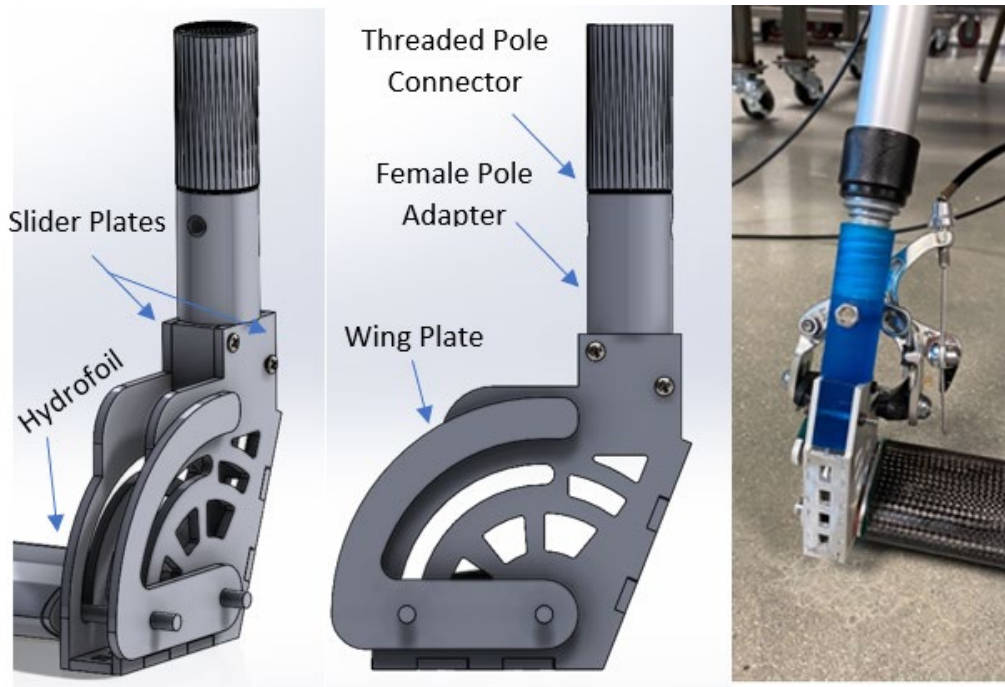


Figure 33: Hydrofoil and bike brake final design (left and middle) and manufactured product (right)

### 4.4.3 Clamp Opener

Attached to the opposing side of the hydrofoil and bike brake system is the dorsal fin clamp opener. Taking inspiration from existing bar clamps, the clamp opener uses the same concepts to open and trigger the clamp. The device consists of an oval steel metal rod that runs through it with two rectangular plates containing a slightly larger oval to allow the rod to pass through (not shown in the Figure 34). One plate is for the trigger release and the other is for moving the shaft causing the clamp to open. When the plate is perpendicular to the direction of the rod, the plate allows the rod to slide. When the plate is not at 90 degrees, the sharp corners on the inside of the plates bite into the steel rod, preventing it from moving. A spring is used between the plate and the device body to keep the plate perpendicular when the clamp trigger is not squeezed. When the squeeze trigger is pulled, it rotates about a point inside the device and contacts the metal plate. This rotation causes the plate to angle, biting into the rod. After the plate bites the rod, the plate can no longer slide. As the trigger is pulled more, the additional rotation causes a reaction force from the plate onto the device causing the device to slide up the rod.

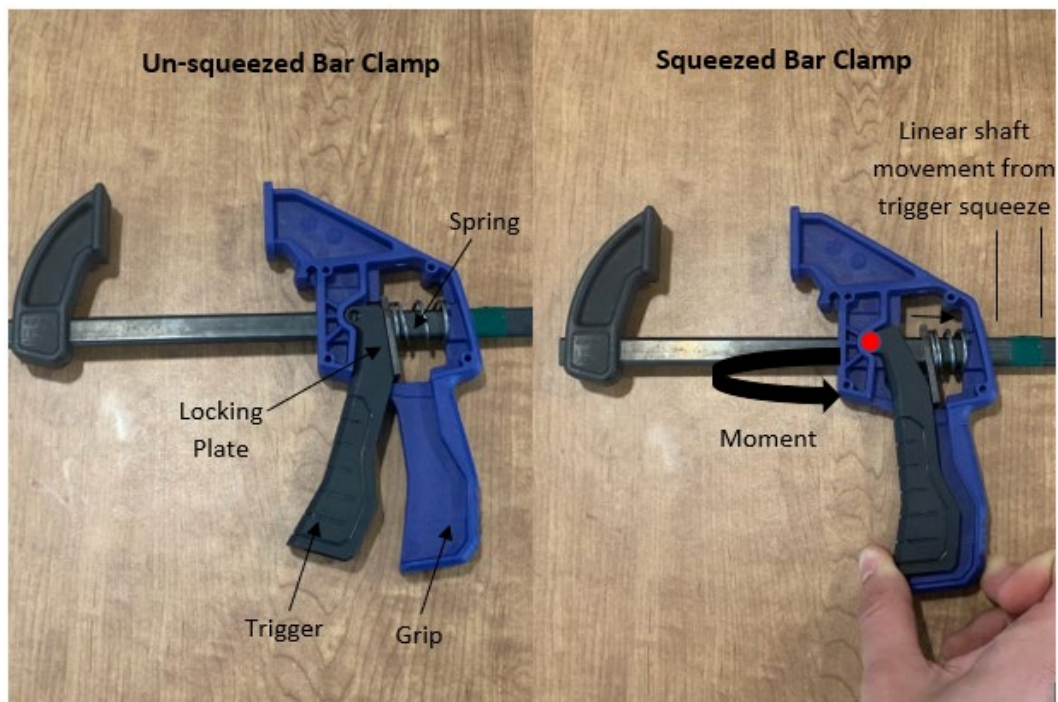
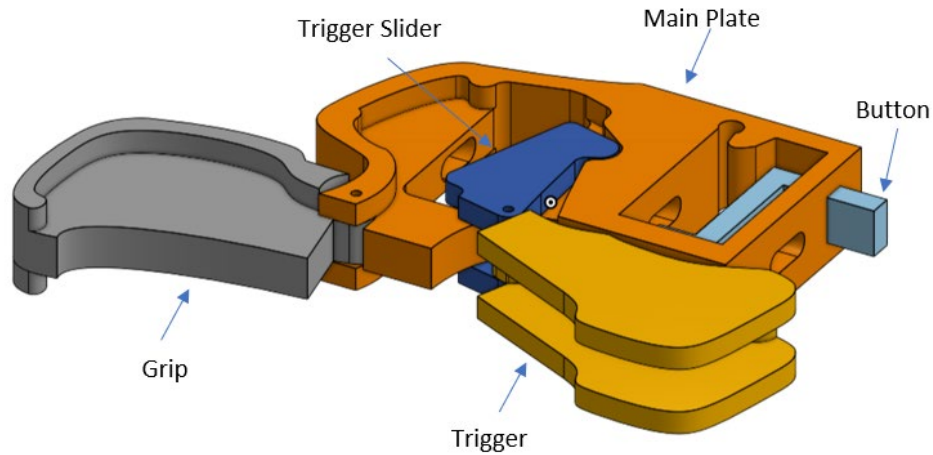


Figure 34: Mechanism of bar clamp

#### 4.4.3.1 Clamp Opener: Iteration 1

The first iteration of the clamp opener follows similar geometric shapes to existing bar clamps, as seen in Figure 35. This iteration did not explicitly implement pins or an extended piece to hold the clamp. This prototype was used to explore the functionality of the trigger pieces. A "button" (light blue) allows for an automatic release of the clamp holder pins that we improved upon in future iterations. When the button contacts the

shark's dorsal fin, it engages a release lever (not shown) which releases the steel rod from its locked position.



*Figure 35: Clamp opener iteration 1*

#### 4.4.3.2 Clamp Opener: Iteration 2

The second iteration followed a similar design to the first, but it included an extra rectangular piece for inserting two fixed pins (in the two holes) to hold the clamp. The steel rod that runs through the entire device has a separate pin attached (not shown in Figure 36). One of the fixed pins holds the clamp from the inside of the torsion spring. The other fixed pin holds the clamp on the inside of the clamp arm. The pin attached to the sliding rod holds the other clamp arm. As the device trigger is pulled, the sliding pin slides away from the fixed pins and spreads the clamp arms apart.

The orange body was modified to a less complex shape. Additionally, the trigger, grip, and grip slider pieces were modified such that they can fold into a flat line along the base of the body to minimize drag from the water. Lastly, the button on this iteration reaches both vertically down and horizontally across as shown in Figure 36. The location of the button relative to the clamp is approximately between the two clamp arms to allow for easier contact with the dorsal fin. 3D printing and fabricating a prototype of this iteration revealed holding the grip and trigger did not allow for enough of a grip to load the trigger. Additionally, the whole system was bulky.

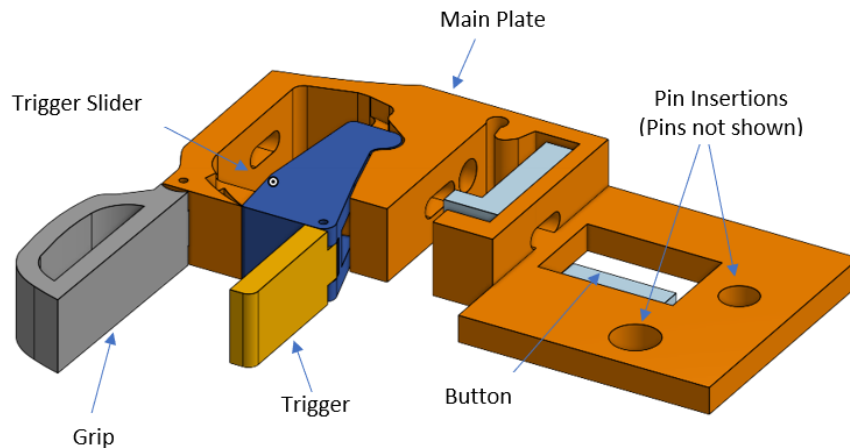


*Figure 36: Clamp opener iteration 2*

#### 4.4.3.3 *Clamp Opener: Iteration 3*

This third iteration's folding ability, aerodynamic shape, orientation of the release button, and trigger loading separates it from existing bar clamps. A hydrofoil type shape produces a low-drag design. In order to achieve a hydrofoil shape, the protruding hand grips from a standard bar clamp could not be used due to their high drag. Foldable grips which only open during the setting of the tag, and are stored away during tagging, eliminates the need for cables running up to pole to operate the device. This reduces the device complexity and aids in the versatility and adaptability of the overall device system.

Although the third design iteration was a large improvement from past iterations, two small design oversights produced fatal flaws that affected the functionality of the device. This was the first iteration that included an enclosed internal locking mechanism and a two-piece clamshell shape (top and bottom plates). With this design, the clamp slider piece shown in Figure 37 was initially only once piece. When the top and bottom plate were screwed together, and the trigger slider was inserted through the bottom opening, it clamped the pieces together even when the screws were removed. This meant the device could not be taken apart as it was intended too. An easy fix was to split the trigger slider into two halves, but not before the original one-piece part had to be snapped off from the device in order to separate the plates. The second major issue with the design was inserting the shaft, springs, and locking plates (which must sit in the middle of the cross section) exactly where the top and bottom parts meet. Not only did this require the user to balance the shaft in the open slot when assembling the device, but it also bisected the hole where the spring applies a force to the release plate. This made it nearly impossible to keep the spring in place when attaching the top and bottom pieces together.

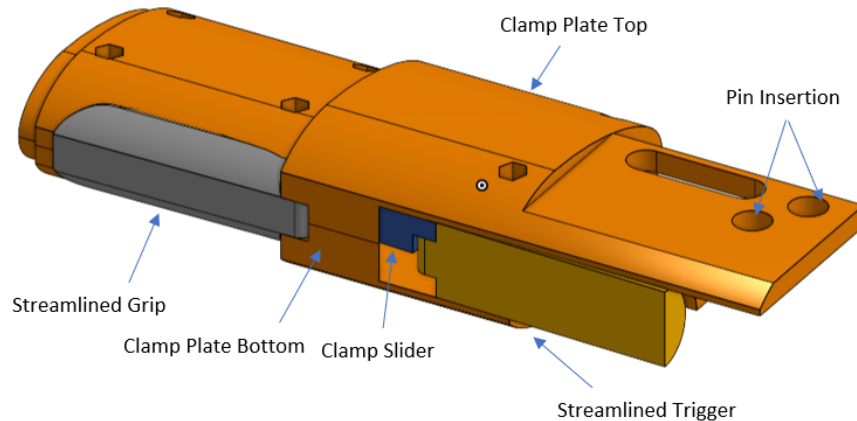


*Figure 37: Clamp opener iteration 3*

#### 4.4.3.4 Clamp Opener: Final Iteration

The final iteration of the clamp opener follows closely to iteration three except that it includes all the pins, a new release trigger, and an additional support on the bottom of the body. To allow for easier assembly and machining of these complex components, the body was separated into three separate plates that can be screwed together. The top and bottom plates effectively mirror each other, and the middle piece maintains the support structure of the device. The top and bottom plates allow for extra support for the pins and reduces the effects of stress and deformations on the material. The pins (light blue) are press fit into the two holes of the two outer body plates.

In the previous two iterations of this design, the release trigger is reoriented in the opposite direction so that the trigger would protrude into the space between the opened orientation of the clamp arms. When the operator maneuvers the opened clamp around the dorsal fin, the dorsal fin contacts the release trigger, causing the clamp to slam shut, releasing the clamp from the device and securing the clamp onto the dorsal fin. The biggest benefit of this system includes mitigating any potential accident from the operator releasing the clamp early before it the clamp was in the correct location. The self-setting trigger release, located towards the front of the clamp arm opening, ensures the clamp is only released when the dorsal fin is fully seated inside the clamp.

In the previous iteration, the pins were oriented such that one pin held the clamp arm approximately 6 cm from the torsion spring. Bending stress calculations for the magnesium link, revealed the stress on the magnesium link when a force is applied (just past its location on the clamp arm) is high enough to cause the magnesium link to fracture. The orientation of the pins was changed to eliminate this possibility. As seen in Figure 38

below, the pins are oriented so that the stationary pin holds onto the clamp adjacent to the torsion spring, and the mobile pin holds the clamp about 6 cm away from the torsion spring using an offset arm. With this design, the clamp can be oriented so that the location of the magnesium link on one of the clamp arms is past the pin attachment point.

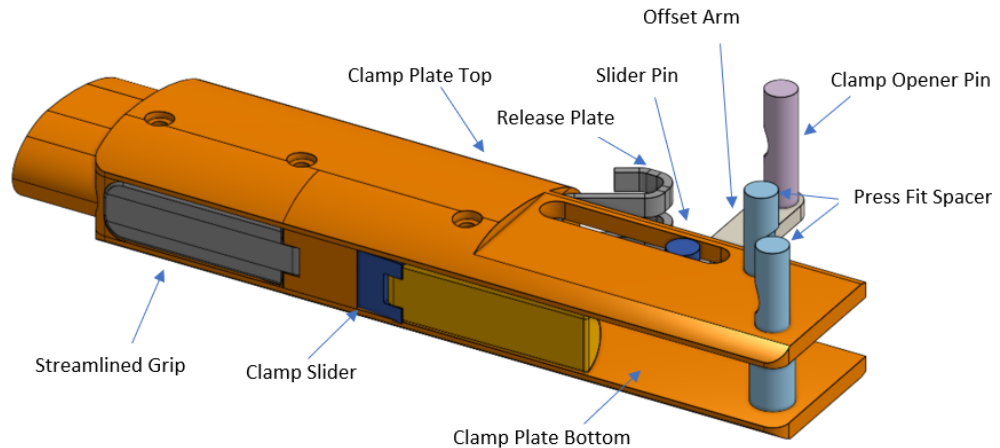


*Figure 38: Clamp opener final iteration*

Part of the new release mechanism also includes a curved shape release trigger (gray) that allows for more surface area in contact with the dorsal fin. The trigger and grip are modified minimally for easier manufacturability. This version includes a more adaptable piece on the left side of Figure 38 for connecting this directly into the open end of the hydrofoil. Lastly, the PLA end which goes into the hydrofoil includes an indent where a TPU O-ring can slide in to allow for a water-tight seal in the hydrofoil. The manufactured version of the clamp opener iteration is shown in Figure 39.



*Figure 39: Manufactured clamp opener with offset arm*

After initial testing of the offset arm clamp opener shaft, the design was successful when the clamp was inserted, and the pin was used to open the clamp. When the release plate was actuated with nothing in between the clamp arms, the device sprung closed, and the clamp released as intended. However, once an object with similar thickness of a shark dorsal fin activated the release, the offset arm meant to reduce the force of opening the clamp, wedged itself against the object (Figure 40). This stopped the shaft from continuing to slide and release all of its tension, meaning the clamp still had residual force against the opening pin and would not release itself from the device. An opener shaft was made without the offset arm to mitigate this effect; in this version, the clamp opener pin now resides in the slot of the bottom plate (Figure 41).



*Figure 40: Offset arm wedged against object, preventing clamp from closing completely*



*Figure 41: Final clamp opener version after testing*

Overall, the final pole design incorporates two sub-assemblies which connect on either side of a hydrofoil crossbar and attach to a standard painting pole of adjustable lengths. This design aims to satisfy the Dr. Skomal's needs for a versatile pole to safely tag great whites. The final manufactured assembly is seen in Figure 42.



*Figure 42: Final manufactured assembly*

#### 4.4.4 Manufacturing of the Final Design

The pole system is manufactured out of four materials: resin, PLA polymer, 5052 aluminum, and 316 stainless steel. The large forces required to open the clamp exceeded the strength of the PLA 3D printed prototype pieces and required stronger materials to withstand the forces. Since the parts are subjected to consistent exposure to saltwater, the metals have high corrosion resistance. Stainless steels such as 18/8 and 304 are more common and less expensive but lack the corrosion resistance needed for this application. The marine grade stainless steel alloy is 316 stainless steel which resists oxidation from saltwater. For a similar reason, 5052 aluminum alloy was chosen over 6061 aluminum since 5052 is more corrosion resistant and meant for saltwater applications. The clamp opener shaft, offset arm (Figure 44, right), release, and pins are made of 316 stainless steel (Figure 43). The top and bottom clamp opener body pieces, grip (Figure 44, left), trigger, fixed pins, and pole end hydrofoil rotation pieces are 5052 aluminum. Appendix E shows the breakdown of parts and their respective materials. Since the top and bottom plates are machined aluminum and support the forces created by the clamp, the enclosed parts of the design were 3D printed. 3D printing the main body piece of the clamp allowed for use of the 3D infill settings which use geometric patterns to add structural support, decrease printing times, and reduce mass instead of being solid. Additionally, the complicated internal geometry required for the opener shaft would be too difficult to CNC machine out of a block of metal.

3D CAD files were transformed into files the CNC lathe and mill could understand. Using a program called ESPRIT, parts were made through subtractive manufacturing, the process used by the CNC machines to turn a raw block of stock material into the intended design. CNC machining requires significant setup time to fixture the raw stock in the machine properly and to set workpiece and tool offsets. For each operation, the correct tools must be loaded into the machine, the tool offsets must be set, the part be securely clamped, and the workpiece offset must be set in the same location as the corresponding ESPRIT operation file.



*Figure 43: Slide shaft finished sub-assembly*



*Figure 44: Grip piece (left) and offset arm (right)*

The most time-consuming part to machine was the trigger piece which required four operations and was extremely difficult to fixture securely into the vice grips of the machine since there was very little flat surface to clamp on. The first operation did not leave enough surface to securely clamp on to and run the second operation without the piece flying out of the machine. After trial and error, the ESPRIT file was modified to run operation two first. The flat surface produced by the operation allowed for supergluing the part onto a sacrificial piece of aluminum before running the original first operation to make the rounded surface. Figure 45 (left) shows the initial first operation which produced the rounded surface. The extra material was supposed to be removed in operation two, but the round surface would not stay in the vice. In Figure 45 (middle), the two pieces in the back of the image are the second attempt at machine the trigger, and the flat surface on top is what we superglued to another piece of metal so we could remove the remaining material below. Figure 45 (right) shows the machined trigger piece after the final operation.



*Figure 45: Initial trigger operation one (left), actual first trigger operation (middle), final trigger piece (right)*

The hydrofoil and bike brake portion of the design are manufactured using abrasive fluid jet cutting as well as 3D printed resin polymer. The locking and release plates shown in Figure 46 were cut with AFJ technology and are made from 0.100-inch 316 stainless steel. The flat pole end fitting pieces including the wing piece were laser cut from SendCutSend out of  $\frac{1}{8}$  in 5052 aluminum. These pieces are assembled and secured to one another using tack welding. The threaded piece of the female pole fitting is 3D printed using resin polymer and attaches to the rest of the female pole fitting pieces using M3 screws. The bike brake screws through a hole in the female pole fitting using the existing bolt meant to fixture the brake to a bike. CAD drawings for all previous iterations of the clamp opener are in Appendix F, and the CAD drawings for the final design are in Appendix G.

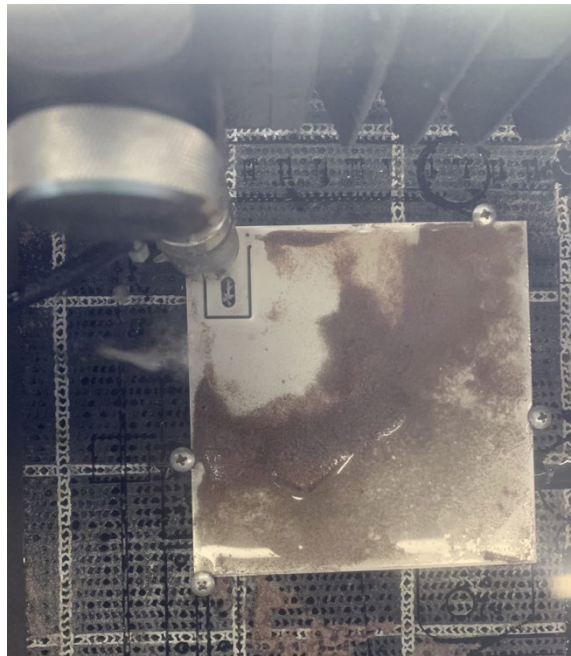


*Figure 46: Abrasive fluid jet cutting locking plate*

## 5 Design Verification

### 5.1 Deflection Calculations for Pole

To determine the necessary material and geometry of the pole to minimize deflection, as well as the forces acting on the hands of the user, the pole was modeled as a cantilever beam (Figure 47-50). In this model, the pole was a 14-foot supported cantilever beam with the two hands of the user three feet apart at one end and the tag at the other end connected to a 2-foot bar perpendicular to the pole. The rear hand acted as a fixed constraint generating a vertical reaction force and a reaction moment, and the front hand acted as a simple support generating a vertical reaction force perpendicular to the pole. This model had two configurations. The first part is in the air, where the weight of the tag (5 lb) and the pole (as determined by the density and geometry of the pole) acted as the supplied forces perpendicular to the pole (parallel to the direction of gravity). The second model observed forces while the system is in the water where the weight of the tag was assumed negligible because it will be neutrally buoyant, so the only force in the water would be the drag force on the hydrofoil, tag, and tag attachment mechanism. The model in air had the pole perpendicular to the user to find the maximum reaction force on the hands. For the model of the tag within the water, we used a worst-case scenario drag coefficient of 1, resulting in a 7.5 lb drag force. The hydrofoil encounters a 1.4 lb drag force, so the total system encounters approximately 9 lbs of drag. In water, the pole was assumed to be at 45 degrees to the water creating 7.6 lb perpendicular and parallel components of force.

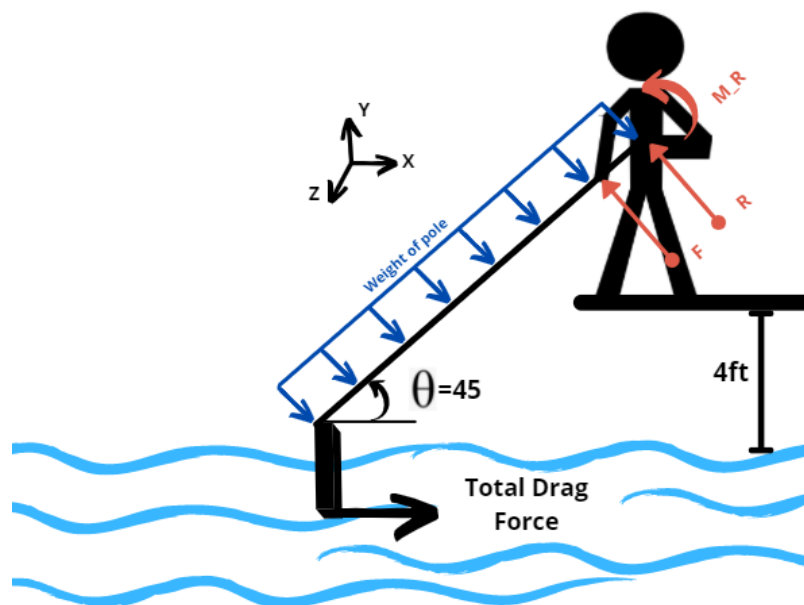


Figure 47: Free body diagram of pole in water. In blue: known forces, in red: unknown reaction forces and moment

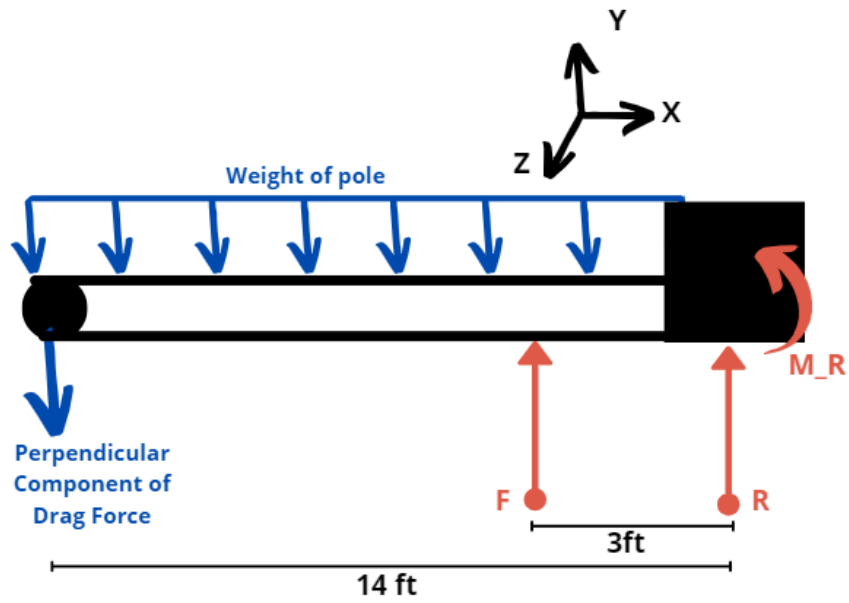


Figure 48: Simplified model of pole as a deflected beam in water. In blue: known forces, in red: unknown reaction forces and moment

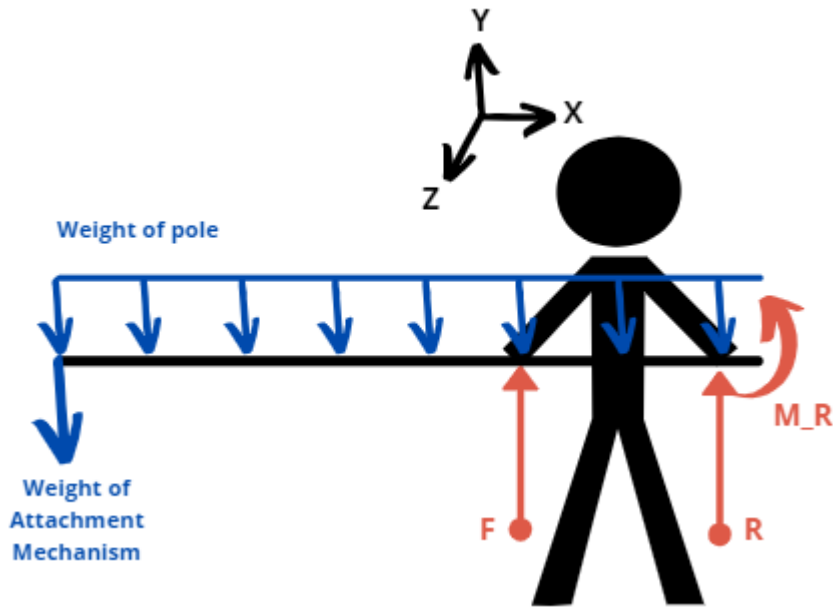


Figure 49: Free body diagram of pole in air. In blue: known forces, in red: unknown reaction forces and moment

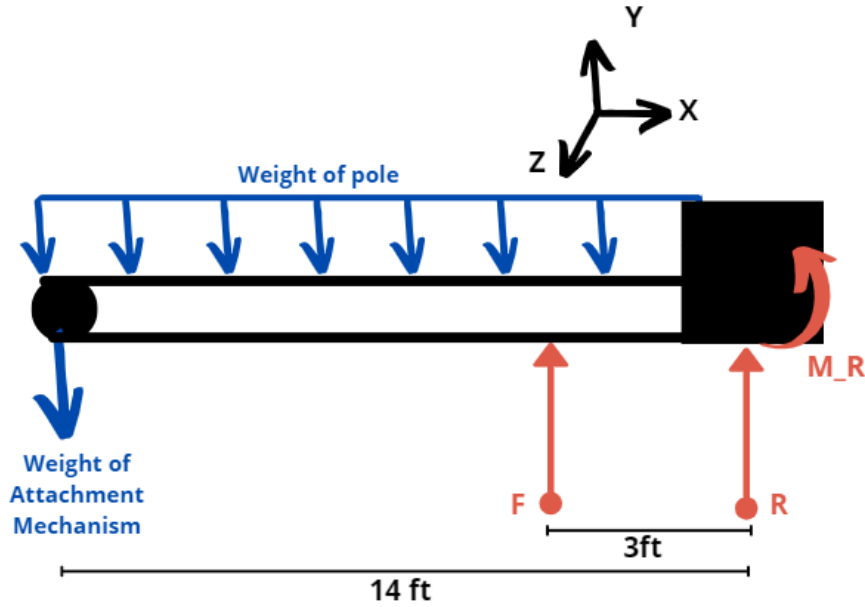


Figure 50: Simplified model of pole as a deflected beam in air. In blue: known forces, in red: unknown reaction forces and moment

Dr. Skomal decided he wanted to continue to tag with an existing telescopic painting pole. A Mathcad file (Appendix H) was used to solve for deflection and resultant forces using singularity functions. The results from these calculations are in Tables 2-3 below. The new deflection results for this pole fits into our defined constraint of a deflection less than 0.5 in.

Table 2: Material properties and weight of Dr. Skomal's pole.

Material Properties (Aluminum Pole)	Modulus of Elasticity	Weight	Mass Density
$r=0.93$ in $t=0.04$ in	12.3282 Mpsi	4.02 lbs	0.0092 lb/in <sup>3</sup>

Table 3: Resultant forces and deflection of Dr. Skomal's pole under our assumed loads.

<i>Results</i>	<i>In Air</i>	<i>In water</i>
<i>F on Front Hand (lb)</i>	14.567	19.977
<i>F on Rear Hand (lb)</i>	-5.547	-8.292
<i>M on Rear Hand (lb-in)</i>	427.31	594.326
<i>Deflection (in)</i>	0.001721	0.003261

The maximum safe load on the human carpal bones in compression is 46 lbs [42]. At the 46 lb limit, the cartilage between the carpal bones is in maximum compression; beyond the 46 lb limit, there is increased risk of fatigue injury. Using the “worst case scenario” of the tag weighing 5 lbs does not lead to significant concern for the use of this pole because the resultant forces on the hands are well below 46 lbs. The other “worst case” of the tag release device having a drag coefficient of 1 (drag force of 9 lbs) when combined with the hydrofoil also does not lead to forces on the hands that are even half of the limit we set for safety at 19.977 and 8.292 lbs.

## 5.2 Force Gauge Measurements

### 5.2.1 Clamp Opening Force

To measure the force it takes to open the clamp, we set up the testing apparatus shown in Figure 51. One arm of the clamp was fixed to the counter, and a force gauge was fixed to the other arm at a known distance from the 90-degree bend in the arm at the torsion spring; these distances were 4 cm, 6 cm, and 20 cm. The force gauge was then pulled straight up until the free arm was at a specified distance away from its initial position. The peak force was recorded at this distance for three samples at each deflection. At 4 cm and 6 cm away four different deflections were measured and at 20 cm away five different deflections were measured.

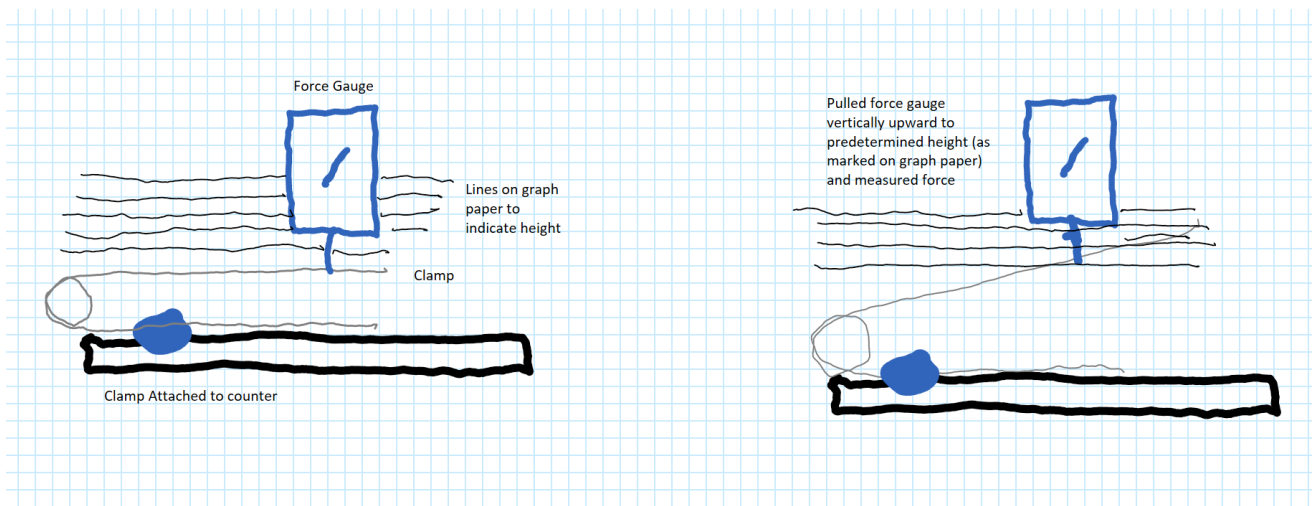


Figure 51: Top: Set up for the clamp opening force test. Bottom: Graphic for a clearer visual of the set up for the clamp opening force test

The distances were then related to the angle the clamp was opened from its initial position using the following equation:

$$\theta = \sin^{-1}\left(\frac{\text{height opened}}{\text{distance from 90}}\right)$$

The force it took to open the clamp at each position was then plotted versus the angle it was opened in radians (Figure 52). The plots for both 6 cm and 20 cm away show a linear relationship between the angle the clamp is opened and the force it takes to open it, both with an R-squared value of almost one. The 4 cm away plot has a significantly lower R-squared value, which may be because it took considerable force to open the clamp from that position by hand, and readings may not have been accurate.



Figure 52: Opening force over angle open (in radians) for the gauge at Top: 4 cm from 90, Middle: 6 cm from 90, Bottom: 20 cm from 90

Section 1.3.4 of Appendix D includes torsion spring calculations of a similar design as the clamp. The forces calculated in those equations for a torsion spring with a 20 cm length would be 500 N at 3.14 radians and 250 N at 1.57 radians. Extrapolating the linear regression shown in the bottom of Figure 52 has the force at 3.14 radians as 360 N and at

1.57 radians to be 190 N. The differences in these values can be explained in part by the differences in the assumed geometry and material used in the calculations in Section 1.3.4 of Appendix D and the geometry and material of the clamp. The difference in values can also be because while the data showed a linear pattern up to 0.25 radians it may not be accurate to assume the force-angle curve continues to be linear at 1.57 radians.

### 5.3 Sensitivity and Angles of Release Mechanism

In order to evaluate the sensitivity of the release mechanism on the clamp holder, we performed tests to determine how difficult it is to trigger the clamp release. Since we could not test on an actual shark, it was difficult to obtain results that would accurately describe the required force to tap the device against the fin. This was mainly because the foam shark fin we used could not be held sturdily enough to engage the release trigger. As a result, we had to test the trigger by moving the fin and hitting or “flicking” it against the release. These tests demonstrated that the trigger releases the clamp with a forceful flick, lending evidence that the force required could be easily produced by moving the pole system to hit the trigger against the fin as intended.

Various angles of approach of the shark fin to engage the release were also tested to ensure that the fin would not become stuck on the release lever. To complete these tests, the foam shark fin was used to simulate the attachment of Dr. Skomal’s clamp as if the shark were approaching the clamp from different angles. When the clamp is at its fully opened position and loaded into the clamp opener, the angle between the two arms is approximately 0.641 radians making the ends of the arms 14.5 cm apart. Our tests demonstrated that the angle of approach did not significantly impact the function of the device, as long as the front of the dorsal fin entered the clamp on the left side of the release trigger. We performed these same tests in a pool to simulate a more accurate tagging environment. Figure 53 shows the two test setups.

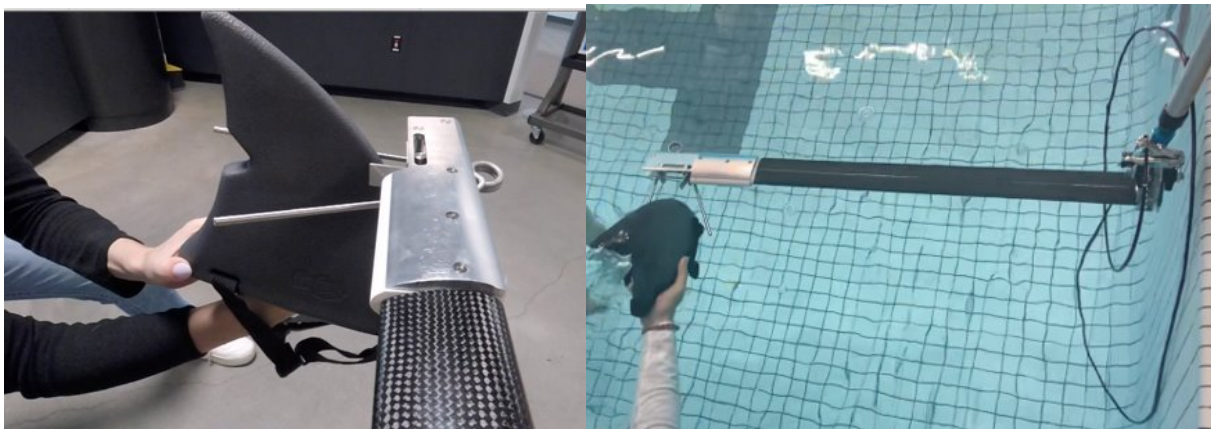


*Figure 53: Release mechanism testing for sensitivity and angles (left) and in pool (right)*

## 5.4 Buoyancy and Water-tight Testing

Buoyancy was an important factor in the functionality of our device in water. As a hydrofoil is supposed to be positively buoyant due to its hollowness, we wanted to assess the buoyancy of the hydrofoil attached to the clamp holder. We performed simple buoyancy tests which consisted of placing the hydrofoil attached to its end piece (connected to the clamp holder) in a large bucket of water. We evaluated the buoyancy effect of the clamp opener on the end of the hydrofoil compared to the hydrofoil by itself.

The effectiveness of the hydrofoil depends on the ability of the hydrofoil end caps to prevent water from seeping into the foil. To test this, we placed the PLA end caps from our original prototype on each end of the hydrofoil and put the entire apparatus into a tote of water with a dumbbell holding it down (Figure 54). Within four minutes, the hydrofoil filled with water. Since PLA is a porous plastic, we knew that this might be a concern, so we were not planning on using PLA as the end cap material. But this initial test gave us a baseline and proof that a better material and a sealant was necessary to seal the hydrofoil.



*Figure 54: Hydrofoil watertight test with PLA endcaps*

We later performed a test of the whole system in a pool (see Section 5.6). During this test a small amount of water did enter the hydrofoil with the final endcaps in place. However, the final O-rings were not in place for this test. The O-rings will prevent water from entering the hydrofoil.

## 5.5 Stress Analysis

### 5.5.1 Compressive Stress Calculations

Since the clamp will be mounted around the clamp opener at about 6 cm away from the 90-degree angle of the torsion spring, we used the linear regression generated from the clamp opening force test to estimate the compressive stress on the end plate of the clamp

opener (see Section 5.2.1 for testing setup and results). We estimated that the ends of the arms of the clamp would need to be about 17.78 cm apart during tagging; this corresponds to an open angle of approximately 0.688 radians. Plugging that value into the linear regression equation shown in Figure 52, we found a compressive force of 197.966 N. Figure 55 below shows the free body diagram of the plate with the force the clamp would apply on it.

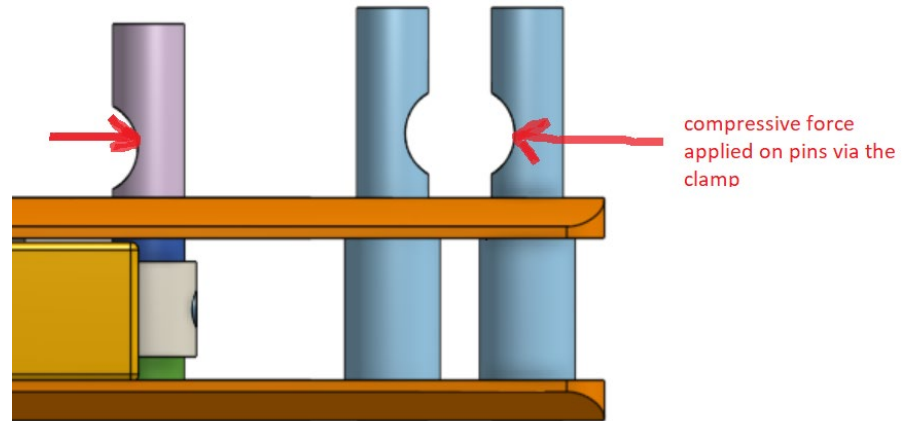


Figure 55: Free body diagram of the clamp opener with compressive forces applied by the clamp.

To find the compressive stress on the plate we used the following equation:

$$\sigma = \frac{F}{A} = \frac{F}{\text{bolt diameter} * \text{plate thickness}}$$

This resulted in a compressive stress of 3.14 MPa, well below the yield stress for 5052 aluminum, resulting in a safety factor of approximately 61.

### 5.5.2 ANSYS Software Analysis of Stresses

We performed another assessment of stress deformation on the clamp opener through ANSYS software analysis. A fixed support was placed at the end of the clamp opener where the hydrofoil attaches to allow for a deformation analysis to occur. We placed a 198 N force (found from the clamp opener force gauge test) horizontally on the fixed pin in line with the slot and another 198 N force on the smaller pin on the sliding bar to represent the clamp arms around the pins. These forces both faced inward towards each other to mimic the tendency of the torsion spring arms to close in towards each other. Figure 56 shows the results of the total deformation analysis. The red indicates where maximum deformation occurs, while the dark blue indicates the minimum. These results gave us an understanding of the deformation that could occur on the clamp opener when the user is loading the clamp to its open position and when the clamp is around the pins

until it closes around the dorsal fin. While the deformation appears to be very large, the software scales the view to  $1.2 \times 10^3$  times the true scale to amplify the deformation. A convergence analysis was performed to ensure that the deformation result converged, and the mesh of the model was small enough to capture the deformation of the material (Figure 57). When assessing the actual maximum deformation value, the result is approximately 0.082 mm (0.0032 in), as seen in the left side of the image.

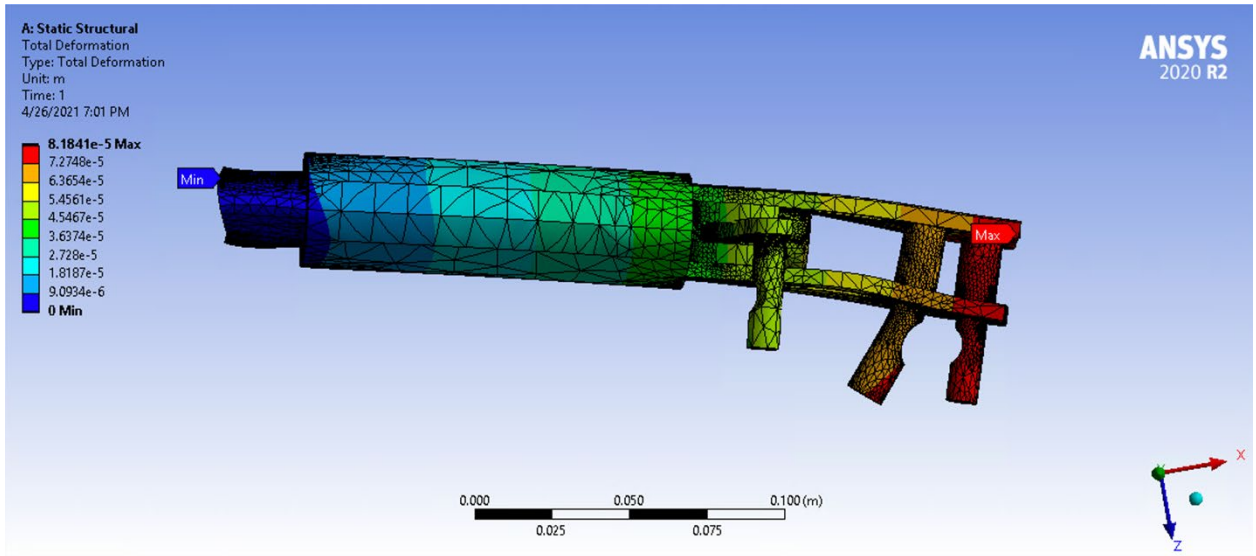


Figure 56: Results of total deformation ANSYS analysis

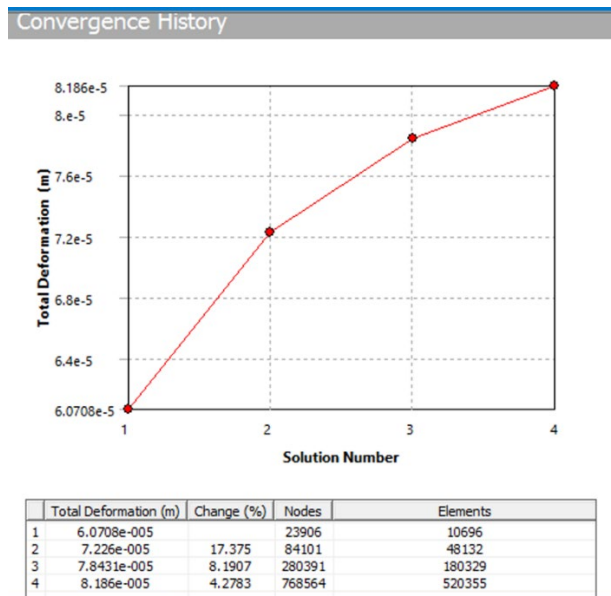
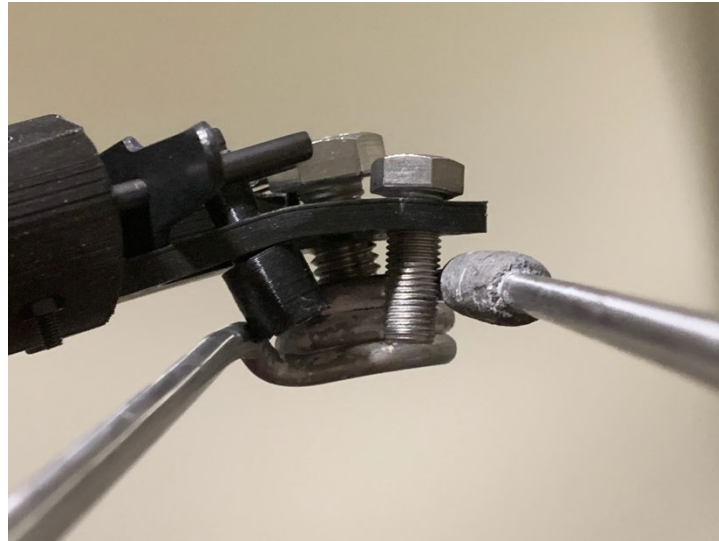


Figure 57: Results of ANSYS convergence analysis

While the scaling of the deformation from the software is exaggerated from that of 316 stainless steel, 5052 aluminum, and PLA materials within the assembly, we noticed a similar deformation when prototyping our clamp opener fully in standard PLA 3D printed plastic. Figure 58 shows the PLA printed outer body with large screws used as the pins and a metal sliding bar. As mentioned previously, this prototyping with PLA encouraged us to choose stronger materials for the final design.



*Figure 58: Testing of clamp opener deformation in PLA plastic material*

Based on an ANSYS analysis of von Mises stress using the same materials and 198 N opposing forces on both pins as above (Figure 58), we calculated the factor of safety for 316 stainless steel. The calculations are shown below, using a yield strength of 316 stainless steel of 205 MPa:

$YS = \text{yield strength of 316SS}$

$\sigma_e = \text{equivalent von Mises stress}$

$$FOS = \frac{YS}{\sigma_e} = \frac{205 * 10^6 Pa}{2.1988 * 10^7 Pa} = 9.32$$

This high factor of safety indicates that the equivalent stress from the 198 N pin forces using the materials we chose is insignificant. A safety factor of more than nine demonstrates that the stainless still can withstand the stresses encountered from the clamp opening force without coming close to its yield strength.

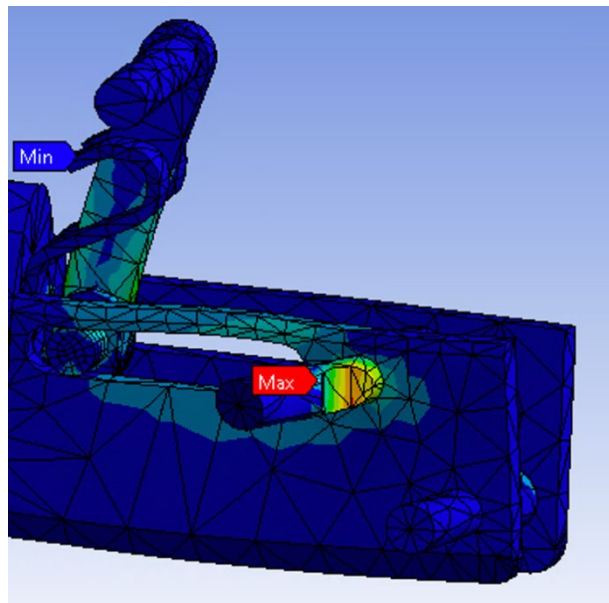
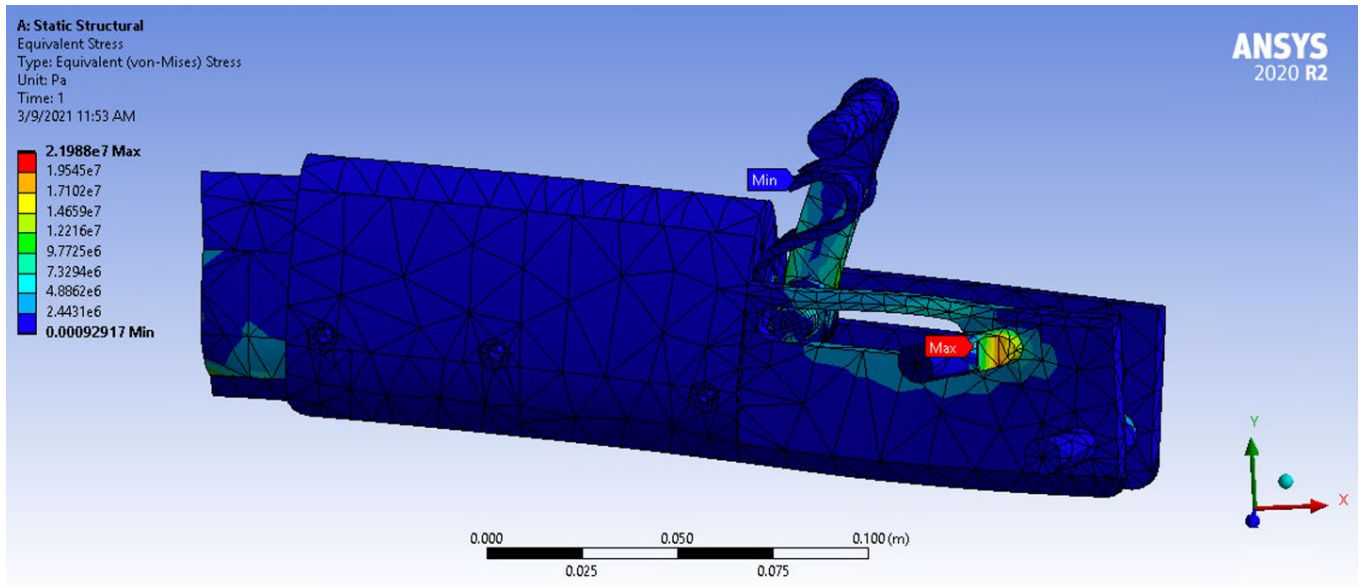


Figure 59: Results of von Mises stress analysis in ANSYS (top); stresses on pin (bottom)

## 5.6 Full System Tests

To test the entire assembled system, we brought the device to a large indoor pool for qualitative results. This test was used to evaluate the performance of the full assembly in water. We qualitatively determined how the system felt, whether the hydrofoil functioned properly, and whether the clamp detached from the clamp opener while submerged.



*Figure 60: Image of pool testing set up where we held the device stationary in the water*

First, we assembled the full device and held it in the water. There was not any noticeable strain in the hands to hold the pole up; however, the hands did have to resist a torque around the pole to hold it in the right orientation (hydrofoil parallel to the surface of the water). This effect was mitigated by walking with the device along the side of the pool to stimulate flowing water. While standing still with the hydrofoil in the water, the hydrofoil and clamp opener tended to twist in the user's hands to be perpendicular to the surface of the water. This effect was also reduced by walking with the device. To evaluate the clamp release mechanism while underwater, we performed the same test described in Section 5.3 with the only difference being that the whole assembly was used and that it was submerged. The clamp released onto the foam dorsal fin without any difficulties while underwater.



*Figure 61: Image of pool testing where we moved the whole system through the water by walking along the pool deck*

After removing the device from the water, we discovered that water had seeped inside the hydrofoil. Since the pool trial was for testing purposes, we had not yet epoxied the endcap to the end of the hydrofoil; however, even after being tested in the water for an hour, the water collection within the foil was minimal. Moreover, the tagging pole is only intended for short-term use, under an hour at a time, so once the endcaps are tightly sealed with epoxy, water seeping will be of minimal concern. Overall, the whole assembly

functioned better while we mimicked flowing water; furthermore, there was less physical strain required on the user's part, and the hydrofoil self-leveled

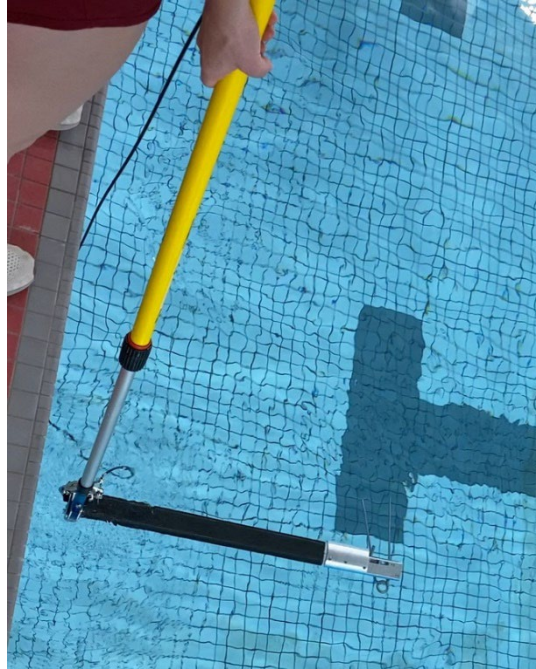


*Figure 62: Image from pool testing with the clamp loaded into the clamp opener, taken before testing the release mechanism in water*

## 6 Final Design and Validation

The final design of the shark tagging apparatus can be seen in Figure 63. This design contains the bike brake system on the right side of the hydrofoil and the clamp opener on the left side of the hydrofoil. The top of the bike brake system (bike brake not shown) includes threading which any sized standard painting pole can screw into. This system allows for adaptable sizing depending on the boat and pulpit size and based on the user's tagging situation. This final design satisfies the primary goal of creating a versatile great white shark tagging device that works from various distances while still ensuring the safety of both the user and the shark.

To achieve this result, our first task of this project included background research and literature reviews on any relevant information to our client's need. We gained insight from previous marine animal tagging poles which inspired us in certain aspects of our design. We also utilized design matrices throughout the early design phases of the project, allowing for all group members to contribute numerous individual and complementary ideas. Throughout each step of new design iterations and early alternative designs, we performed safety and functional calculations to aid in our decisions moving forward. We also created as many physical prototypes as time allowed with personal 3D printers to bring our ideation into realization and gain a better understanding of the improvements we could make. Testing and software analyses also contributed to progress of the final design as they presented potential concerns that we might not have thought about until seeing components of the design in action. Overall, we employed a combination of research, design matrices, calculations, prototyping, and testing in an iterative design cycle which culminated in our final redesigned shark tagging device.

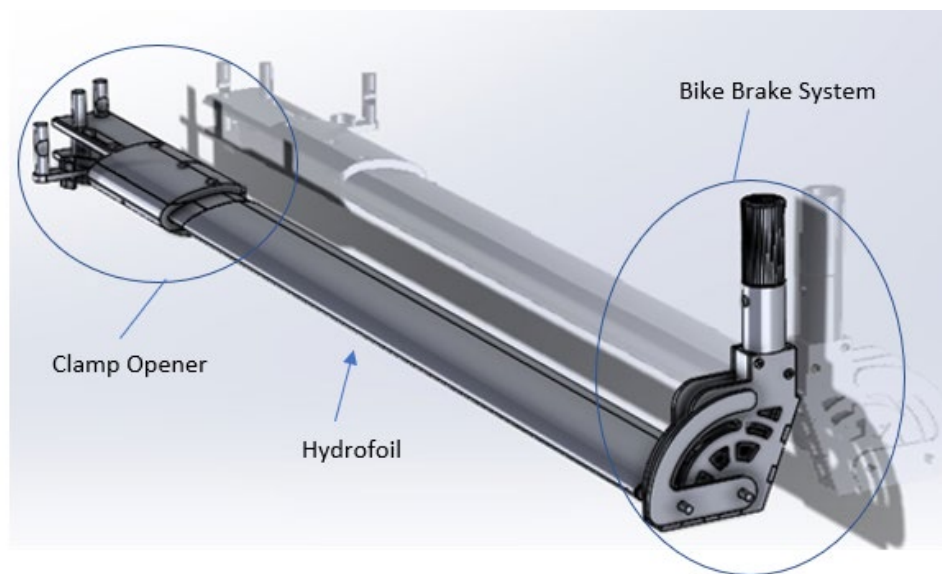


*Figure 63: Final tagging apparatus design*

The following sections of this chapter describe how our device broadly impacts various sectors including economics, environment, society, politics, ethics, health and safety, manufacturability, and sustainability.

## **6.1 Economics**

Being able to tag and track sharks to better understand their habits can lead to keeping both sharks and humans safer. Sharks are necessary to the marine ecosystem as discussed in the background section, so it is important to keep sharks alive. Some people hunt sharks for the purpose of taking their dorsal fins and teeth to make a profit. The practice of tagging sharks to protect them from these hunters can impact the economy in that it decreases the market for the unethical selling of shark fins and teeth. However, the positive effect on the economy and society by keeping sharks alive outweighs this decreased market.

Sharks contribute to the economy in many warmer areas in both tourism and shark-diving excursions. Our tagging system indirectly impacts the economy in that it allows for sharks to be researched and tracked for both shark safety (which maintains shark tourism) and human safety (which allows for more beachgoers to feel safe enough to go to beaches in high shark risk areas).

## **6.2 Environmental Impact**

As this project deals primarily with tagging in the ocean, the environmental impacts on marine ecosystem must be considered. The primary concern is to reduce the potential for metal or plastic components of our clamp design to pollute the ocean as a result of the tagging process. The current clamp uses a magnesium link as its detachment mechanism from the shark fin, which erodes in the saltwater, forcing the entire metal clamp to fall off and sink into the ocean. Adding a buoyancy feature to the clamp system allows the clamp to be retrievable after the magnesium sleeve erodes in the saltwater. In turn, Dr. Skomal and other researchers can retrieve the parts and reuse them for future tagging efforts, while at the same time this prevents the clamp material from sinking to the bottom of the ocean and harming the marine environment. Our pole design contains a hydrofoil component which adds buoyancy to the overall system, allowing for the pole to be retrieved quickly in the case that the user accidentally drops it in the water. This also eliminates any environmental impact of the pole components polluting the ocean. When choosing materials for the pole design, we considered how they would interact in a marine environment to make sure that they were safe to use for our purpose.

## **6.3 Societal Influence**

Our project will have an indirect impact on ordinary people in their daily lives, as the application of our pole design to tag sharks for the purpose of learning about their predatory habits and migration patterns can inform societal decisions. The pole system we designed may allow for more researchers to tag sharks in areas other than the Cape Cod

region, providing safety to more beaches in the U.S. and even other countries. The knowledge gained from the CATS Cam data can alert beaches of frequent shark sightings through the Sharktivity app (mentioned in the introduction) or other sources. This awareness affects how people behave on beaches and influences when or where to take extra safety precautions. The pole product itself will likely not have any marketing influence on ordinary people, since it is geared toward experienced marine researchers.

#### **6.4 Political Ramifications**

One potential political influence of this project is that it allows for more marine researchers across the globe to tag sharks safely, while still following ocean standards. Chumming (baiting the shark with raw fish and blood near the side of the boat) is a practice that has been commonly used to tag sharks in the past, but it has been banned in certain U.S. states and in other countries as well, forcing researchers to find new methods of tagging sharks from their boats. Since our pole design is intended to be used at a distance from the shark being tagged, it eliminates the practice of chumming, giving shark researchers another viable option to tag sharks safely.

This could influence the behavior of international marine scientists in the global market for marine animal tagging, especially in countries such as Australia and South Africa, where the waters are infested with sharks, and previous shark tagging systems have been tested. CATS is also a company with founders based in Australia and Germany, therefore leading to a global market for our pole to be utilized with other CATS technology in various countries.

#### **6.5 Ethical Concerns**

One important ethical consideration was to ensure that the pole and clamp cannot cause any long-term injury to the sharks that are tagged. This could include abrasions to a shark's body or dorsal fin as a result of the tagging process. We designed our pole to work with an existing clamp which is known to be safe for sharks, and we made sure that our pole did not have any exposed sharp objects or materials that could harm the shark.

As mentioned in the economics section, another ethical concern that this project can potentially reduce is the hunting of shark fins and teeth. The practice of hunting a shark to remove its fins and then releasing it back into the water is unethical treatment of animals for a profit. By designing a better means of tagging sharks (for tracking and understanding their migration patterns), this project can indirectly be linked to eliminating some of these unethical practices.

#### **6.6 Health and Safety Issues**

The primary focus of this project is to contribute to the safety and enjoyment of humans on beaches. The Sharktivity app helps notify civilians, beach authorities, and shark researchers about shark sightings on various beaches to give ample time for evacuation of

beaches and the water if necessary. The tagging system that we designed in this project is for the purpose of attaching camera and tracking systems to sharks, allowing for more awareness of shark proximity. Having a means of tracking sharks and understanding their predatory habits can give beachgoers peace of mind when enjoying a day at the beach during the shark season and help lifeguards and beach officials with proper safety preparations. While the tagging pole and clamp do not directly contribute to a satisfying life for everyday people, the system indirectly contributes to an overall more enjoyable and safer pastime.

When designing our pole, we also wanted to ensure the safety of the user. Part of this process included our pole bending calculations, where we solved for the resultant forces on the hands to assure that they never exceeded 46 lbs of force on the metacarpal bones, which could lead to cartilage and then joint damage. Additionally, since the user will be standing on the pulpit of a boat while tagging, our design eliminates the need to lean over the rail too far, potentially leading to further injury. The last component of user safety included ensuring that the system would put the user's hand or arm at risk of injury when loading the clamp with the clamp opener. We addressed this by using pins with slots in them to keep the clamp arms in place and prevent them from slipping off and prematurely activating the torsion spring.

## **6.7 Manufacturability**

Our prototype required some external manufacturing due to the group's lack of experience with machining complicated parts as well as time constraints and lack of access to the proper equipment. We also utilized personal 3D printers for many phases of the initial prototyping process. For the actual production of the design, the tagging mechanism could be reproduced with access to CNC (milling and lathing) and water jetting equipment, as well as a resin 3D printer. Ideally, even the 3D printed components of the project could be machined with access to more material options and funding, as our main reason for opting for resin was to save money on materials and increase strength without negatively impacting the total weight of the design.

Once all the proper components are machined and printed, the components of the pole and clamp opener can be easily attached by welding and screws. The unique design of the clamp opener posed more of a challenge to machine, as it requires very specific tolerances and dimensioning; therefore, we opted to decompose the design into multiple parts that fit together to allow for easier manufacturability and reproducibility.

## **6.8 Sustainability**

Our original intent for this project was to design both a clamp and pole to tag sharks. Our clamp design focused on ensuring that the clamp could be reused for multiple tagging efforts, rather than fall off the shark and sink into the ocean. This reusability promotes sustainability of materials because having a reusable clamp means that researchers do not

have to request a new manufactured product for every single shark they want to tag. Similarly, in our pole design, we opted for materials that do not easily react in a saltwater environment to maintain the structure and functionality of the pole components for longer periods of time without replacing them. The general production of our pole design does not require excessive amounts of machining or energy to reach a final product. Additionally, since most researchers will only need one or two of these poles on hand (the same pole is designed to be used for each tagging opportunity), and not many researchers in the world tag sharks in this way, the production of these poles will not have a significant negative impact on sustainable practices and species.

## 7 Discussion

As described in Section 5 our system passed verifications for both safety and functionality. Deflection calculations of the whole system revealed minimal risk for injury to the user. Testing of the force required to open the clamp and further stress analysis of the plates of the clamp opener showed that the clamp opener will be able to withstand the forces generated by the clamp itself. Tests on the efficacy of the release mechanism proved that the release is functional at any tagging angle in both air and under water. Full system tests revealed the importance of the self-leveling aspect of the hydrofoil in flowing water.

Our final design is meant for use in the ocean. As we did not have access to choppy water for testing, we tested the device's efficacy in an indoor pool. We also did not have the opportunity to test the pole's ability to attach a clamp onto a shark both for safety reasons and because the project timeline did not align with shark season; therefore, our results on the efficacy of the design in a tagging environment are limited to the environment we modeled as described in Section 5. Additionally, we did not have the CATS Cam housing for our tests, as it is an expensive piece of technology with limited quantities available; therefore, without the positively buoyant CATS Cam housing, our test results in water may be skewed.

Since our design is relatively unique to the marine tagging industry and focuses specifically on a design challenge for Dr. Greg Skomal's research, we do not have many benchmarks to compare our results to. The current mechanism that Dr. Skomal uses to release the specific clamp and tag system is a short pole that cannot be safely used for tagging great white sharks. We aimed to provide a solution to this safety concern by creating a design that can be attached to the end of any length pole. As a result of this adaptability, our device can attach to Dr. Skomal's adjustable painting pole, allowing him to safely tag great whites off the pulpit of his boat. Additionally, in the previously mentioned existing design, the user must release the tag manually by holding down a trigger; in our design, the release is automatic upon contact with the dorsal fin, requiring no extra step on the user's part.

## 8 Conclusions and Recommendations

Tracking shark movements off the coast of Cape Cod has become increasingly important as the seal population has rebounded. Understanding shark movements allows for accurate estimates regarding when to shut down public beaches for swimmer safety. The act of tagging a great white can be dangerous as well; therefore, our goal was to design a device that increases user safety for deploying a tag onto great whites. After conducting background research on great whites, types of marine tagging, existing tagging devices, and injury prevention, we were able to formulate various design ideas and compare them through a design matrix. This matrix informed our final design decisions which we continued to iterate on throughout the project term. We successfully were able to design, develop, and manufacture a tagging apparatus for safely attaching a tagging system to great whites from a moving boat.

Although our design is intended for use from the pulpit of the boat, it can be adapted to any length of pole and therefore can be used for tagging a variety of sea creatures. The self-aligning aspect of the hydrofoil allows the design to be used in any conditions, calm or choppy. Marine tagging is a niche industry; therefore, the market for tag deployment mechanisms is small, allowing this device to be used for a variety of tagging efforts.

We could always continue to make improvements to our design, but due to time constraints, we wanted to ensure functionality and safety. Some possible improvements to our design include making the bike brake piece more hydrodynamic and lighter by changing material choice or geometric design. Another possible design improvement would be to reduce the length of the hydrofoil to make it easier for the user to control the pole without losing the self-aligning aspect of the design. Due to time constraints, we did not test a shorter hydrofoil length because we would not have time to order a new full-length hydrofoil if the shorter hydrofoil failed. We also recommend using a more durable material for the main body of the clamp opener such as ABS plastic or manufacturing it through injection molding. We realized late in the assembly process that having a notch in the main body of the clamp opener to easily access the grip piece from its stored position would also be desirable.

Due to the COVID-19 pandemic we did not have as much time on campus to design and manufacture every piece perfectly. Furthermore, due to the custom nature of our design, we were able to purchase only a few components. A few parts were outsourced to be manufactured elsewhere and some were manufactured on campus. Originally, we planned to design a clamp and a pole, but due to limited time with campus access due to COVID-19 we instead prioritized finalizing the pole. See Appendix D for the design process followed for our initial design ideas for clamps.

Future projects building on this work could include designing a new clamp to work with our device or adapting the current design to be retrievable and reusable. Another possible project could be to work with CATS Cam to create a tag that powers itself using water flow as the shark swims. While marine tagging is not a widely followed industry,

researchers continue to seek out new technology to aid in their marine studies; as such, it is becoming increasingly prevalent around the globe, leading to more opportunities for exciting future projects.

## 9 Works Cited

- [1] AWSC. (September 5). *Why White Sharks?* [Online]. Available: <https://www.atlanticwhiteshark.org/why-white-sharks>
- [2] M. C. Society. (2020, September 5). *Great White Sharks ~ MarineBio Conservation Society* [Online]. Available: <https://marinebio.org/species/great-white-sharks/carcharodon-carcharias/>
- [3] M. A. Naresh, V. Sanjeevi, R., "Mechanical behaviour of shark skin," *Journal of Biosciences*, vol. 22, no. 4, pp. 431-437, 1997.
- [4] B. B. Dean, B., "Shark-skin surfaces for fluid-drag reduction in turbulent flow: a review," *Philosophical Transactions of the Royal Society*, vol. 368, pp. 4775-4806, 2010.
- [5] H. W. C. Chien, XY. Tsai, WP. Lee, M., "Inhibition of biofilm formation by rough shark skin-patterned surfaces," *Colloids and Surfaces B: Biointerfaces*, vol. 186, pp. 1-9, 2020.
- [6] D. L. Zhang, Y. Li, X. Chen, H. , "Numerical Simulation and Experimental Study of Drag-Reducing Surface of a Real Shark Skin," *Journal of Hydrodynamics*, vol. 23, no. 2, pp. 204-11, 2011.
- [7] T. Lingham-Soliar, "Dorsal Fin in the White Shark, *Carcharodon carcharias*: A Dynamic Stabilizer for Fast Swimming," *Journal of Morphology*, vol. 263, pp. 1-11, 2005.
- [8] M. A. W. O.J.D. Jewell, E. Gennari, A.V. Towner, M.N. Bester, R.L. Johnson, S. Singh, "Effects of Smart Psotion Only (SPOT) Tag Deployment on White Sharks *Carcharodon Carcharias* in South Africa," *PLoS One*, vol. 6, no. 11, 2011.
- [9] M. A. B. E. Mul, M. Biuw, A. Rikardsen, "Implications of tag positioning and performance on the analysis of cetacean movement," *Animal Biotelemetry*, vol. 7, no. 11, 2019.
- [10] B. D. Groot, "Buoyancy regulation in sharks: The importance of the fins and body," *Doctoral dissertation, Faculty of Science and Engineering*.
- [11] F. E. S. Fish, L.D., "The Role of the pectoral fins on body trim of sharks," *Fish Biology*, vol. 56, pp. 1062-1073, 2000.
- [12] J. J. Videler, *Fish Swimming*. London: Chapman and Hall, 1993.
- [13] J. R. Simons, *The direction of the thrust produced by the heterocercal tails of two dissimilar elasmobranches: the Port Jackson shark, *Heterodontus portusjacksoni* (Meyer), and the piked dogfish, *Squalus**. 1970.
- [14] Available: [http://www.elasmo-research.org/education/white\\_shark/ws-images/fins.gif](http://www.elasmo-research.org/education/white_shark/ws-images/fins.gif)
- [15] A. Martin. *Fins to the Left, Fins to the Right*. Available: [http://elasmo-research.org/education/white\\_shark/fins.htm](http://elasmo-research.org/education/white_shark/fins.htm)
- [16] "Why do sharks have to keep swimming?," ed, 2020.
- [17] G. B. Skomal, CD. Chisholm, JH. Thorrold, SR., "Movements of the white shark *Carcharodon carcharias* in the North Atlantic Ocean " 2017.
- [18] B. D. Bruce, Stevens, J.D. & Malcolm, H., "ovements and swimming behaviour of white sharks (*Carcharodon carcharias*) in Australian waters," *Marine Biology*, vol. 150, pp. 161-72, 2006.
- [19] D. Long, "White Shark," in *Encyclopedia Britannica*, ed, 2020.
- [20] M. Musyl, Domeier, M., Nasby-Lucas, N., Brill, R., McNaughton, L., Swimmer, J., Liddle, J., "Performance of pop-up satellite archival tags," *Marine ecology progress series*, vol. 433, pp. 1-28, 2011.
- [21] F. K. Carey, JW. Brazier, O. Gabrielson, G. Casey, JG. Pratt, HL. , "Temperature and Activities of a White Shark, *Carcharodon carcharias* " *American Society of Ichthyologists and Herpetologists (ASIH)* vol. 1982, no. 2, May 28 1982.
- [22] N. Hammerschlag, Martin, R. & Fallows, C, "Effects of environmental conditions on predator-prey interactions between white sharks (*Carcharodon carcharias*) and Cape fur seals (*Arctocephalus pusillus pusillus*) at Seal Island, South Africa," *Environmetnal Biology Fish*, vol. 76, 2006.

- [23] G. H. Burgess, Callahan, M, "Worldwide patterns of white shark attacks on humans," *Academic Press inc*, 1996.
- [24] J. Stevens, "Shark Tagging: A Brief History of Methods," *Australian Society for Fish Biology*, pp. 65-8.
- [25] B. Team. *Tagging and Monitoring fish*. Available: <https://bullbuster.net/community/articles/bullbuster-in-action/everything-an-angler-needs-to-know-about-tagging-programs>
- [26] V. I. o. M. Science, "Dart and Roto Tags," 2020.
- [27] K. B. Holland, A. Meyer, CG. Kaijura, S. Wehterbee, BM. Lowe, CG., "Fie Tags Applied to a Single Species in a Single Location: The Tiger Shark Experience," *Reviews: Methods and Technologies in Fish Biology and Fisheries Electronic Tagging and Tracking in Marine Fisheries*, pp. 237-247, 2001.
- [28] L. Bergeron. (2009). *Tags reveal white sharks have neighborhoods in the North Pacific, Stanford researchers say*. Available: <https://news.stanford.edu/news/2009/november2/white-shark-research-110309.html>
- [29] (9/18/2020). *Shark Tracking Devices*. Available: <http://www.himb.hawaii.edu/ReefPredator/Tools.htm>.
- [30] N. G. Hammerschlag, AJ. Lazarre, DM. , "A Review of Shark Satellite Tagging Studies," *Journal of Experimental Marine Biology and Ecology*, 2010.
- [31] J. P. Hoolihan, Luo, J., Abascal, F. J., Campana, S. E., De Metrio, G., Dewar, H., Domeier, M. L., Howey, L. A., Lutcavage, M. E., Musyl, M. K., Neilson, J. D., Orbesen, E. S., Prince, E. D., and Rooker, J. R, "Evaluating post-release behaviour modification in large pelagic fish deployed with pop-up satellite archival tags," *Journal of Marine Science*, vol. 68, pp. 880-9, 2011.
- [32] G. B. Skomal, "Evaluating the physiological and physical consequences of capture on post-release survivorship in large pelagic fishes.," *Fisheries Management and Ecology*, vol. 14, pp. 81-9, 2007.
- [33] M. R. M. Heithaus, G.J. Buhleier, B.M. Dill, L.M., "Employing Crittercam to study habitat use ad behavior of large sharks," *Marine ecology progress series*, vol. 209, pp. 307-10, 2001.
- [34] A. C. N. Gleiss, B. Liebsch, N. Francis, C. Wilson, R.P., "A new prospect for tagging large free-swimming sharks with motion-sensitive data-loggers," *Fisheries Research*, vol. 97, no. 1-2, pp. 11-6, April 2009.
- [35] T. G. Chapple, AC. Jewell OJD. Wikelski, M. Block, BA., "Tracking sharks without teeth: a non-invasive rigid tag attachment for large predatory sharks," *Animal Biotelemetry*, vol. 3, no. 14, 2015.
- [36] D. M. R. Avery, C.M. Edgar, C.M., "Sports-related wrist and hand injuries: a review," *Journal of Orthopaedic Surgery and Research*, vol. 11, no. 99, pp. 1-15, 2016.
- [37] E. R. C. Weber, E.Y., "An experimental approach to the mechanism of scaphoid waist fractures," *Journal of Hand Surgery*, vol. 3, no. 2, pp. 142-8, 1978.
- [38] L. M. Teurlings, G.J. Wright, T.W., "Pressure Mapping of the Radioulnar Carpal Joint: Effects of Ulnar Lengthening and Wrist Position," *Journal of Hand Surgery*, vol. 25B, no. 4, pp. 346-349, 2000.
- [39] (2020). *Energetis Osteopathy Treatments & Courses*. Available: <https://terapix.wixsite.com/osteodouce>
- [40] M. H. Majima, E. H. Matsuki, H. Hirata, H. Genda, E., "Load Transmission Through the Wrist in the Extended Position," *The Journal of Hand Surgery*, vol. 33, no. 2, pp. 182-188, 2008.
- [41] E. H. Genda, E. , "Theoretical Stress Analysis in Wrist Joint - Neutral Position and Functional Position," *Journal of Hand Surgery*, vol. 25 B, no. 3, pp. 292-295, 2000.

- [42] S. F. P. Viegas, R. Peterson, P. Roefs, J. Tencer, A. Choi, S., "The effects of various load paths and different loads on the load transfer characteristics of the wrist," *Journal of Hand Surgery*, vol. 144, no. 3, pp. 458-65, 1989.
- [43] C. L. Kolstrup, "Work Environment and Health among Swedish Livestock Workers," *Swedish University of Agricultural Sciences*, vol. Doctoral Thesis, 2007.
- [44] J. C. F. Siebert, "Resurrecting Virginia Algonquian from the dead: The reconstituted and historical phonology of Powhatan," *Studies in Southeastern Indian Languages*, p. 290, 1975.
- [45] (2011). *Master The Art of Fish Chumming!* Available: <https://www.americagofishing.com/fish-chum/fish-chum-and-chumming.html>
- [46] H. Orecchio-Egresitz, "New rules to protect sharks," in *Cape Cod Times*, ed, 2015.
- [47] (2017). *Solidworks Help*. Available: [http://help.solidworks.com/2017/english/solidworks/acadhelp/c\\_standards\\_acadhelp.htm](http://help.solidworks.com/2017/english/solidworks/acadhelp/c_standards_acadhelp.htm)
- [48] *Standard Interpretations*, 1984.
- [49] "Electromagnet," in *Encyclopedia Britannica*, ed, 2020.
- [50] Adafruit. (2020). *Solenoids: 5V Electromagnet*. Available: <https://www.adafruit.com/product/3874>
- [51] A. Company. (2020). *Electromagnets and Coils*. Available: <https://apwelectromagnets.com/>
- [52] D. Alexander, *Fluid Biomechanics*. Academic Press, 2017.
- [53] Y. T. Cengel, R.H. Cimbala, J.M., *Fundamentals of Thermal-Fluid Sciences*, 3 ed. McGraw Hill, 2008.
- [54] A. K. Ashrafi, M. Ghassemi, H., "Numerical Study on Improvement of Hydrofoil Performance using Vortex Generators," *International Journal of Engineering*, vol. 28, pp. 305-313, 2015.

## Appendix A: Project Schedule

Redesigned Shark Tagging Schedule		
Task	Initial Start Date	Completion Date
<i>A-Term</i>		
Preliminary Research	9/1/20	9/20/20
Annotated Bibliography	9/6/20	10/16/20
Outline & Begin Writing First Draft	9/15/20	10/3/20
Discuss & Draw Design Ideas	10/3/20	10/16/20
Complete & Submit First Draft	10/12/20	10/16/20
<i>B-Term</i>		
Edit A-Term Draft	10/21/20	10/26/20
Finalize 5 Design Ideas	10/28/20	11/4/20
Outline & Begin Design Section	10/25/20	11/6/20
CAD Model Initial Designs of Pole & Clamp	10/21/20	12/11/20
Generate Design Matrix	10/21/20	11/23/20
Select Final Design for Clamp & Pole	11/23/20	12/11/20
Finalize & Submit Design Section	12/4/20	12/11/20
<i>C-Term</i>		
Edit B-Term Design Draft	1/18/21	1/28/21
Order Materials	1/20/21	2/25/21
Edit CAD Models of Pole	1/20/21	2/10/21
Initial Prototype Phase (3D Printer)	2/2/21	2/18/21
Revise CAD Models	2/18/21	2/25/21
Final Prototype Phase (Resin 3D Printer, Etc.)	2/25/21	3/3/21
Test Design	3/3/21	3/16/21
Final Design Assembled and Tested	3/14/21	3/31/21
Finalize & Submit Final Paper	2/10/21	4/1/21

# Appendix B: Pole Design Matrix

Customer Requirements	Weight/Importance	Electromagnetic Pole		Grabbing Pole	
		Score	Explanation	Score	Explanation
Low Cost	0.7	1 (.7)	Requires more electrical components and magnets which increase cost.	2 (1.4)	There are multiple parts but they would all be cheap.
Easy to Use	1	3 (3)	Very easy to use, just disconnect the power source when clamp is in place.	1(1)	Only needs to be squeezed, but it can only be used perpendicular to the shark.
Durable	0.8	3 (2.4)	Dependent on material, but magnets may not be durable and work well after being in saltwater.	3 (2.4)	Dependent on material.
Light-weight	0.8	2 (1.6)	Depends on pole material but power source or magnet could cause heavier weight.	3 (2.4)	Pole is hollow, thus lightweight.
Low potential for failure	1	2 (2)	Could have electrical malfunction or current stopped too soon which would release clamp on shark too early.	1 (1)	Could release prematurely as it depends on the hand strength of the user squeezing the pole.
Safe for User	1	2 (2)	No potential for harm to the user.	3 (.6)	No potential for harm to the user.
Adaptable approach angle	0.8	3 (2.4)	Able to adapt to various angles with a swivel attachment.	1 (.8)	Can only be used perpendicular to the shark.
Simple in complexity	0.5	1 (.5)	Multiple parts and electrical components but simple mechanism of release.	2(1)	Multiple parts but simple mechanism .
Re-makeability	0.3	2 (.6)	Requires some electrical parts.	2 (.6)	Simple mechanism but may have several custom parts.
	18.3 = perfect	15.2	0.830601093	11.2	0.612021858

		Flex Release Pole	
Customer Requirements	Weight/ Importance	Score	Explanation
Low Cost	0.7	3(2.1)	Adapts to existing telescopic pole and requires minimal other expensive parts.
Easy to Use	1	3(3)	Only requires user to engage the clamp. No other action or mechanism is required for the pole.
Durable	0.8	2(1.6)	Dependent on material but does not have any mechanisms that can fail aside from clamp adapter piece if overflexed.
Light-weight	0.8	3(2.4)	Existing pole is manageable in weight. Crossbar and clamp adapter are relatively light as well.
Low potential for failure	1	2(2)	Clamp adapter could snap if material is not flexible enough to stretch at its widest position.
Safe for User	1	3(.6)	No potential for harm to the user.
Adaptable approach angle	0.8	2(1.6)	Moderately adaptable ahead of time with different angle of crossbar adjustments.
Simple in complexity	0.5	3(1.5)	Moderate number of parts but no mechanism in the pole itself.
Re-makeability	0.3	3(.9)	3D printed parts, some machined, and existing pole.
	18.3 = perfect	15.7	0.857923497

## Appendix C: Pole Design Pairwise Matrix

Customer Requirements	Weight/Importance	Electromagnet	Flex Release	Explanation
Low Cost	0.7	0	1	The cost of the electromagnet pole would be more expensive because there are more parts and the electromagnet is expensive.
Easy to Use	1	0	1	The flex release is easier to use because there are less moving parts and you don't have the complexity of using the electromagnet.
Durable	0.8	0	1	Electromagnets will need to be replaced over time due to saltwater, but both physical poles would likely be similar in durability.
Light-weight	0.8	0	1	The flex release pole would be significantly lighter because it does not possess an electromagnet and uses lighter materials.
Low potential for failure	1	0	1	Drag forces from the water and added weight of the electromagnet could cause the magnet to be pulled off.
Safe for User	1	0	1	The electromagnet would add extra weight to the end of the pole making it heavier for the user.
Adaptable approach angle	0.8	1	1	Both poles would allow for the same approach angles.
Simple in complexity	0.5	0	1	The flex release pole has significantly fewer parts and has no electrical components.
Re-makeability	0.3	0	1	The electromagnet might require parts to be changed out more frequently, and having to remake electrical components and wiring is more complex than the flex pole.

## **Appendix D: Clamp Design**

### **1 Design Process for the Clamp**

Due to COVID-19 campus access for manufacturing was limited. In response our group prioritized producing a final product for the pole over producing a finished clamp. The extent of our design process for the clamp is described below.

#### **1.1 Needs Analysis**

Initially our plan was to create a new tagging system to be used with the CATS Cam technology, which would have included a clamp mechanism and a pole to apply it. However, as mentioned above, time and resource constraints impacted our decision to not complete the clamp design to full manufacturing.

The most important aspect of the clamp design is that it needs to stay on the shark during swimming and through any rough waters. Because of the nature of the CATS Cam system, the clamp does not need to stay on indefinitely, but instead, it should fall off the shark at a specified time. Since there was no way we could have tested our clamp on a shark, we decided the clamp would need a clamping force similar to previous designs.

The second most important aspect of the clamp centers around its usability for Dr. Skomal. Dr. Skomal asked for a system that could be deployed from the pulpit of his boat since he already has one that functions from the sides of the boat. For this to be achievable, the clamp needs to be able to deploy onto a shark far away from Dr. Skomal, which means the detachment mechanism needs to be reliable and easily manipulated from 10-16 feet.

The next section describes the design matrix we used and how we broke down the basic needs of the clamp into qualifiable requirements.

#### **1.2 Design Matrix**

In weighing various design options for this project, we employed a simple design matrix. We decided on the customer requirements of the project to rank each design option. Based on Dr. Skomal's needs for the tagging system, we summarized these requirements in Table 1. Each of the requirements is given an importance level from 0.1 (least important) to 1 (most important) with multiple of the same score allowed. We

determined these weights based on initial input for the design from Dr. Skomal and through research on what has worked in existing clamp and pole tagging systems. We ranked each requirement on a scale of 1 (worst) to 3 (best). We used the weight scores as multipliers for each ranking. The full design matrices can be found in Appendix A-B. In the full matrix, the first number for each category is the ranked number, and the number in parentheses is the ranked number multiplied by the weight of that specific category. We added the weighted rankings to calculate a total score for each design.

*Table 1: Customer Requirements and Importance Scores for Clamp*

Customer Requirements	Weight/Importance (0.1-1)
Low Cost	0.4
Easy to Use	0.8
Durable	1
Lightweight	0.7
Low Potential for Failure due to Design	1
Safe for shark	0.4
Adaptable sizing	0.8
Simple in Complexity	0.5
Re-makeability	0.3
Easy Approach Angle	0.7
Retrievable	0.9

The “*low-cost*” requirement involves keeping the design under the given budget of 1,000 USD. This requirement received an importance of 0.4 since it is relatively important that the project is capable of being produced under budget, but it is not as important a factor in deciding designs as the functionality requirements.

“*Easy to use*” for the clamp refers to the clamp being able to attach to the shark quickly while requiring minimal effort to engage its mechanisms. This requirement scored 0.8 for clamp importance because it is crucial that the clamp and pole only require minimal

user effort in a fast-moving environment with many variables (ocean waves, moving shark, moving boat, wind, etc.).

The “*durability*” category means the clamp will not break during the attachment process and will last for multiple uses through the shark season. This also means that the clamp will not fall apart while on the shark, especially before the tag is meant to release for user retrieval. “*Durability*” received a score of one for the clamp because it is one of the two key factors which are necessary to decide whether to proceed with a design such that it is useful and functional for Dr. Skomal.

The next requirement, “*lightweight*”, depends on material selection and contributes to how easy the clamp is to use on the end of the pole. If the clamp is too heavy on the end of a pole between 8 to 16 ft in length, the user will experience significant physical strain in the attachment process due to the generated bending moment on the pole. Also, if the clamp is too heavy, the addition of more buoyancy materials will be necessary to prevent it from sinking. This requirement scored 0.7 since it plays a role in the safety of the design for the shark and more importantly, the user. It also contributes to how easy the system is to use and the total cost (depending on materials).

The “*low potential for failure*” requirement involves two components which decide whether the system has failed. First, incomplete attachment occurs if the clamp is unable to attach to the shark. Second, premature detachment is another indication of failure which occurs if the clamp falls off the shark before the preset release time. This requirement also scored the highest with a score of one as functionality and success of the system are the primary goal of any design.

The requirements of “*safe for shark*” simply means that the design will not injure the shark in the tagging process. The score was 0.4 since the feeling of any weight or tightness from the clamp is insignificant to the shark, although preventing long-term artificial damage to the fin is also a key consideration.

The clamp customer requirement category of “*adaptable sizing*” refers to the clamp being able to fit to any size dorsal fin of great white sharks. This scored a 0.8 because the

sizes of the fins will vary, and the user would not be able to quickly change clamps to fit a different sized fin within such a short time frame.

*“Simple in complexity”* refers to the number of parts in the clamp, as well as the simplicity of the mechanisms in the design. The clamp scored a 0.5 for this requirement since simplistic designs are often easier to use, and having fewer parts leads to a lower probability of failure.

The *“re-makeability”* requirement means that the designs can be easily reproduced without many customized parts. Having too many parts which are unable to be remade without customization will make it difficult and expensive for Dr. Skomal to produce multiple tagging and pole systems for his research. This received a score of 0.3 because it is a good consideration for the designs, but it is not necessary for the success and functionality of the overall system.

*“Approach angle”* refers to how easily the clamp can access the shark fin for complete tagging. For example, the attachment angle could be directly behind, in front of, or to either side of the dorsal fin. The clamp approach angle requirement scored a 0.7 because the user only has a short period of time to deploy the tagging system onto the shark, which requires the orientation of the clamp to work in the user’s favor.

Lastly, the *“retrievable”* requirement primarily applies to the clamp, as the tagging system is what stays on the shark to collect data before falling off. The clamp and tag should be retrievable, meaning that almost all parts need to be collected from the ocean and reused for future tagging. *“Retrievability”* received a score of 0.9 because it is essential that Dr. Skomal be able to reclaim the tagging system relatively intact for future use. Also, if the design is almost fully retrievable, we can avoid polluting the ocean with excess parts.

We utilized this design matrix throughout the entire design process to assess various designs and iterations. The scores from the design matrix helped us make informed decisions about designs to identify certain design aspects that could be combined for a more optimal final design. The following sections outline the phases of the design process and explain why we chose to move forward with certain designs over others.

### 1.3 Clamp Alternative Designs

This section outlines each stage of our design process, describing the elastic clamp, remora suction pad, modified CATS-Cam and Crittercam, mousetrap, and the collapsing bar clamp designs in detail. Using the design matrix, we explain why we chose to not move forward with the preliminary designs, and in the next section, we explain how we chose our final design.

#### 1.3.1 *Elastic Clamp Design*

One clamp design from the preliminary design stage is an elastic clamp which consists of an elastic material, such as rubber, in the shape of a wide elastic band as the clamp. The CATS-Cam tagging system would attach to one side of the elastic band, and the other side would have a Galvanic-Timed-Release (GTR) connecting the two sides of the band to complete the loop as shown in Figure 1. The GTR would have an approximate corrosion time associated with it which would indicate approximately how long the clamp would stay on the shark. The clamp is designed to fit snugly around the first dorsal fin of the shark, molding to the shape of the fin once it is in the proper position.

The second component of this design is the attachment device which acts as the exchange between the pole and the elastic band to attach the band to the shark. This device resembles a tool used in farm animal castration, but on a larger scale. In this case, the attachment device would be implemented solely for the purpose of stretching the clamp wider than the dorsal fin so that the user can easily slide it over the fin. The mechanism consists of a system of linkages which the user can control by manipulating the handles (with a spring between them) to stretch or contract the elastic band. As seen on the right side of Figure 2, the four spokes would act as pins for the elastic to stretch around, allowing for the mechanism to control the size of the band. The final component of this design is the pole which would control the attachment device and the position of the clamp placement from the pulpit of the boat. The pole would be connected to the attachment device at an angle so that the attachment device lines up perpendicular to the dorsal fin as shown in Figure 3.

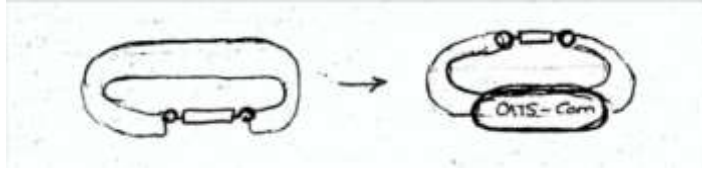


Figure 1: Elastic “clamp” with GTR on one side of the band (left) and CATS-Cam on the other side of the band (right).

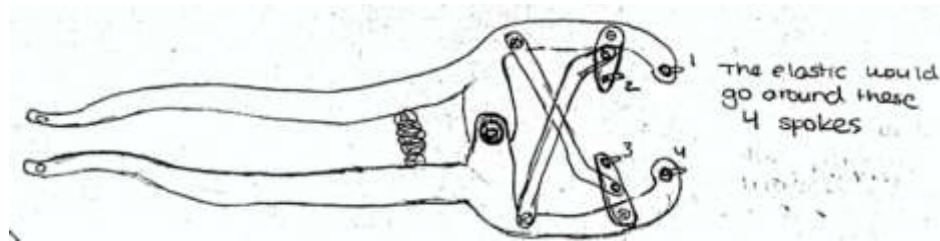


Figure 2: Attachment device for elastic clamp.

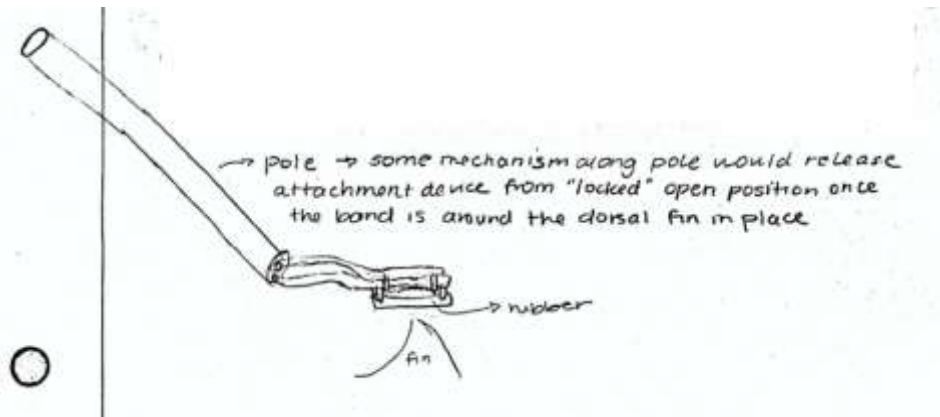


Figure 3: Pole with attachment device at an angle for placement of elastic clamp.

While this design scored well on the design matrix in some categories such as low cost, lightweight, simplicity, and re-makeability, it only scored 14.5/22.5 overall (see Appendix A). While the clamp itself is a simple device, the necessity of the attachment device to act as the transfer between the pole and the clamp creates excessive parts and a greater likelihood for incomplete tagging. The elastic might also be difficult to stretch over a fast-moving shark and from a moving boat, therefore giving this design a low score in

ease of use and a high potential for failure. Additionally, depending on the elastic material used, the roughness of the shark's fin could lead to tearing in the band and premature detachment, giving it a low score in durability. Overall, even though this design seemed to be one of the cheapest, lightest, and least complex clamp options, these customer requirements were not as important as the more functional requirements regarding the success of the tagging.

### 1.3.2 Remora Suction Pad Design

Remora fish firmly attach to many marine animals including great white sharks. The mechanism of attachment for a remora fish is a suction pad surrounding lamellar compartments (Figure 4A) composed of spinules (Figure 4B and 4C) [1]. The suction pad of the remora is more useful for attachment to smooth marine animals such as whales, where the spinules of the remora are useful for creating friction to attach to more rough skin surfaces, such as the great white [2]. The spinules of the remora are calcified projections.

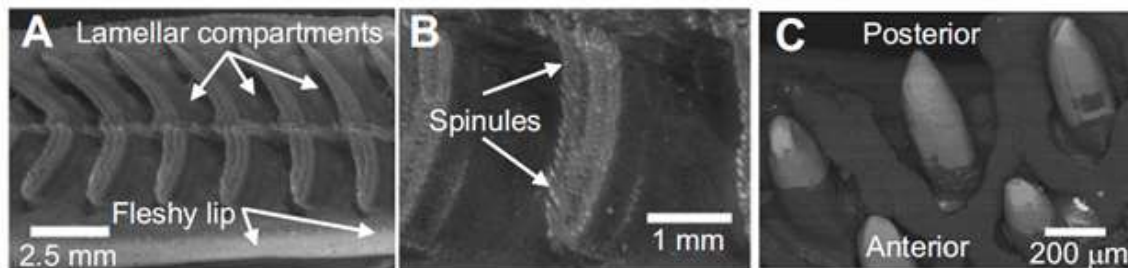


Figure 4: A: the lamellar Compartments of a remora fish. B: A closer look at the spinules in the lamellar compartment. C: Magnified image of the spinules [1].

This design aimed to mimic the remora suction pad as an attachment mechanism. The design includes an elastic material shaped into a long suction cup which contains rows of micro-projections meant to mimic the lamellar compartments and spinules. The micro-projections would be at an angle of 15 degrees to latch into the shark's scales. This value was determined by using the average attack angle of the dermal denticles, see: Background: Shark Anatomy, Skin Properties.

While the remora's attachment mechanism works well in nature, a synthetic version of it may not perform well for this goal. The primary reason this design may not work for this application is that the elastic material has a high likelihood of tearing on the riblets of

the shark's skin, which could result in premature detachment. Premature detachment could also result from water seeping under the suction pad and removing the suction mechanism. Additionally, this design does not allow any control over how long the tag stays on the shark.

### 1.3.3 Modified CATS-Cam and Crittercam Design

The modified CATS-Cam and Crittercam design, as seen in Figure 5, consists of several parts. The overall function of the design consists of a clamp with friction pads aligned on the inside. Within the clamp is a zip tie that secures the clamp around the rear of the dorsal fin. In Figure 5, Part A is where the CATS-Cam attaches to the clamp. Part B is the zip tie which goes inside the clamping system and is tied together at Part E. The zip tie has two ends: one end is tied together (Part E), and one end is loosely hanging outside of the clamp. The goal of this system was to have the user place the mechanism over the dorsal fin and tighten the zip tie. Through either a push of a button or a required force, the zip ties would tighten and stay secure once the clamp was in the necessary spot. The zip ties would stay secure because once locked, the zip tie does not expand or contract in length. The design would essentially fall off due to a biodegradable zip tie and a GTR mechanism.

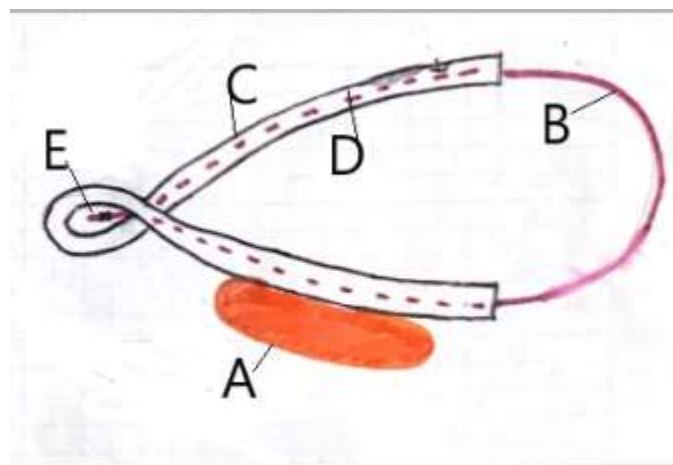


Figure 5: Modified CATS-Cam and Crittercam design

The modified CATS-Cam and Critter Design scored a 14.6/22.5 in the design matrix as shown in Appendix A. This design was promising in theory because it combined a multitude of designs that have proven to be successful in past tagging mechanisms. It scored well in durability, safe for shark, and retrievability. However, when looking at the

realistic nature of the design, it proved to be too complex for the given design time frame. The Crittercam, one of the two tagging mechanisms that inspired this design, had to use pneumatics with a scuba tank to cut the zip tie. Utilizing such additional equipment was a concern, as it would only further complicate the process. Additional aspects such as potential for failure and cost of overall design also led to the conclusion that the modified CATS-Cam and Crittercam design would not be a feasible final design.

#### 1.3.4 Mousetrap Design

The mousetrap design is a clamp concept that works similarly to a standard mousetrap, except on a larger scale. The clamp itself consists of a torsion spring connecting the two arms of the clamp and a pressure pad with a hook to set the trap. As shown in Figure 6, this design could exist in two initial orientations, 180-degree and 90-degree travel. The pole wraps around the mousetrap clamp in its open position and holds the hook that connects to the pressure pad. The clamp is designed to be set like a mousetrap prior to placement in the water. Once in the water, the user simply needs to align the clamp in the proper position on the side of the shark's dorsal fin and tap the pressure pad against the fin, activating the mousetrap mechanism.

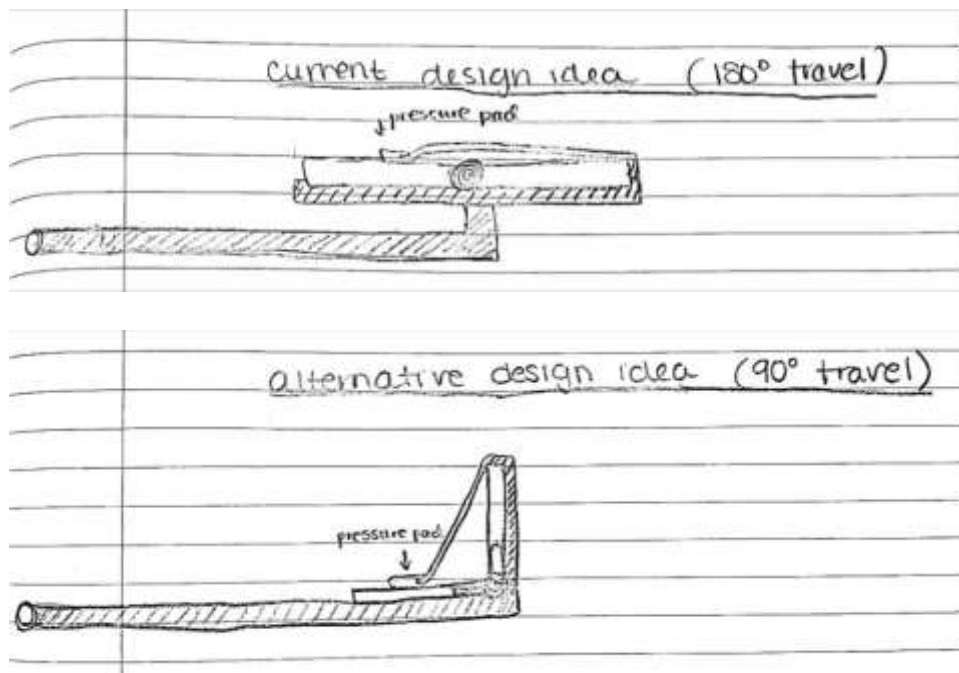


*Figure 6: Mousetrap design with 180-degree travel (top) and 90-degree travel (bottom) of torsion spring*

The mousetrap design scored in the top three clamp designs with 19.2/22.5 as shown in Appendix A. Although this design scored well, after further research into how standard mousetraps work and some safety calculations, we elected to not move forward with this design. Mousetraps often have sensitive and firm settings to control how much force it takes to activate them. For the purpose of this design, we could design our clamp to be firm to withstand more force from the ocean, but the drawback is that the pressure pad might be too difficult for the user to engage the clamp (by tapping the pad against fin) with a very long pole and other moving variables. The firmer setting of the pressure pad could still be engaged prematurely from the forces of water or tapping a different part of the shark's body, effectively preventing a tag from being attached to that specific shark. Additionally, while the 90-degree design uses less force than the 180-degree design when slamming closed, the bar connecting to the pressure pad mechanism obstructs a clean tap to the shark's fin, adding an additional barrier to the sensitivity level of the pressure pad. Lastly, after performing calculations regarding the safety of the spring travelling from both 90 degrees and 180 degrees, we found that the spring rate, moment, and energy of the spring would be very unsafe for the user and likely the shark as well. The calculations are shown below:

$E_{steel} = 206GPa$   
 $N_a = \text{number of active coils} = 3$   
 $D = \text{mean diameter of coil} = 20mm$   
 $d = \text{wire diameter} = 5mm$   
 $L = 155mm$   
 $T = \text{Deflection of spring}$   
 $M = \text{Moment}$   
 $PE = \text{Potential energy}$

$$k = \frac{M}{\theta_{rev}} = \frac{206000 * 5^4}{10.8(20) * 3 * \theta_{rev}}$$

$$M \approx 200,000 \text{ N-mm}$$

$$k = \frac{200,000}{2\pi} = 32,000 \text{ N-mm/rad}$$

**For Mousetrap at 90-degree travel:**

$$M = 200,000 * \frac{90}{360} = 50,000 \text{ N-mm}$$

$$F = \frac{M}{L} = 320 \text{ N} = 72 \text{ lbf}$$

$$PE = \frac{1}{2} k q^2 \text{ Where } q = \text{twist of } 90 \text{ degrees} = \frac{\pi}{2}$$

$$PE = \frac{1}{2} (32,000) * \left(\frac{\pi}{2}\right)^2 = 39,000 \text{ mJ} = 39 \text{ J}$$

**For Mousetrap at 180-degree travel:**

$$M = 200,000 * \frac{180}{360} = 100,000 \text{ N-mm}$$

$$F = \frac{M}{L} = 640 \text{ N} = 140 \text{ lbf}$$

$$PE = \frac{1}{2} k q^2 \text{ Where } q = \text{twist of } 180 \text{ degrees} = \pi$$

$$PE = \frac{1}{2} (32,000) * (\pi)^2 = 160,000 \text{ mJ} = 160 \text{ J}$$

The first set of calculations use the angular deflection of the spring to find the spring rate, k, for a specific set of parameters based on the Gleiss et al. design described in Background: Previous Mechanisms for Tagging Sharks. Using the applied moment, M, we were able to find the moment for both the 90-degree and 180-degree travel as shown in the second set of calculations. From these values of M, we found the force applied at 155 mm, the length of the clamp arm. For the 90-degree design, this force was 320 N, or approximately 72 lbf, and for the 180-degree design, the force doubled. We then calculated the potential energy of the spring in the open position for each angle using the spring rate and the angle of twist, q, in radians. These calculations produced a result of 39 J and 160 J, respectively. Therefore, from the preliminary safety calculations, even the 90-degree travel generates enough potential energy which could injure the user's hand if the mousetrap design were to prematurely close before being placed in the water. For these reasons, we chose to eliminate this design, as user and shark safety are of utmost importance.

### 1.3.5 Collapsing Bar Design

The collapsing bar clamp design is constructed from two arms, connected internally with a spring. A third piece between the two arms protects the spring. The CATS-Cam will attach at this piece. This piece also contains a scissor lift mechanism with a top platform that will hold the spring open and in turn hold the two arms apart. When attaching the clamp to a shark's fin, the user needs to push the platform against the fin to engage the linkage holding the platform. As the platform collapses inward, the spring will have nothing holding it open, so it will contract, and the clamp will close tightly around the shark fin. As the top platform is wider than the bottom platform and hollow, the links will fit inside of the top platform when fully collapsed. Because not all shark fins will be the same shape, a gel or moldable material will line the inner "J" shape of the arms for a snug and comfortable fit on any fin. Figure 7 and Figure 8 show the original sketch of this design as well as the first iteration of a CAD model.

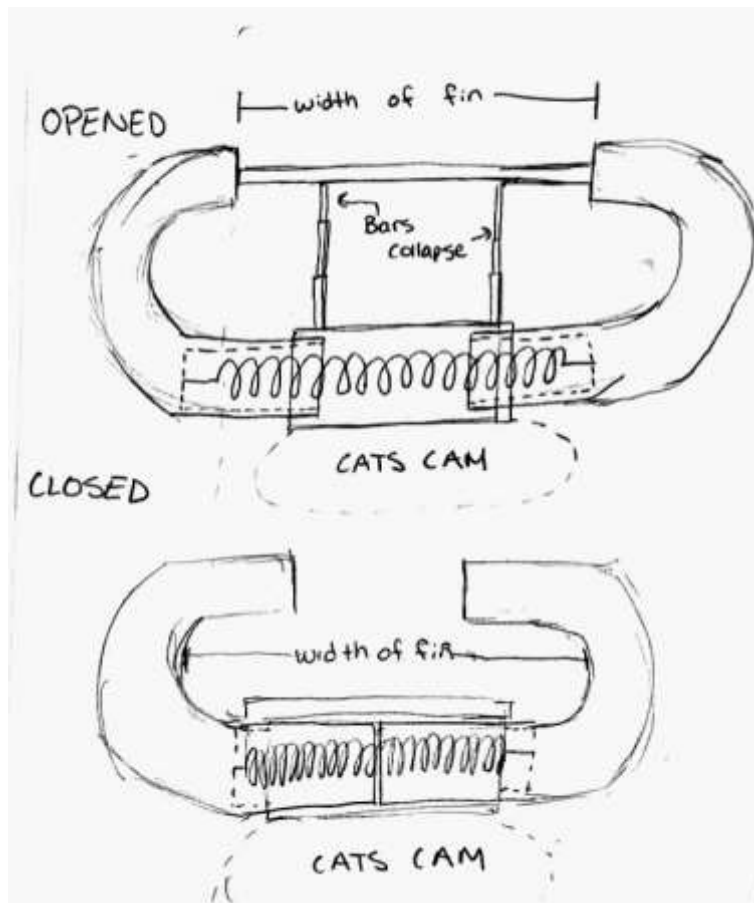


Figure 7: Collapsing bar initial sketch

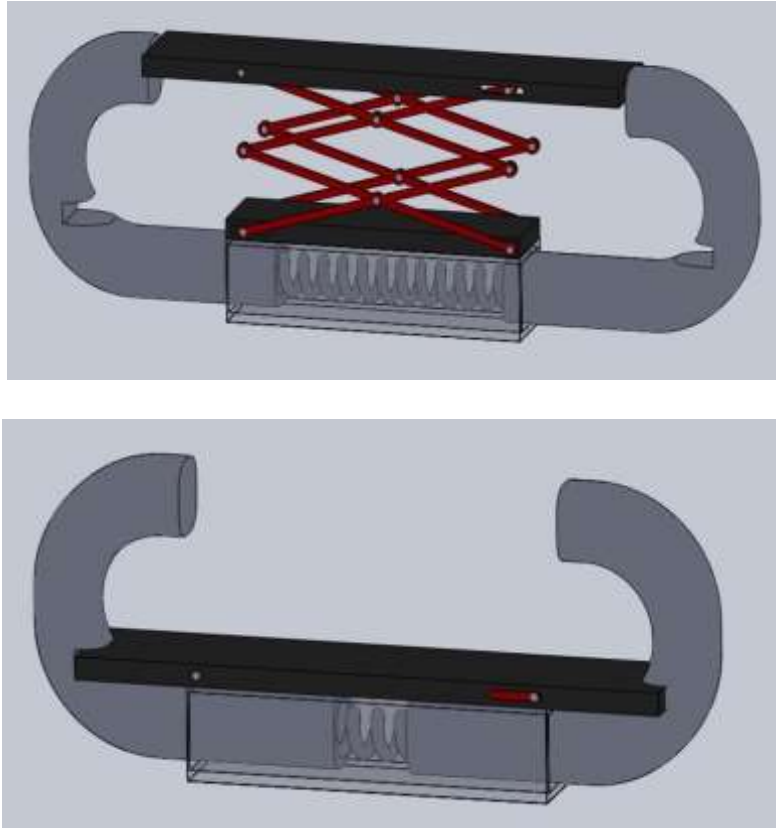


Figure 8: *Collapsing Bar CAD 1st Iteration in opened (top) and closed (bottom) positions*

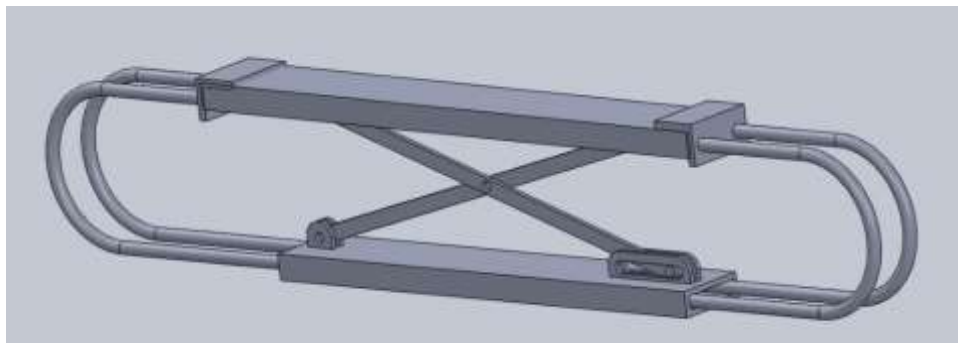
While the collapsing bar could be a potentially successful and feasible design for the final clamp, there were a few drawbacks of the original design that we addressed to improve the overall functionality of the clamp.

The main drawback of the early collapsing bar clamp design was its high potential for failure during the tagging process. This resulted from the bar simply resting in between the two arms and relying only on the force of the spring to keep it in place. With this design, the current and drag from the moving boat and the ocean on the clamp could easily knock

the bar out of place, resulting in incomplete deployment of the tag. To rectify this design flaw, two snap buttons were added to the top of each side of the bar. These snap buttons would attach to a piece connected to the arms, allowing for a more secure connection and a much lower likelihood that the force of the water would knock it out of place.

We needed to address the need for a multitude of parts required for the original collapsing bar design. With more parts, there exists a higher potential that one of them will break or not work properly during tagging. To improve upon this flaw, the second design includes fewer components. The reduction in parts results from an updated version of the scissor lift mechanism that lowers the collapsing bar. In the original design, there were eight links in the scissor lift, which were two crosses tall on each side. This number of links was unnecessary because the mechanism's only purpose was to allow a way for the bar to lower without detaching from the clamp, and it did not need to hold any load. The improved design uses only two links with one cross in the center, having the same effect with far fewer pieces.

Using fewer components also significantly decreases the weight of the tag. We reduced the overall weight by using four much thinner arms spaced one inch apart, connected with two separate springs as seen in Figure 9. This lighter design simultaneously increased stability by allowing the clamp to be flush against the shark's fin, reducing the drag on the clamp.



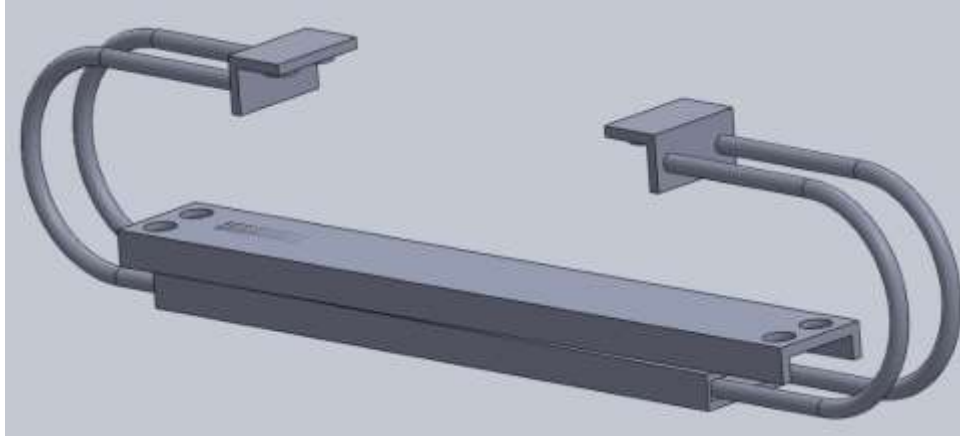


Figure 9: *Collapsing Bar CAD 2nd Iteration in opened (top) and closed (bottom) positions*

In the initial design matrix, this design scored well with an overall score of 17.2/22.5, the third highest score on our matrix. As displayed in the matrix, the collapsing bar clamp design scored consistently across the board, with its weakest point being in low potential for failure. Due to feasibility and safety concerns of the mousetrap design, we further considered the collapsing bar. Once we had established the final two clamp designs, we developed a pairwise matrix to compare these two designs Appendix C. The pairwise matrix utilized the same customer requirements as the full matrix, except the designs were scored with a zero or one. After completing the pairwise matrix, it was abundantly clear that the soft-lock design (explained in the next section) would be more successful than the collapsing bar. In each category being assessed, the collapsing bar scored lower or the same as the soft-lock, and the collapsing bar did not outperform the soft-lock in any of the customer requirements. Additionally, the collapsing bar scored a zero in everything except safe for the shark, lightweight, and retrievable.

#### 1.4 Final Clamp Design Stages

Our chosen clamp design, the “soft-lock design,” is a modified version of the Gauss et al. design, see Background: Previous Mechanisms for Tagging Sharks. These modifications are meant to assist Dr. Skomal with tagging great white sharks from the boat pulpit as opposed to from the side of the boat as intended with the Gauss et al. design. Our first modification is the addition of two links as seen in Figure 10. These links span from one side of the clamp arm to the other. The two links are free to move up towards the torsion spring but are inhibited from moving too far towards the end of the clamp arms. When the

clamp is in a fully open position, the force from the torsion spring causes the links to form an over-clamped linkage. The clamp force keeps the links in the over-clamped position by causing the links to contact a stopper that constrains the angle between the links. The positioning of the two limited motion links creates a locking mechanism that disengages by bumping the link joint against the leading edge of the great white shark's dorsal fin. This forces the linkages to spread the clamp arms open slightly until the two links are fully extended and colinear. As soon as the links begin to angle towards the torsion spring, the over-clamped orientation is broken allowing the clamp to quickly close.

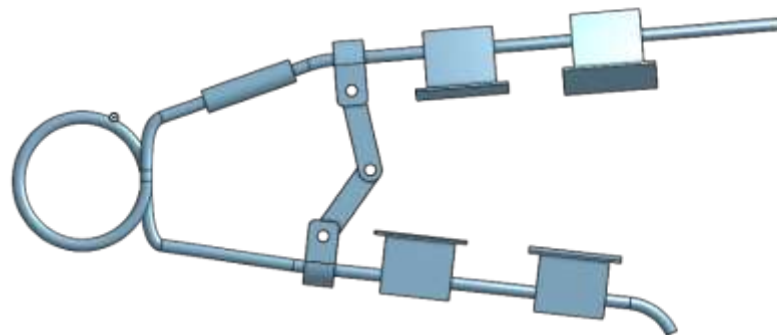


Figure 10: *Clamp Design with Over clamped Linkages*

An advantage of this design is its ability to keep the clamp open without the pole operator manually having to squeeze the lever while orienting the clamp around the dorsal fin. The self-locking mechanism keeps the clamp open which allows the tagging operator to focus on orienting the tag in the correct position. The clamp's easy release performs all the work towards clamping the tag onto the shark quickly and effectively. This also allows for a

cheaper, less complex application pole as it would no longer require a mechanism to open and close the clamp.

The second design modification focuses on the clamp arms and friction pads. The clamp arms on the Gauss et al. design do not bend or contour to the curvature of the great white shark's dorsal fin. This means that the friction pads do not lay perfectly flat on the surface of the shark fin. Depending on the size and shape of the dorsal fin, the force of the torsion spring may not translate perfectly to the friction pad, potentially leading to an insufficient amount of friction between the shark and friction pad. If the friction between the shark and the friction pad is less than intended, the clamp and tag may prematurely fall off. Instead of using a similar friction pad design as before, we have opted to modify a 10-inch rear wiper blade from a car. The wiper blade connects to our clamp arms at its midpoint allowing the force of the torsion spring to be equally distributed along the entire wiper arm. The flexible wiper surface created by the metal tension springs in the rubber blade is intended to conform to the curvature of car windows but also makes it perfect to create a custom-contoured fit to the intricacies of any size dorsal fin. The physical blade that wipes water off the window is removed, allowing for custom mounts to clip onto the flexible rubber and unchanged metal tension springs. These mounts also create a backing plate for a foam buoyancy material and friction pads (explained in the following sections). Since car wiper blades are designed for inclement weather and extreme driving conditions such as heat, cold, salt, and high speed, the wiper is built with a strong aerodynamic steel frame coated in zinc dichromate for corrosion resistance.

As shown in Appendix A, the soft-lock design scored well in all the customer requirement categories. This design scored better than the collapsing bar in all categories, making it the best choice for our final design.

#### *1.4.1 Clamp Release Mechanism: Galvanic-Timed-Release (GTR)*

The detachment mechanism of the clamp from the shark's fin will be a GTR. A GTR or Galvanic-Timed-Release as seen in Figure 11, is an underwater timing device that uses two dissimilar metals that corrode at a predictable rate when exposed to salt water [43]. In the case of our design, the GTR will be used to detach the clamp from the dorsal fin of the shark, thereby also releasing the CATS CAM. Throughout our design process, the GTR went

through several iterations. At first, we contacted Galvotec, a company that produces customized anodes, and asked if they would be able to design a simple magnesium anode. However, we thought it would be easiest to test out a GTR prior to moving forward with a customized anode. We ran into several issues when trying to calculate the size of the anode we would need Galvotec to produce. To avoid having to produce a customized piece of our design and complications with calculations, our group decided to switch to a basic GTR rather a magnesium anode. We will use GTRs with a 7-day release time from Neptune Marine Products, Inc. The GTR has the following properties: a weight of 7 g, a length of 1.5 in and a width with respect to the cylindrical center, of .40 in.



Figure 11: *Galvanic-Timed-Release (GTR)*

A device was designed to aid in the integration of the GTR into the overall clamping system. This device is shown in Figure 12 and attaches to the GTR on one side and to the clamp arm on the other side. The final design includes two of these devices, one on both sides of the GTR. As shown in Figure 11 above, the end of a typical GTR tag is essentially two small hoops, or eye hooks, which are connected to the GTR material between them. These end hoops are placed in the rounded cut-out displayed in Figure 12 (left). The left side of that image shows where the clamp arm would be inserted. Since the clamp arm is cylindrical, an adapter piece is necessary to prevent it from rotating within the GTR attachment device. This piece would be welded or attached to the end of the clamp arm using an adhesive. Our original design for the GTR attachment piece was to have four small snap hooks attached to the sides of the device on the base plate, and four small snap hook grooves at the same relative locations on the top plate. When the top piece is pushed down in the correct orientation, the snap hooks will fit snugly into their respective grooves and prevent any lateral or vertical movement. For a more secure attachment, we decided to alter this design to use bolts instead of snap hooks. This will eliminate any chance of the

plates separating from both sides of the clamp arm. The full GTR attachment clip (in open and exploded views) is shown in Figure 12.

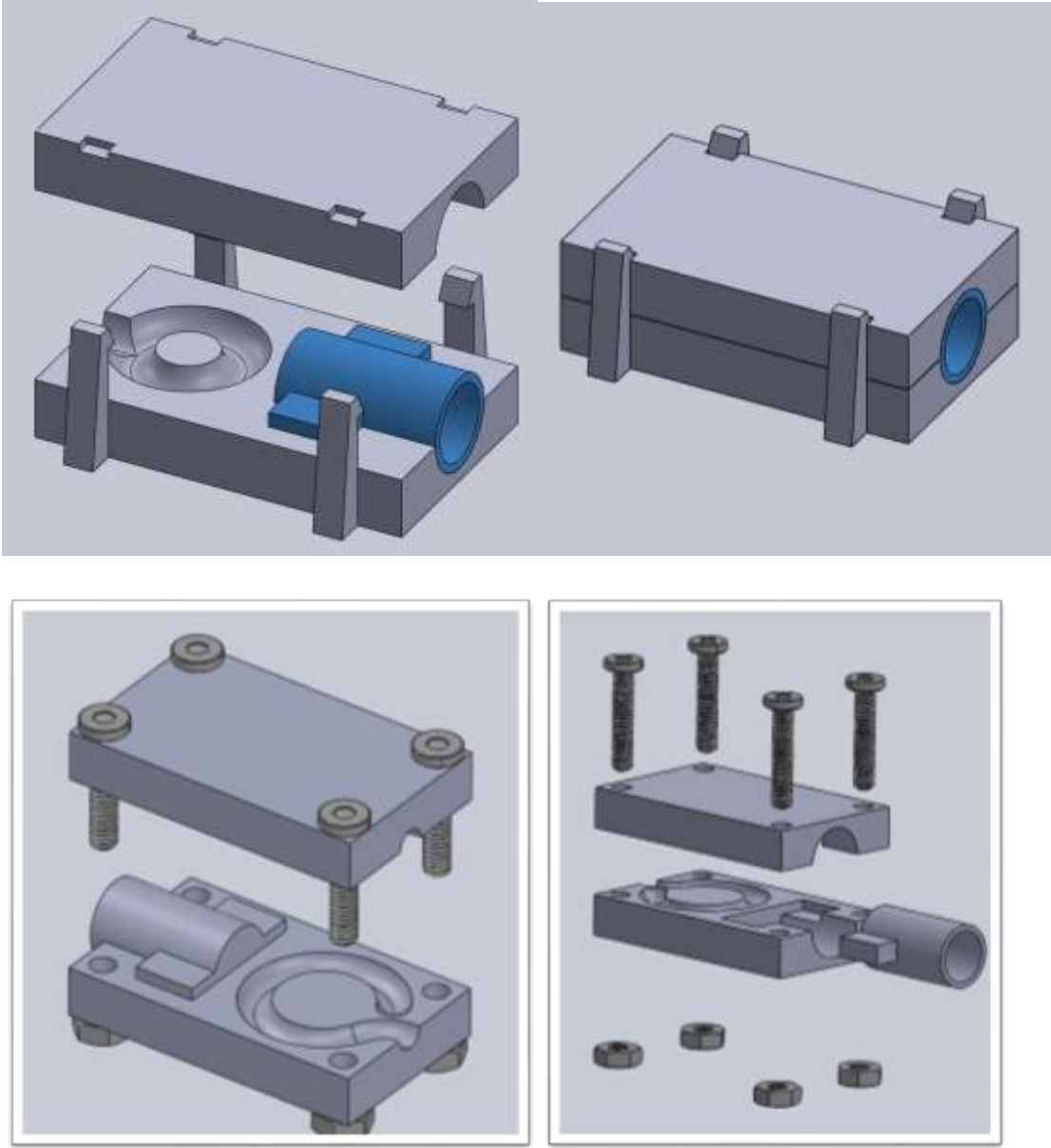


Figure 12: GTR attachment device opened (left) and exploded view (right).

#### 1.4.2 *Buoyancy Materials*

In order to make our clamp system retrievable and therefore reusable, the buoyancy of the entire device must be slightly positive, so that when it releases from the dorsal fin, it will float to the surface of the ocean. In order to do this, a buoyancy foam material will be attached to the mounts that clip onto the bottom of the wiper blade portion of the clamp arm. The foam will need to not only be buoyant enough to float the clamp, but will also need to be resistant to saltwater, biologically inert, and compatible with adhesives (also compatible with the friction pad material) for time periods of up to a week.

Multiple possibilities for this buoyancy material were researched, and the most practical and applicable foam for our application was the “last-a-foam® R-3300 buoyancy foam series, low-density foam for subsea applications” from General Plastics [3]. According to this product’s specifications, it can provide buoyancy in depths up to 2,400 ft. As previously researched, great white sharks do not typically swim at depths deeper than 200 m (~656 ft), therefore the rated depth for the foam is more than adequate. The product specifications also state that the material is biologically inert, compatible with many types of adhesives, able to perform in fresh and salt water, and will not degrade in water. This foam effectively fulfills every requirement necessary for our application.

Another benefit of using this buoyancy foam is that it is available for purchase in sample sizes for only 10 USD. These samples come in dimensions of 6 in x 6 in x 0.5 in thick which would be ideal for this design. Additionally, the foam is available in multiple densities which would allow for further customization to our application to determine the optimal density.

#### 1.4.3 *Friction Materials*

A friction pad will be used to prevent the clamp from sliding up off the dorsal fin it will be attached to the buoyancy material. This friction material will need to have a high coefficient of friction between itself and the shark’s skin. Figure 13 shows the topography of dermal denticles in multiple regions of the shark’s body.

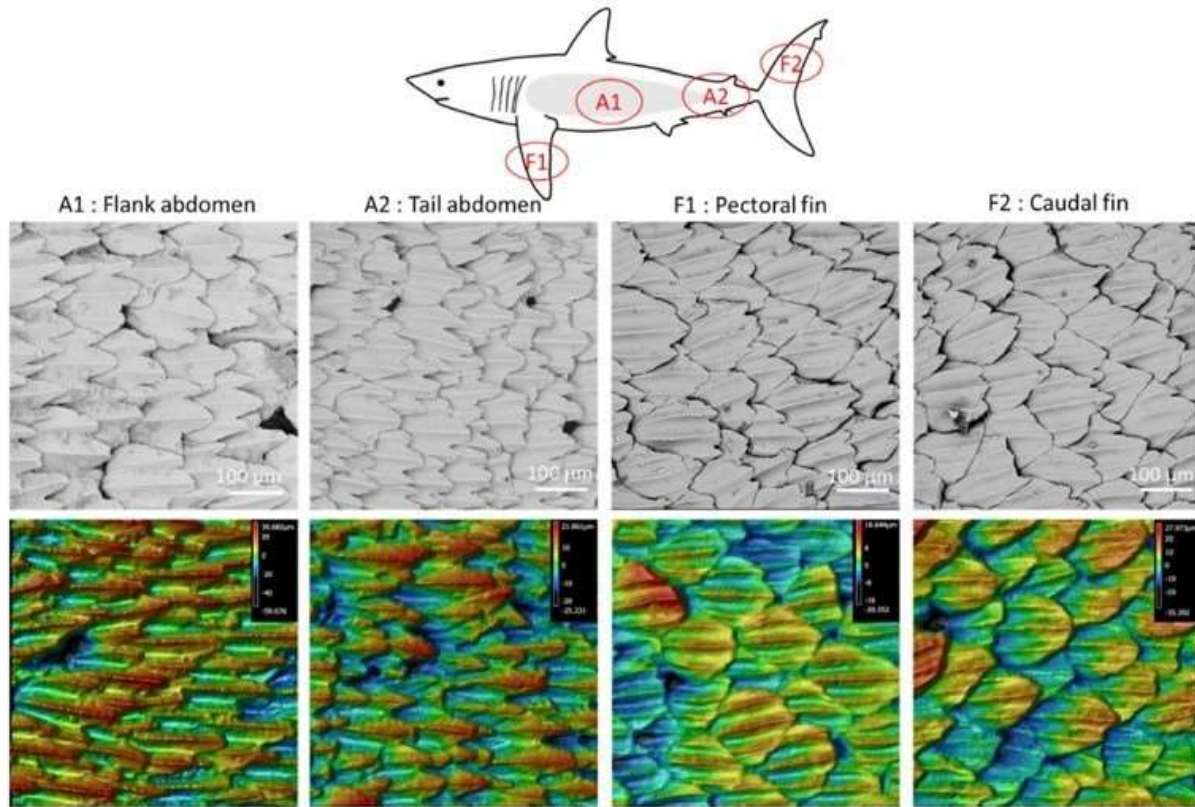


Figure 13: Scanning electron microscope (top) and confocal laser scanning microscope (bottom) images of dermal denticles of the great white shark in four areas of the body [4]

From Figure 13, we determined the peak to valley height of the riblets of the dermal denticles moving vertically. This height difference was then used to compare these regions of the shark's skin to grits of sandpaper; since there are no values for the dorsal fin, the average peak to valley height was used (see Table 2).

Table 2: Ridget heights of regions of the great white shark's body compared to equivalent sandpaper grits

<b>Body Area</b>	<b>Ridget height (valley to peak)</b>	<b>Equivalent Sandpaper Grit</b>
<i>Mid-Abdomen</i>	90 micrometers	225
<i>Tail-Abdomen</i>	46 micrometers	325
<i>Pectoral Fin</i>	39 micrometers	500-325
<i>Caudal Fin</i>	63 micrometers	285-240
<b>Average</b>	<b>59.5 micrometers</b>	<b>285-240</b>

While frictional force is not a function of area, it is dependent on the contact area between the two surfaces. Two very smooth surfaces could generate more friction between them than two very rough surfaces because the overall contact area between grains is higher. As a result, water acts as a barrier between two surfaces and can decrease the coefficient of friction between them [5]. To overcome this, we will use a friction pad with a high coefficient of friction in air. Bani-Hani et al. performed a study on the coefficient of friction between shredded tires and various abrasive surfaces, one of which was sandpaper. The coefficient of friction between sandpaper and various rubber shred sizes are in Table 3 below.

*Table 3: Coefficient of friction between sandpaper and varying sizes of shredded rubber [6].*

<b>Shred Size(mm)</b>	<b>1.18</b>	<b>0.6</b>	<b>0.425</b>	<b>0.3</b>	<b>0.15</b>
<b><math>\mu</math></b>	0.78	0.84	0.9	0.63	0.6

Rubbers that are safe in saltwater and resistant to corrosion from water, NaCl, and magnesium sulfates, include EPDM rubbers, Nitriles, and Kalrez [7]. Tables 4-6 below compare different products for each of these three rubbers based on hardness, tensile strength, resistance to weathering, tear resistance, and water absorption. For these purposes, hardness and weathering resistance are good measures of performance because hardness is a measure of resistance to abrasion.

*Table 4: Comparison of Nitrile products suitable for sea water [8].*

	<i>Buta-N Nitrile</i>	<i>Hydrogenated Nitrile</i>
<i>Hardness</i>	40 Shore A	50 Shore A
<i>Tensile Strength</i>	Good	Excellent
<i>Weathering Resistance</i>	Poor	Good
<i>Tear Resistance</i>	Good	Good
<i>Water Absorption</i>	Good	Excellent

Table 5: Comparison of Kalrez products suitable for sea water [9].

	Kalrez 1050 LF	Kalrez 6190
<i>Hardness</i>	82 Shore A	74 Shore A
<i>Tensile Strength</i>	2698 psi	2657 psi
<i>Weathering Resistance</i>	-	-
<i>Tear Resistance</i>	-	-
<i>Water Absorption</i>	-	-

Table 6: Comparison of EPDM products suitable for sea water [10].

	Commercial Grade 60A	Closed Cell PSA blend	Closed Cell EPDM	Closed Cell Blend
<i>Hardness</i>	60 Shore A	20-25 Shore C	15 Shore C	20-25 Shore C
<i>Tensile Strength</i>	725 psi	149 psi	65 psi	149 psi
<i>Weathering Resistance</i>	Outstanding weathering, UV, and ozone resistance	Very good weathering, UV, and ozone resistance	Very good weathering, UV, and ozone resistance	Very good weathering, UV, and ozone resistance
<i>Tear Strength</i>	-	<449 psi	449 psi	449 psi
<i>Water Absorption</i>	0%	3-5%	<5%	3%

From these comparisons between products, the top rubbers from each category are hydrogenated nitrile, commercial grade 60A EPDM, and Kalrez 1050 F. Because the websites were not all uniform in their methods of measuring and comparing rubbers, tests will be necessary to determine which of these three will provide the best friction surface.

In summary, this clamp design utilizes components of previous designs that have worked and incorporates adaptations to the clamp attachment process, arms, friction pads,

and buoyancy to fulfill Dr. Skomal's intended use. A full design sketch of the clamp with each of its components is shown in Figure 14.

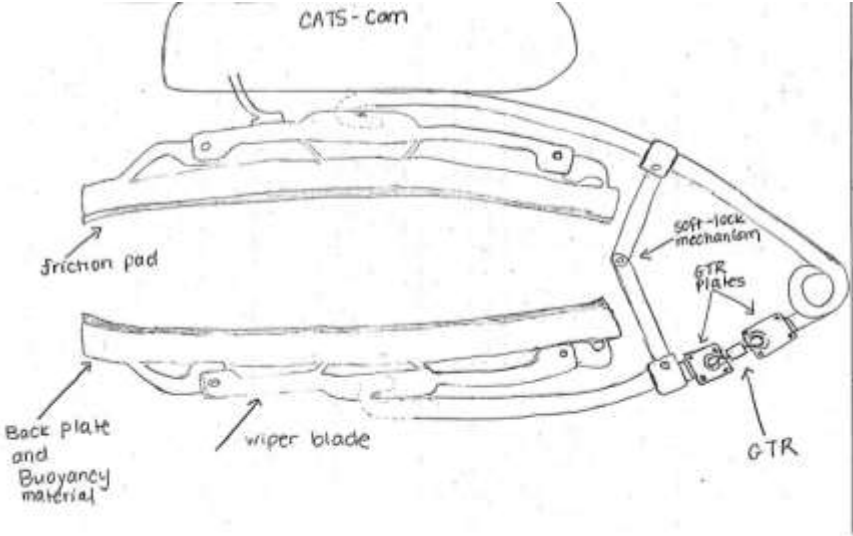


Figure 14: Full clamp design with components

## Works Cited

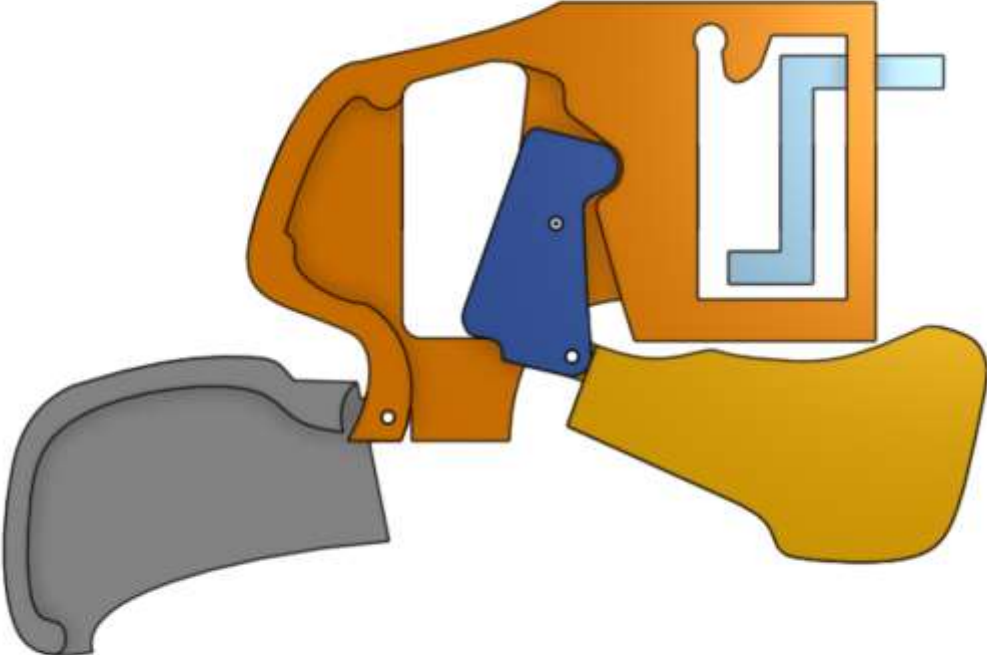
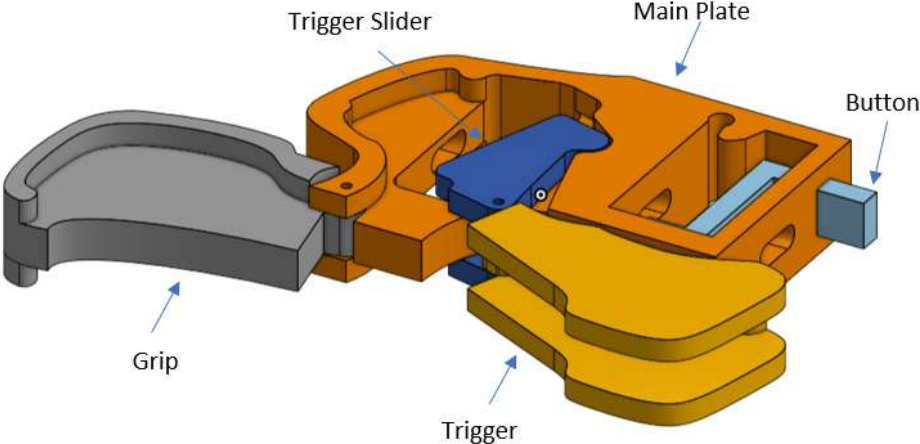
- [1] M. F. Beckert, B.E. Nadler, J.H., "Remora fish suction pad attachment is enhanced by spinule friction," *The Company of Biologists*, vol. 218, pp. 3551-8, 2015.
- [2] M. Beckert, "Mechanics of Remora Adhesion," Doctor of Philosophy in Mechanical Engineering, Mechanical Engineering, Georgia Institute of Technology, 2015.
- [3] (2020). *Subsea Foam Buoyancy Foam Manufacturer*. Available: <https://www.generalplastics.com/markets/subsea?pmc=AW-1>
- [4] H. W. C. Chien, XY. Tsai, WP. Lee, M, "Inhibition of biofilm formation by rough shark skin-patterned surfaces," *Colloids and Surfaces B: Biointerfaces*, vol. 186, pp. 1-9, 2020.
- [5] M. Consulting. *Rubber Friction Research*. Available: <http://www.multiscaleconsulting.com/our-research/rubber-friction>
- [6] E. L. Bani-Hani, J. Mohanan, G., "Data on the coefficient of static friction between surfaces coated with different sizes of rubber granules produced from used tires," *Data in Brief*, vol. 22, 2019.
- [7] M. Inc. (2019). *Rubber Chemical Resistance Chart*. Available: <https://mykin.com/rubber-chemical-resistance-chart>
- [8] M. Inc. (2019). *Rubber Properties*. Available: <https://mykin.com/rubber-properties>
- [9] Dupont. (2020). *Kalrez*. Available: <https://www.knowde.com/stores/dupont/products/kalrez-1050lf>
- [10] RubberCal. (2019). *EPDM Rubber*. Available: [https://www.rubbercal.com/sheet-rubber/epdm-rubber/?gclid=Cj0KCQiAqdP9BRDVARIsAGSZ8AnZpxUMs49yAN0qNadM6gq1YTUgVXout46ryMAnyqZ9NldnuC5YP0IaAo81EALw\\_wcB](https://www.rubbercal.com/sheet-rubber/epdm-rubber/?gclid=Cj0KCQiAqdP9BRDVARIsAGSZ8AnZpxUMs49yAN0qNadM6gq1YTUgVXout46ryMAnyqZ9NldnuC5YP0IaAo81EALw_wcB)

## Appendix E: Material and Manufacturing Process by component

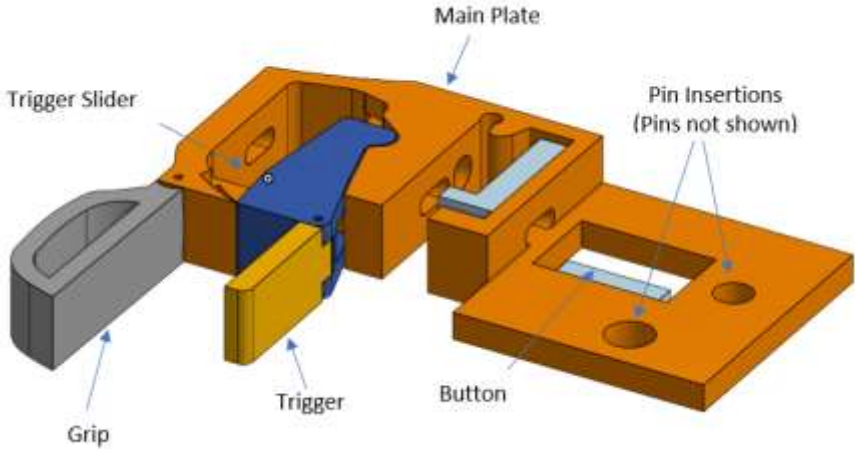
Component	Material	Manufacturing Process
Hydrofoil	Carbon fiber	Purchased as is
Bike brake plates and wings	5052 Aluminum	Laser cut by Send-cut-send
Bike brake bolts	316 Stainless	Purchased as is
Bike brake bushings	N/A	Purchased as is
Bike brake	N/A	Purchased as is
Pole adapter piece	Resin	3D printed
Endplates	5052 Aluminum	CNC Mill
Spacer pins	316 Stainless	CNC Lathe
Sliding pin	316 Stainless	CNC Lathe
Clamp opening pin	316 Stainless	CNC Lathe
Locking Plate	316 Stainless	Water jet cut
Release button	316 Stainless	Water jet cut
Sliding bar	316 Stainless	CNC Mill
Offset arm	316 Stainless	CNC Mill
Top and bottom plate of clamp opener	5052 Aluminum	Outsourced to AM 3D & CNC Fabrication LLC
Internal body of clamp opener	PLA	3D printed
Trigger	5052 Aluminum	CNC Mill
Grip	5052 Aluminum	CNC Mill

# Appendix F: Drawings of Initial Iterations of Clamp Opener Design

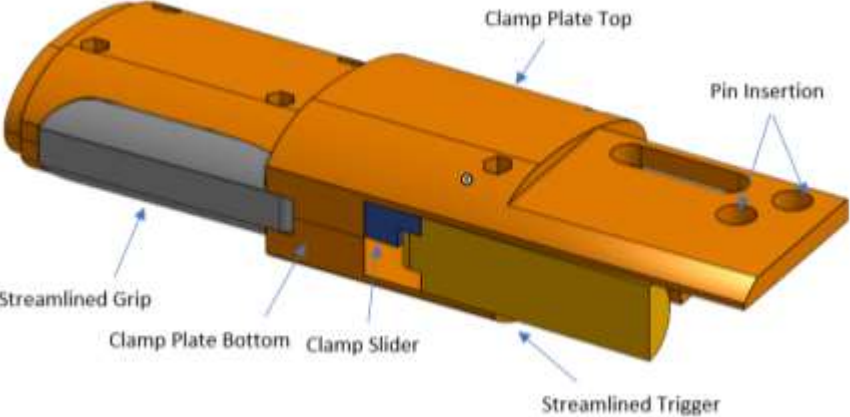
Iteration 1

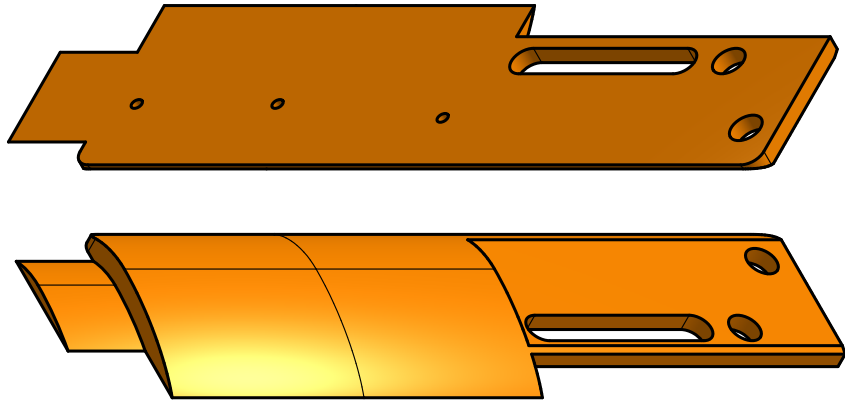
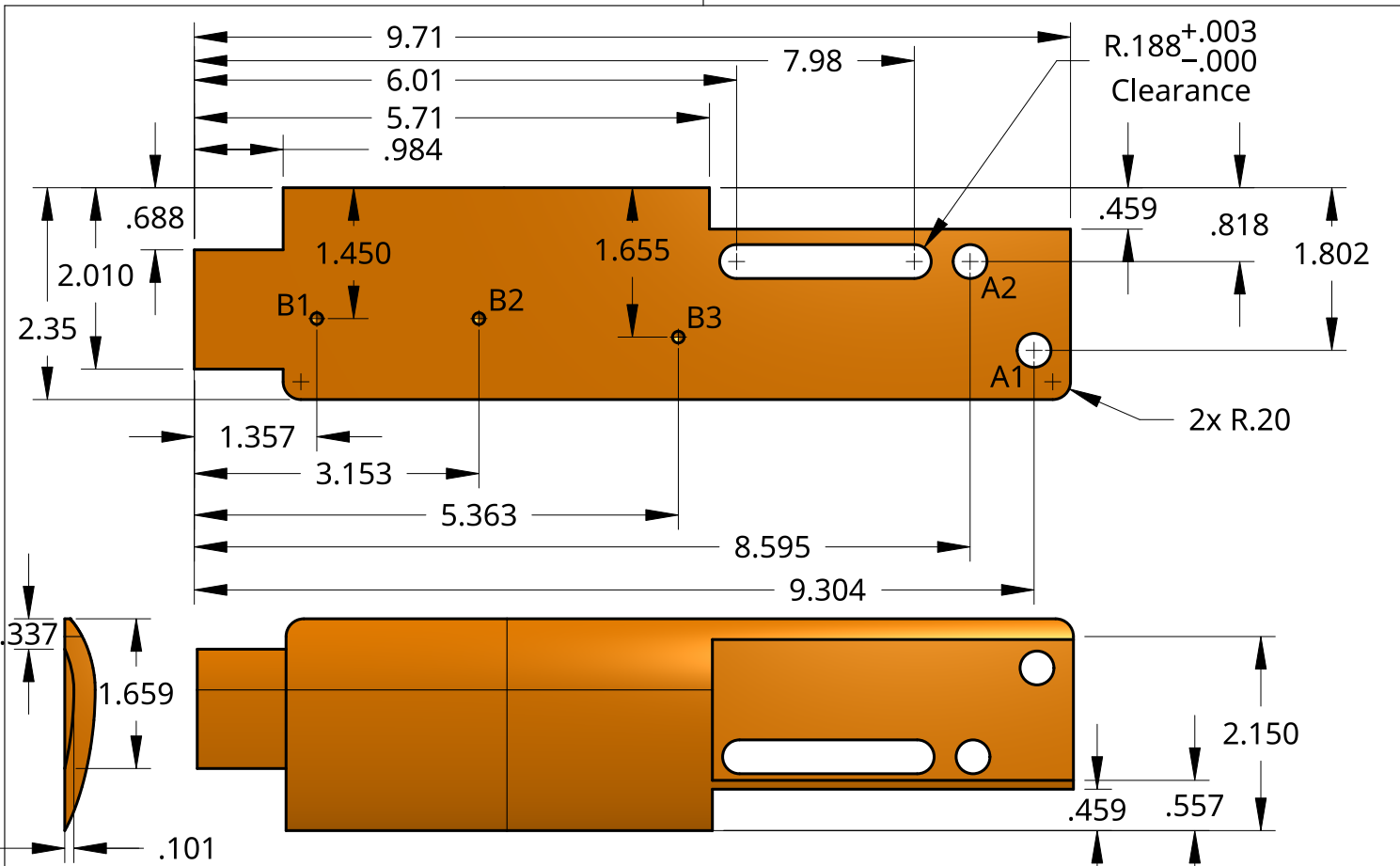


Iteration 2

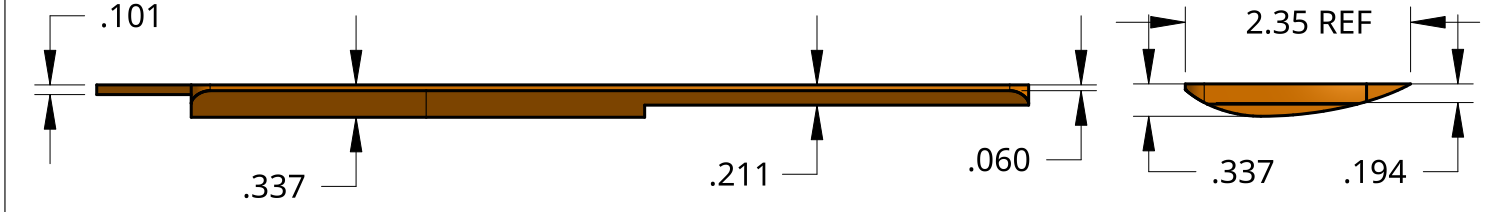


Iteration 3





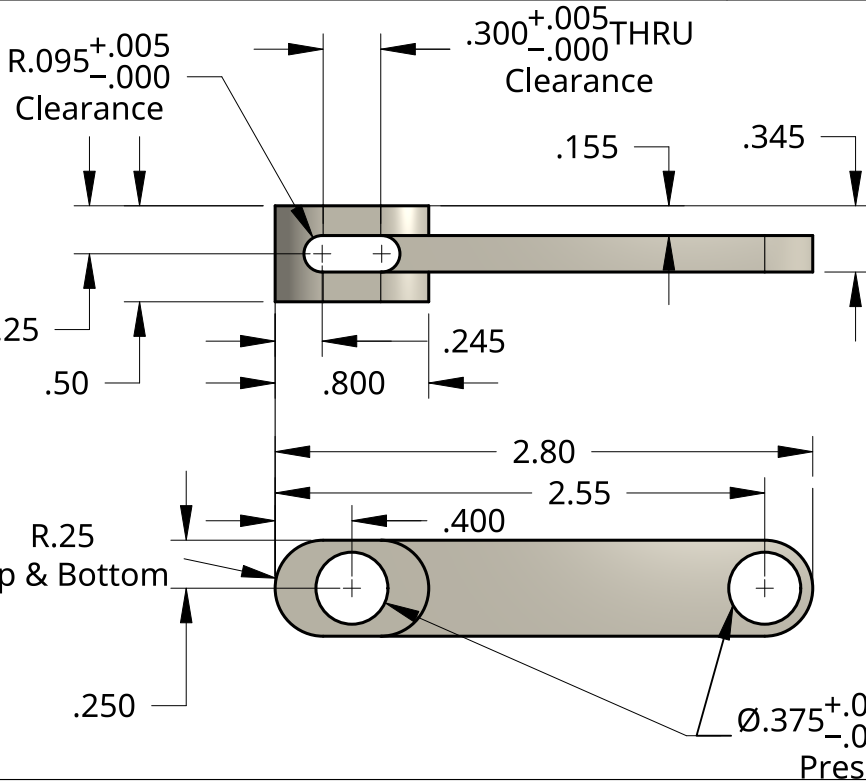
TAG	SIZE	QTY
A1	Ø.375 +.003 -.000 THRU Clearance	2
A2		
B1	∇.200 M4x0.7 Do not Break THRU	3
B2		
B3		



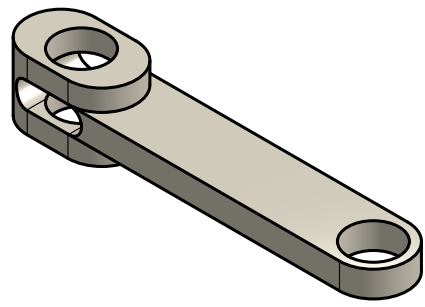
UNLESS OTHERWISE SPECIFIED, DIMENSIONS ARE IN INCHES .XX = ±.01 .XXX = ±.005 .XXXX = ±.000- SURFACE FINISH	DRAWN	NAME	DATE	TITLE <h3>Bottom plate clamp opener</h3>	
	CHECKED	BROOKE DAWSON	02/26/2021		
	APPROVED				
	DO NOT SCALE DRAWING				
BREAK ALL SHARP EDGES AND REMOVE BURRS				SIZE	DWG NO.
THIRD ANGLE PROJECTION	MATERIAL	FINISH		A	
	5052 AI			SCALE	WEIGHT
				1:2	SHEET
					1 of 1

2

1



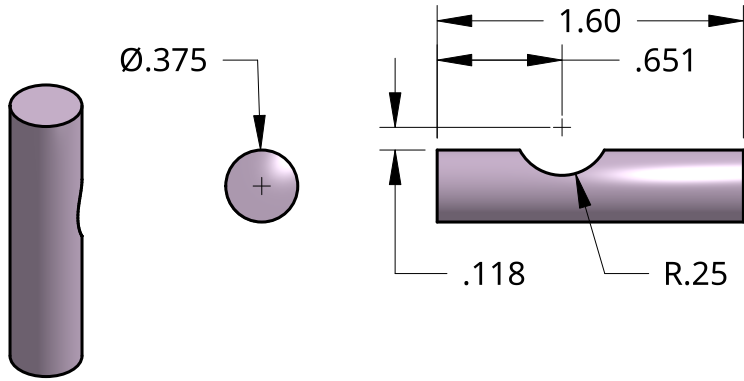
Offset Arm



QTY
1

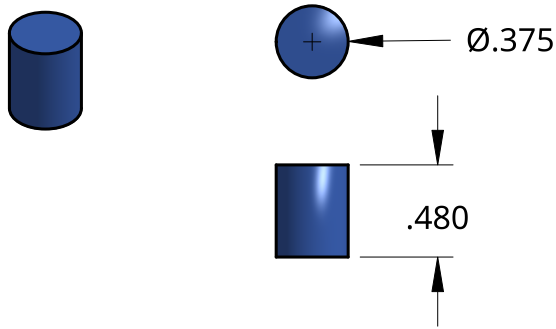
B

B



Clamp Opener Pin

QTY
2



Slider Pins

QTY
3

A

A

UNLESS OTHERWISE SPECIFIED, DIMENSIONS ARE IN INCHES .XX = ±.01 .XXX = ±.005 .XXXX = ±.000- SURFACE FINISH $\sqrt{\quad}$ DO NOT SCALE DRAWING BREAK ALL SHARP EDGES AND REMOVE BURRS THIRD ANGLE PROJECTION	DRAWN	NAME	DATE	TITLE <h3>Clamp Opener Shaft Alternative</h3>	
	CHECKED	ARAM SOULTANIAN	03/02/2021		
	APPROVED				
	MATERIAL	FINISH	SIZE	DWG NO.	REV.
	316 SS		A		
			SCALE	WEIGHT	SHEET
			1:1		1 of 1

2

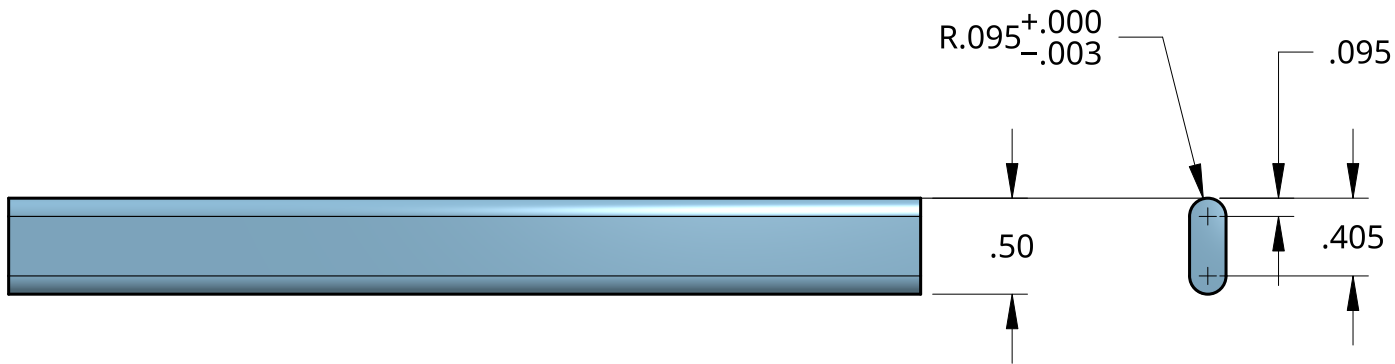
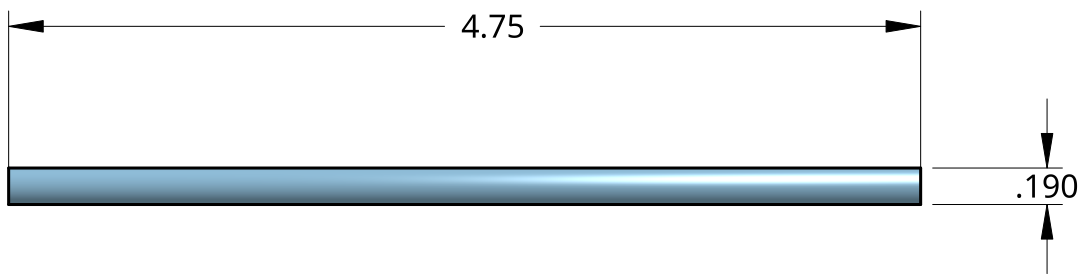
1

2

1

B

B



A

A

Qty
2

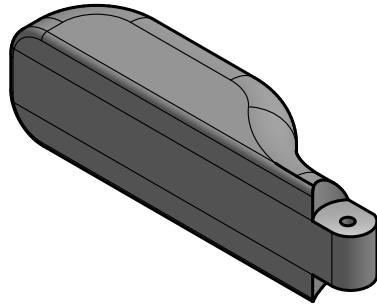
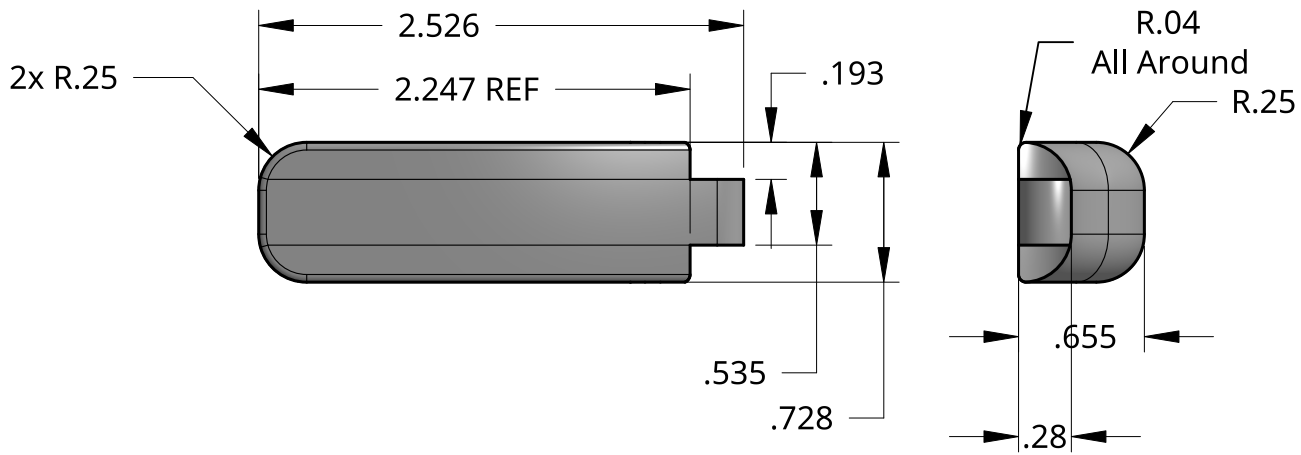
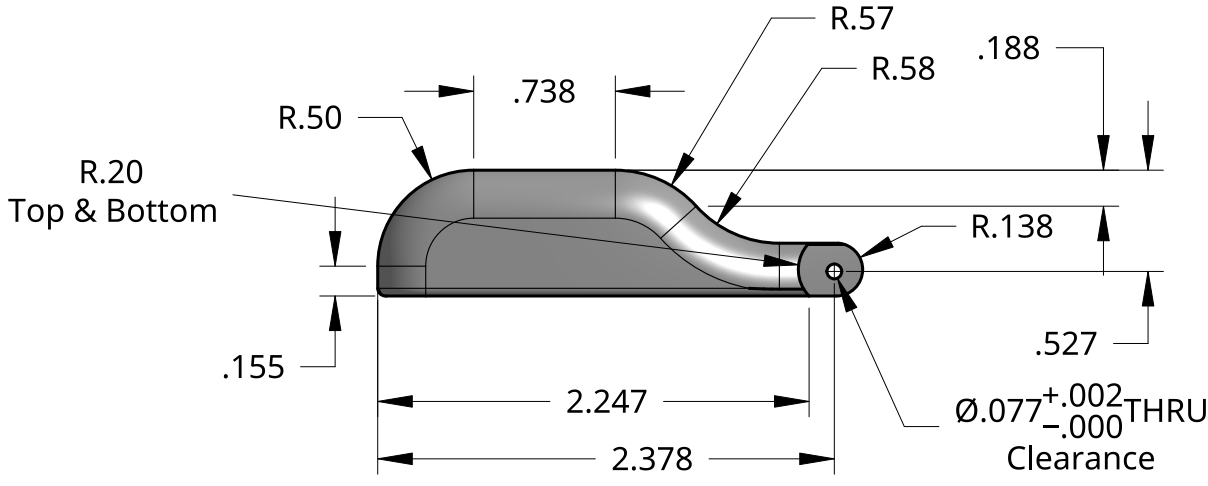
UNLESS OTHERWISE SPECIFIED, DIMENSIONS ARE IN MILLIMETERS .XX = ±.01 .XXX = ±.005 .XXXX = ±.000 SURFACE FINISH	DRAWN	ARAM SOULTANIAN	03/02/2021	TITLE <h3 style="text-align: center;">Clamp Opener Shaft</h3>
	CHECKED			
	APPROVED			
	DO NOT SCALE DRAWING			
BREAK ALL SHARP EDGES AND REMOVE BURRS THIRD ANGLE PROJECTION 	MATERIAL	316 SS	FINISH	SIZE <b>A</b> SCALE 1:1 DWG NO. 1 WEIGHT SHEET 1 of 1 REV.

2

1

2

1



UNLESS OTHERWISE SPECIFIED, DIMENSIONS ARE IN INCHES .XX = ±.01 .XXX = ±.005 .XXXX = ±.000- SURFACE FINISH $\sqrt{\quad}$ DO NOT SCALE DRAWING BREAK ALL SHARP EDGES AND REMOVE BURRS THIRD ANGLE PROJECTION 	DRAWN	NAME	DATE	TITLE <h2 style="text-align: center;">Grip</h2>	
	CHECKED	BROOKE DAWSON	02/26/2021		
	APPROVED				
	MATERIAL	FINISH	SIZE	DWG NO.	REV.
	5052 AI		A		
			SCALE	WEIGHT	SHEET
			1:1		1 of 1

2

1

B

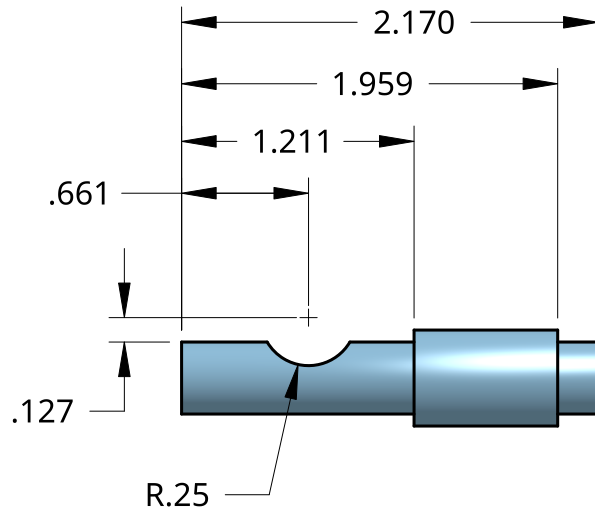
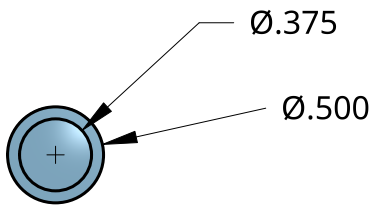
B

A

A

2

1



UNLESS OTHERWISE SPECIFIED,  
DIMENSIONS ARE IN INCHES

.XX = ±.01  
.XXX = ±.005  
.XXXX = ±.000

ANGULAR = ± 1°  
FRACTIONAL = ±

SURFACE FINISH

DO NOT SCALE DRAWING

BREAK ALL SHARP EDGES AND  
REMOVE BURRS

THIRD ANGLE PROJECTION



	NAME	DATE
DRAWN	BROOKE DAWSON	02/26/2021
CHECKED		
APPROVED		

MATERIAL	FINISH
5052 Al	

SIZE	DWG NO.	REV.
A		

TITLE		
Press Fit Spacer		

SCALE	WEIGHT	SHEET
1:1		1 of 1

2

1

B

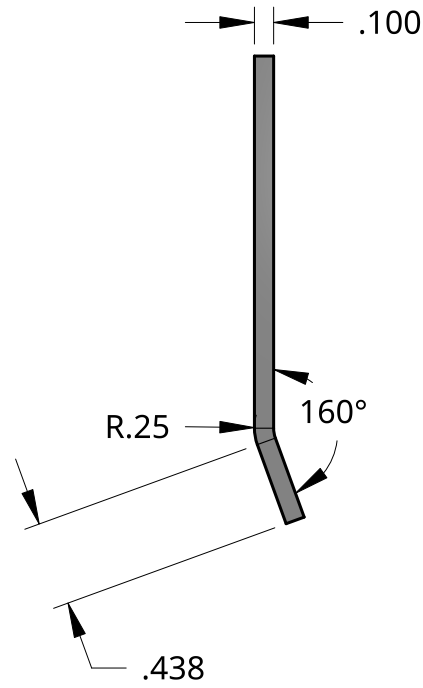
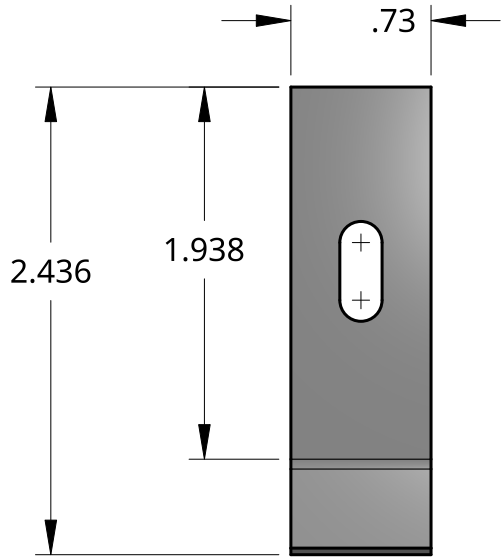
B

A

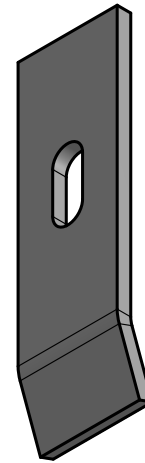
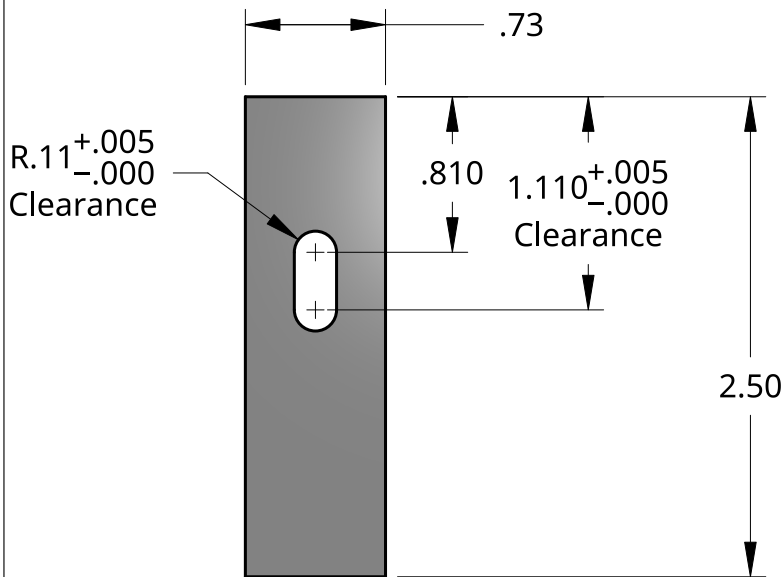
A

2

1



2D Sheet Metal Form  
Waterjet Profile



UNLESS OTHERWISE SPECIFIED, DIMENSIONS ARE IN INCHES .XX = ±.01 .XXX = ±.005 .XXXX = ±.000- SURFACE FINISH <input checked="" type="checkbox"/> DO NOT SCALE DRAWING BREAK ALL SHARP EDGES AND REMOVE BURRS THIRD ANGLE PROJECTION 	DRAWN	NAME	DATE	TITLE <p style="text-align: center;">Release 1</p>	
	CHECKED	ARAM SOULTANIAN	03/02/2021		
	APPROVED				
	MATERIAL	FINISH	SIZE	DWG NO.	REV.
	316 SS		A		
			SCALE	WEIGHT	SHEET
			1:1		1 of 1

2

1

B

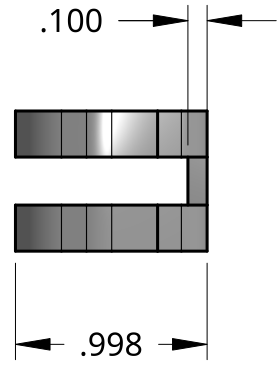
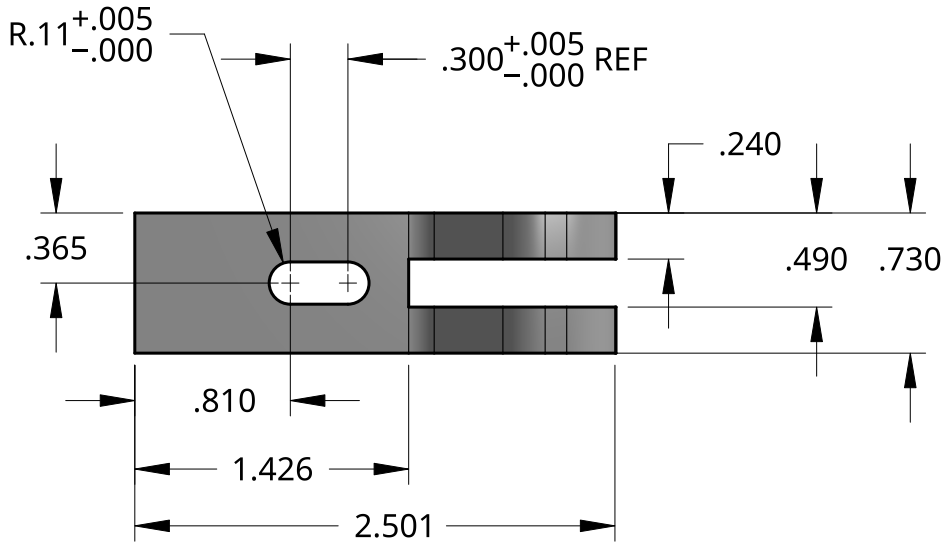
B

A

A

2

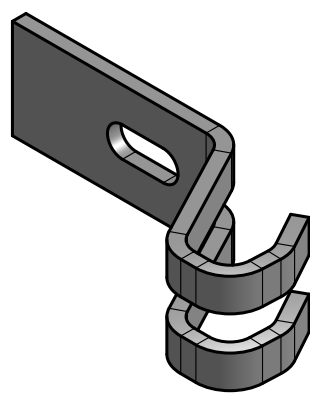
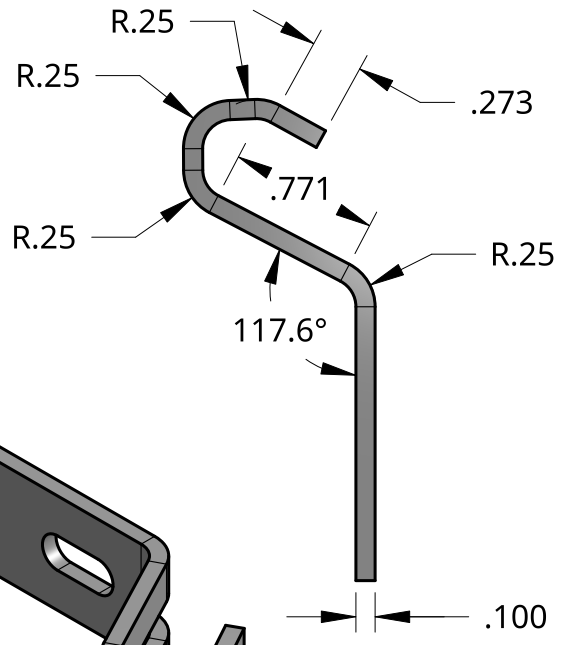
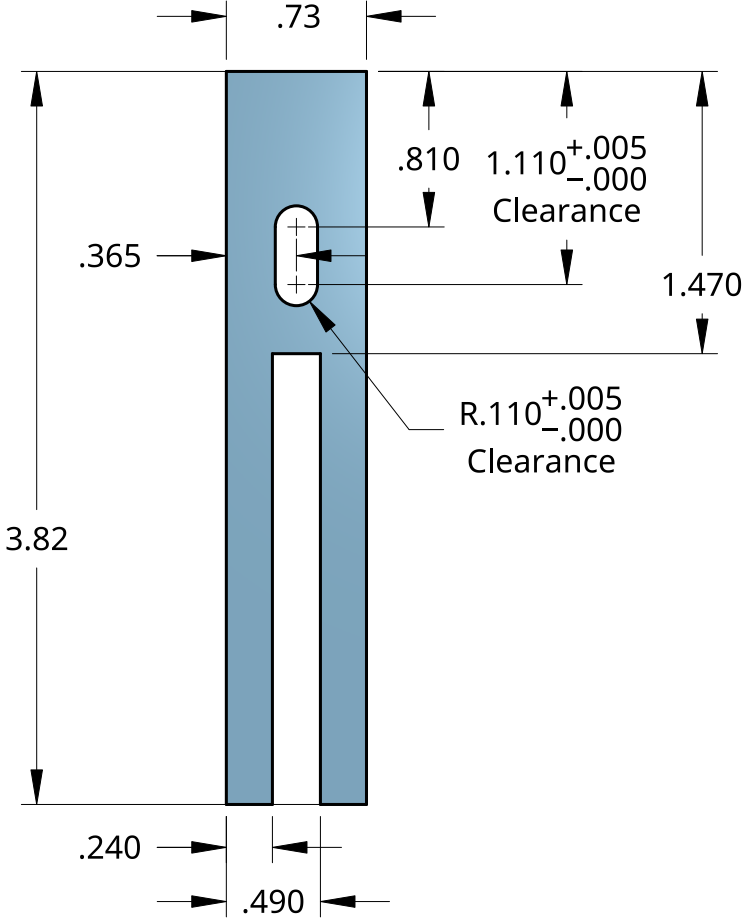
1



B

B

2D Sheet Metal Form  
Waterjet Profile



Bends do not have to  
be perfectly to spec

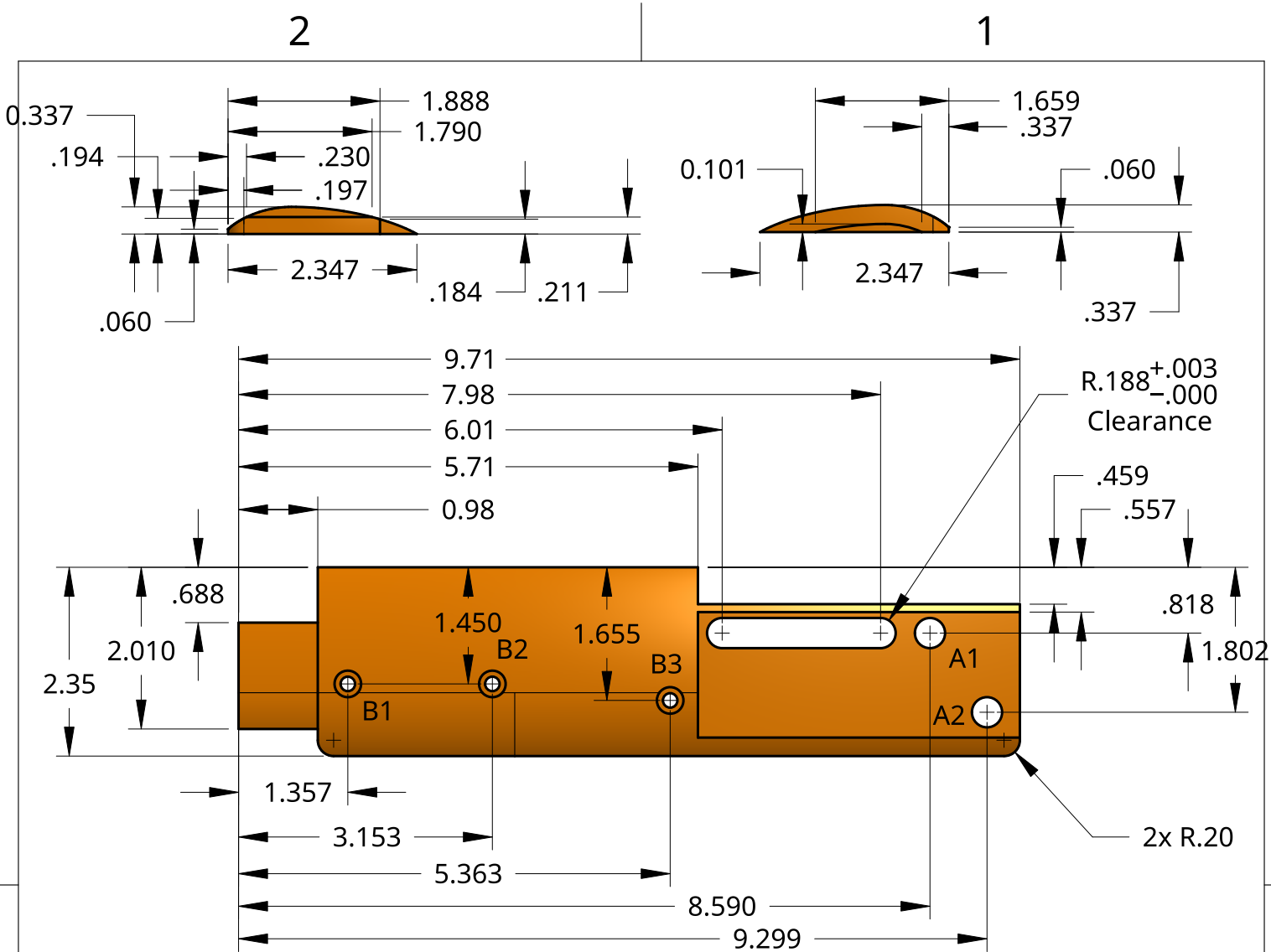
A

A

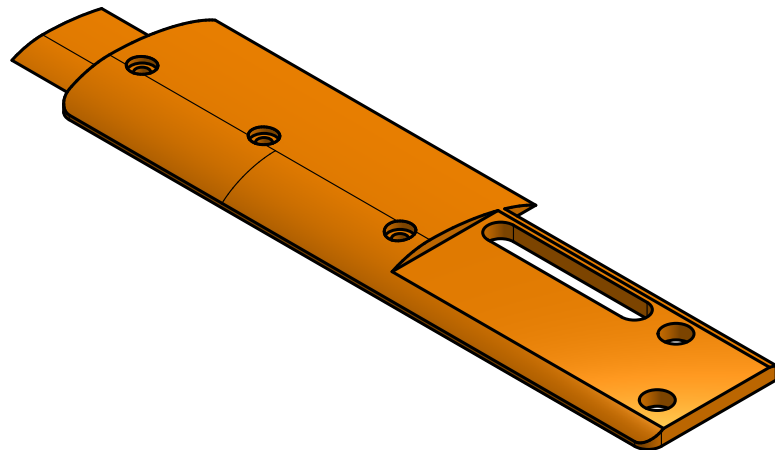
UNLESS OTHERWISE SPECIFIED, DIMENSIONS ARE IN INCHES .XX = ±.01 .XXX = ±.005 .XXXX = ±.000- SURFACE FINISH	DRAWN	NAME	DATE	TITLE  <b>Release 2</b>	
	CHECKED	ARAM SOULTANIAN	03/02/2021		
	APPROVED				
	DO NOT SCALE DRAWING				
BREAK ALL SHARP EDGES AND REMOVE BURRS THIRD ANGLE PROJECTION 	MATERIAL	FINISH	SIZE	DWG NO.	REV.
	316 SS		<b>A</b>		
			SCALE	WEIGHT	SHEET
			1:1		1 of 1

2

1



TAG	SIZE	QTY
A1	Ø.375 THRU +.000, -.002 Press Fit	2
A2		
B1	Ø .180 THRU └─┤ Ø.330 ─┘ .080	3
B2		
B3		
For specific hole locations, see Bottom Plate Drawing		



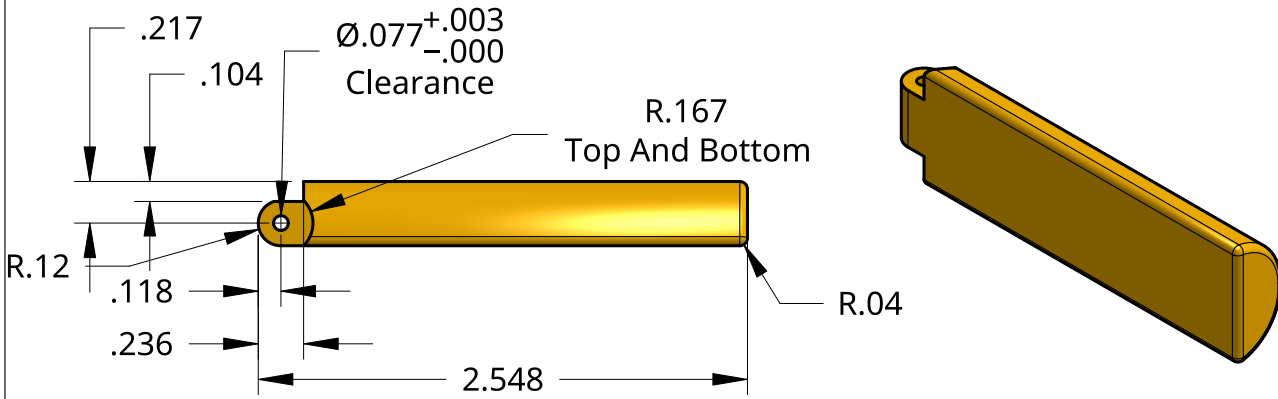
UNLESS OTHERWISE SPECIFIED, DIMENSIONS ARE IN MILLIMETERS .XX = ±.01 .XXX = ±.005 .XXXX = ±.000 SURFACE FINISH $\sqrt{\quad}$ DO NOT SCALE DRAWING BREAK ALL SHARP EDGES AND REMOVE BURRS THIRD ANGLE PROJECTION 	DRAWN	ARAM SOULTANIAN	DATE	02/26/2021	TITLE	Clamp Opener Top	
	CHECKED						
	APPROVED						
	MATERIAL	5052 Al		FINISH		SIZE	A
						DWG NO.	
					SCALE	1:2	
					WEIGHT		
					SHEET	1 of 1	

2

1

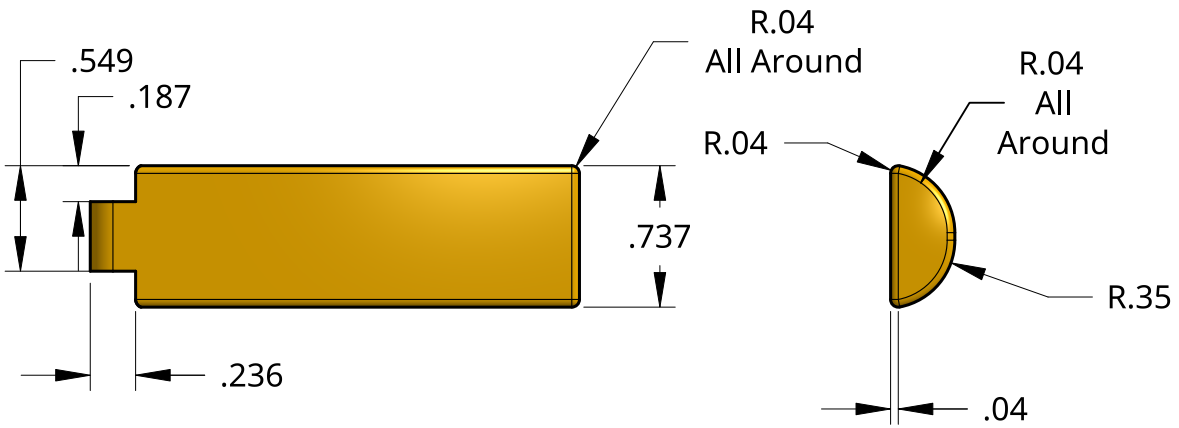
B

B



A

A



UNLESS OTHERWISE SPECIFIED, DIMENSIONS ARE IN INCHES

.XX = ±.01  
.XXX = ±.005  
.XXXX = ±.000

ANGULAR = ± 1°  
FRACTIONAL = ±

SURFACE FINISH

DO NOT SCALE DRAWING

BREAK ALL SHARP EDGES AND REMOVE BURRS

THIRD ANGLE PROJECTION



	NAME	DATE
DRAWN	BROOKE DAWSON	02/26/2021
CHECKED		
APPROVED		

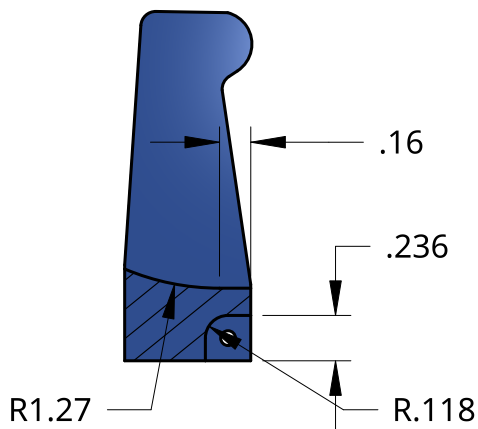
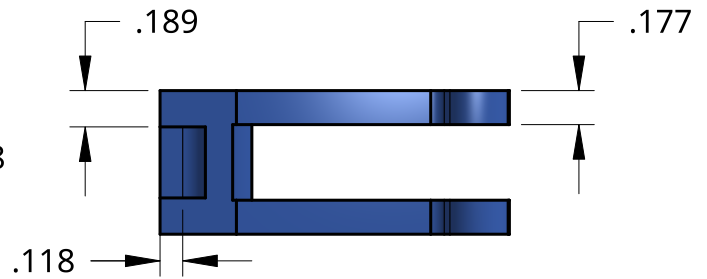
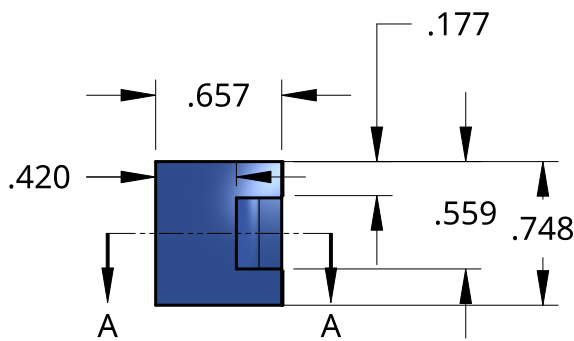
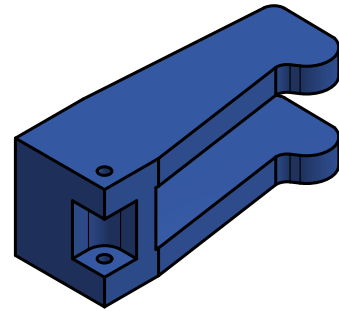
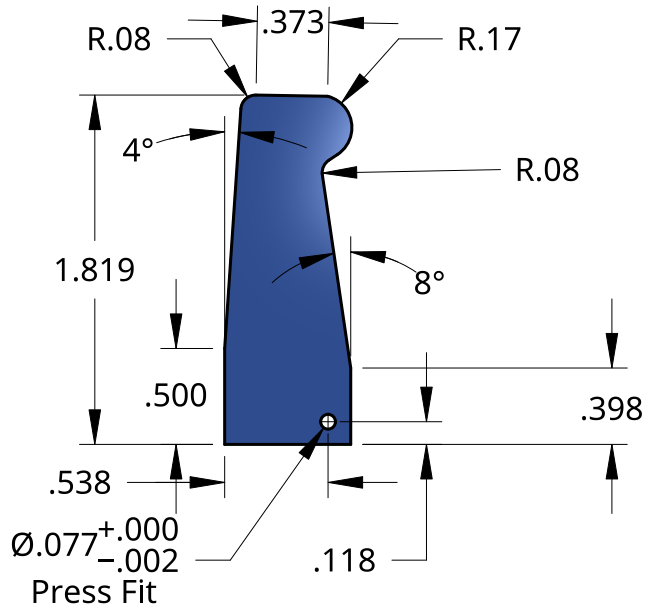
TITLE		
Trigger		
SIZE	DWG NO.	REV.
A		

MATERIAL	FINISH
5052 Al	

SCALE	WEIGHT	SHEET
1:1		1 of 1

2

1



UNLESS OTHERWISE SPECIFIED,  
DIMENSIONS ARE IN INCHES

.XX = ±.01  
.XXX = ±.005  
.XXXX = ±.0005

ANGULAR = ± 1°  
FRACTIONAL = ±

SURFACE FINISH  $\sqrt{\quad}$

DO NOT SCALE DRAWING

BREAK ALL SHARP EDGES AND  
REMOVE BURRS

THIRD ANGLE PROJECTION

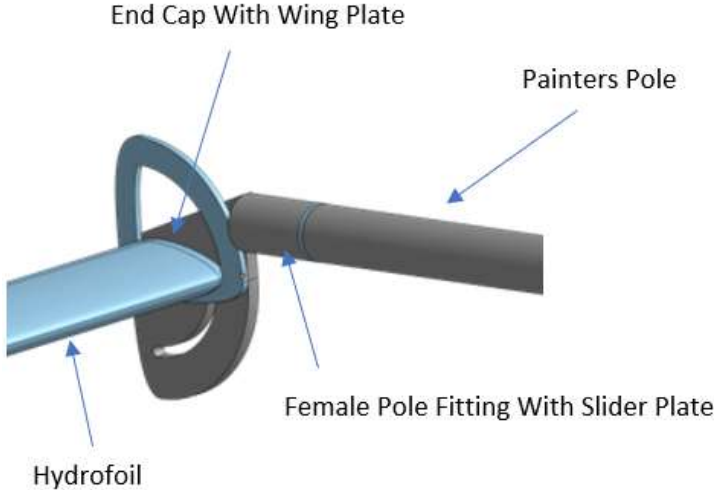


NAME	DATE
DRAWN BROOKE DAWSON	02/26/2021
CHECKED	
APPROVED	

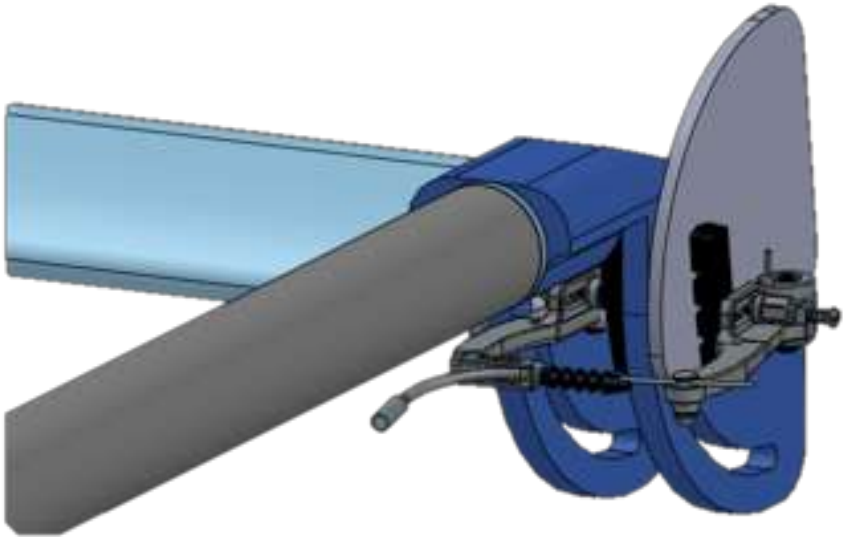
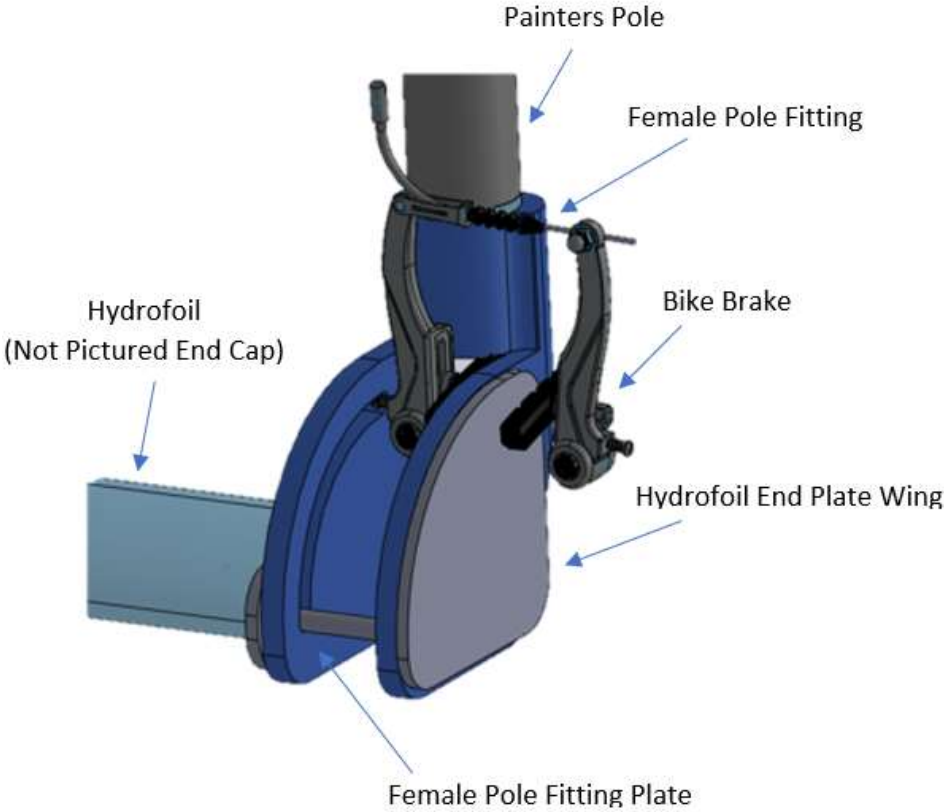
TITLE <b>Clamp Slider</b>		
SIZE <b>A</b>	DWG NO.	REV.
SCALE 1:1	WEIGHT	SHEET 1 of 1

# Appendix H: Drawings of Initial Iterations of Bike Brake Design

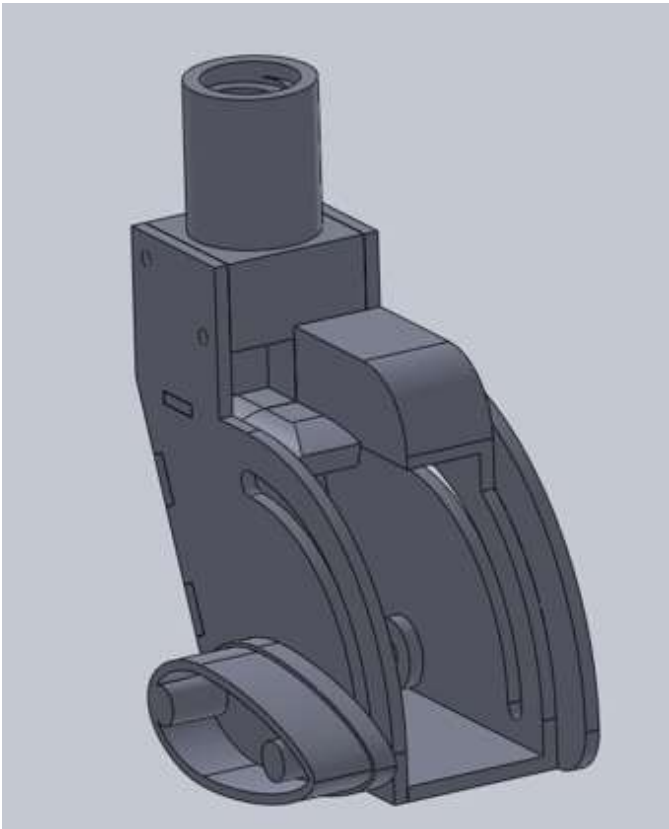
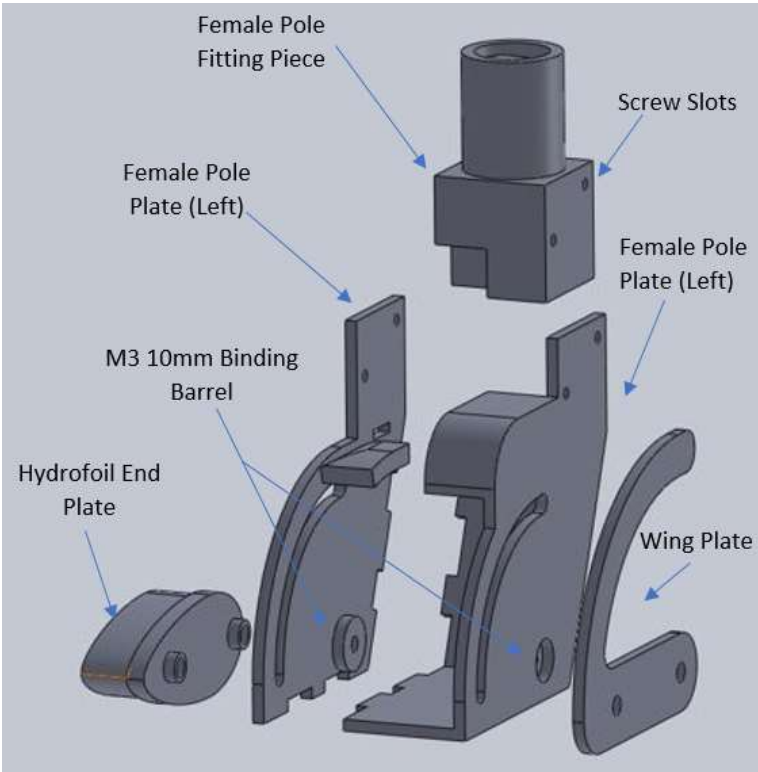
## Iteration 1



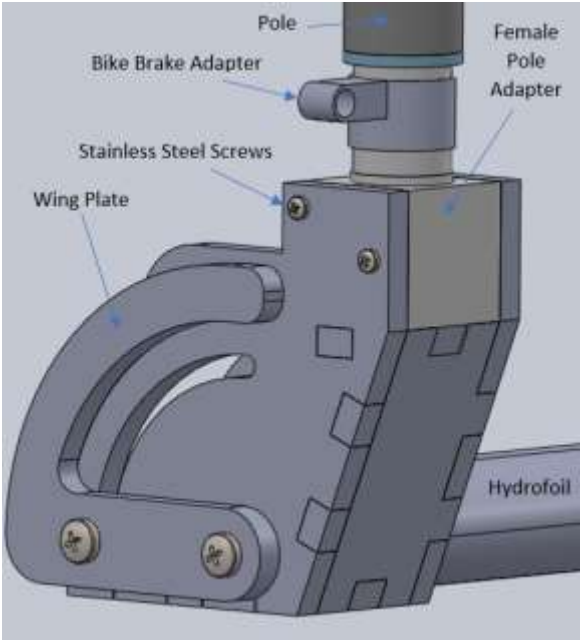
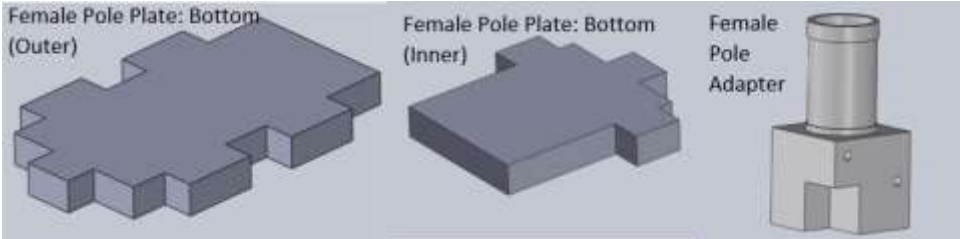
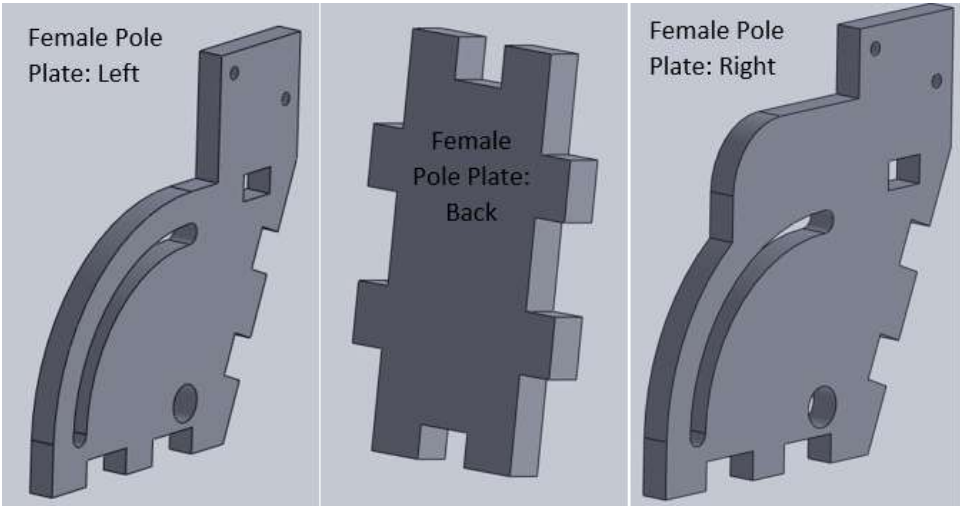
Iteration 2



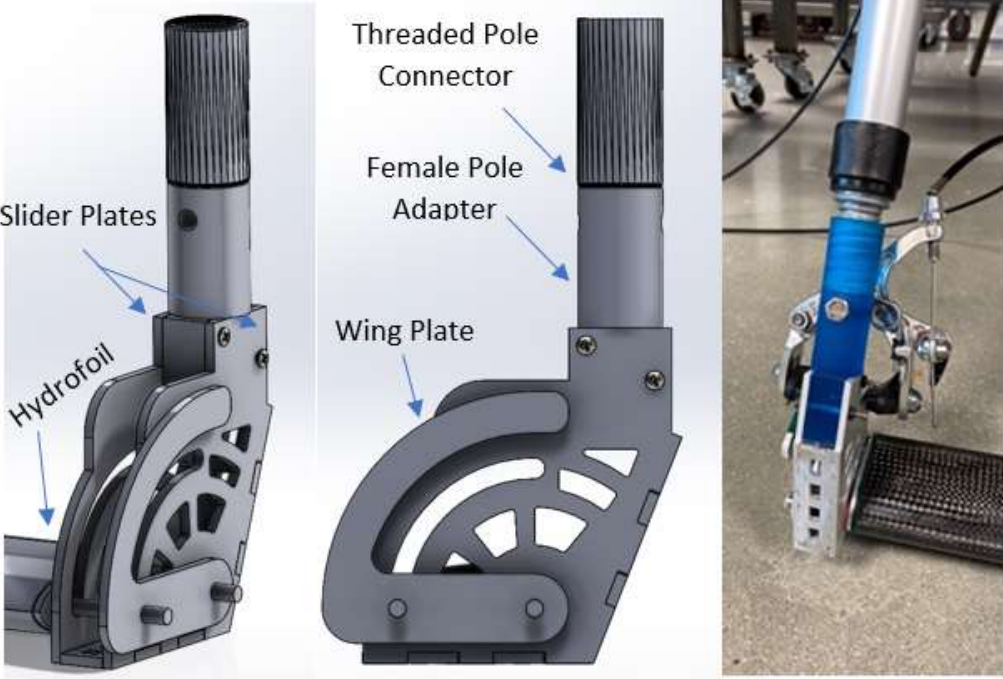
Iteration 3



Iteration 4



# Appendix I: Drawings of Final Iteration of Bike Brake Design



## Appendix J: Pole Deflection Calculations

Calculations for the pole

Assumptions

1. in air the pole is horizontal
2. the hands are 3 feet apart, with the rear hand acting as fully constrained and the front hand as a simple support
3. E and I are constant throughout
4. the pole is 10 feet long
5. The material is aluminum
6. in the water the pole is held at 45 degrees to the water

Model:

1. The rear hand generates a force in the Y and a moment about the Z at 0
2. The front hand generates a force in the Y at A
3. The weight of the tag is a force in the Y at L (for air)
4. The weight of the pole is a uniformly distributed load from 0-L
5. The drag force perpendicular to the pole is a force in the Y at L (for water)

Known Values

$$\text{massdensity} := \frac{159.191}{(12^3)} = 0.092 \quad \underline{\underline{A}} := 3 \cdot 12 \quad r := \frac{1.86}{2} = 0.93 \quad \underline{\underline{L}} := 12 \cdot (\sqrt{2 \cdot 8^2})$$

$$\text{Volume} := \frac{4.02}{\text{massdensity}}$$

$$\text{OD} := 2 \cdot r = 1.86$$

$$\text{Area} := \frac{\text{Volume}}{L}$$

$$\text{ID} := 2 \cdot \sqrt{\frac{-\text{Area}}{\pi} + \left(\frac{\text{OD}}{2}\right)^2} = 1.747$$

$$t := r - \left(\frac{\text{ID}}{2}\right) = 0.057$$

$$E := 12328200$$

Based on Dimensions

$$I := \pi \cdot \frac{(\text{OD}^4 - \text{ID}^4)}{64} \quad \underline{\underline{\text{Area}}} := \pi \cdot \left[ \left(\frac{\text{OD}}{2}\right)^2 - \left(\frac{\text{ID}}{2}\right)^2 \right]$$

Load

$$P := \text{massdensity} \cdot \text{Area}$$

$$w := 5$$

$$\text{In water } w = 7.6647$$

$$\text{In air } : w = 5 \text{ lb}$$

temporary variables

$$M := 800$$

$$\underline{\underline{R}} := 100$$

$$\underline{\underline{F}} := 100$$

$$C1 := 10$$

$$C2 := 10$$

Define singularity function

$$\underline{\underline{S}}(x, z) := \text{if}(x \geq z, 1, 0)$$

Solve for the reactions in equation form using boundary conditions

Given

from the shear boundary condition being 0 at L

$$0 = -M \cdot 0 + R \cdot (L - 0)^0 + F \cdot (L - A)^0 - w \cdot (L - L)^0 - P \cdot (L - 0)^1$$

from moment boundary condition being 0 at L

$$0 = -M + R \cdot (L - 0)^1 + F \cdot (L - A)^1 - w \cdot (L - L)^1 - \frac{P}{2} \cdot (L - 0)^2$$

From angle boundary conditions being zero at 0

$$0 = M(0 - 0)^1 + \frac{R}{2} \cdot (0 - 0)^2 + \frac{F}{2} \cdot (0 - A)^2 - \frac{w}{2} \cdot (0 - L)^1 - \frac{P}{6} \cdot (0 - 0)^3 + C1$$

from deflection boundary conditions being zero at 0 and A

$$0 = \frac{M}{2} (0 - 0)^2 + \frac{R}{6} \cdot (0 - 0)^3 + \frac{F}{6} \cdot (0 - A)^3 - \frac{w}{6} \cdot (0 - L)^2 - \frac{P}{24} \cdot (0 - 0)^4 + C1 \cdot 0 + C2$$

$$0 = \frac{M}{2} (A - 0)^2 + \frac{R}{6} \cdot (A - 0)^3 + \frac{F}{6} \cdot (A - A)^3 - \frac{w}{6} \cdot (A - L)^2 - \frac{P}{24} \cdot (A - 0)^4 + C1 \cdot A + C2$$

$$\underline{\underline{\text{var}}} := \text{Find}(M, R, F, C1, C2) = \begin{pmatrix} 427.31 \\ -5.547 \\ 14.567 \\ -9.779 \times 10^3 \\ 1.286 \times 10^5 \end{pmatrix}$$

$$\underline{\underline{M}} := \text{var}_0 = 427.31$$

$$\underline{\underline{R}} := \text{var}_1 = -5.547$$

$$\underline{\underline{F}} := \text{var}_2 = 14.567$$

$$\underline{\underline{C1}} := \text{var}_3 = -9.779 \times 10^3$$

$$\underline{\underline{C2}} := \text{var}_4 = 1.286 \times 10^5$$

## Singularity Functions

$$x := 0, 0.01L \dots L$$

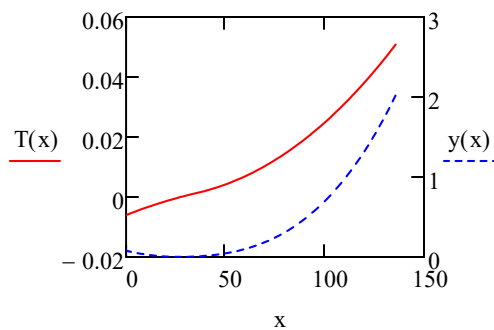
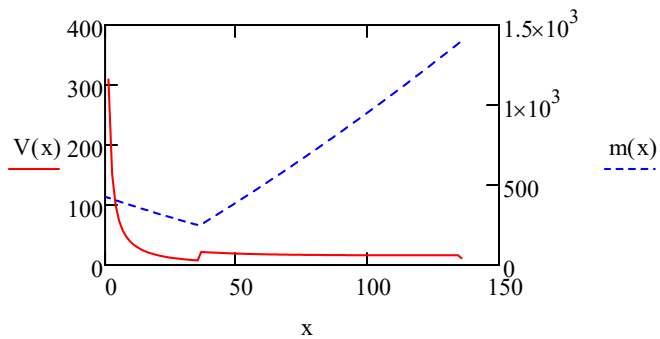
$$q(x) := M \cdot S(x, 0) \cdot (x - 0)^{-2} + R \cdot S(x, 0) \cdot (x - 0)^{-1} + F \cdot S(x, A) \cdot (x - A)^{-1} - w \cdot S(x, L) \cdot (x - L)^{-1} + P \cdot \delta(x - L)$$

$$V(x) := M \cdot S(x, 0) \cdot (x - 0)^{-1} + R \cdot S(x, 0) \cdot (x - 0)^0 + F \cdot S(x, A) \cdot (x - A)^0 - w \cdot S(x, L) \cdot (x - L)^0 + P \cdot S(x, 0)$$

$$m(x) := M \cdot S(x, 0) \cdot (x - 0)^0 + R \cdot S(x, 0) \cdot (x - 0)^1 + F \cdot S(x, A) \cdot (x - A)^1 - w \cdot S(x, L) \cdot (x - L)^1 + \frac{P}{2} \cdot S(x, 0)$$

$$T(x) := \left[ M \cdot S(x, 0) \cdot (x - 0)^1 + \frac{R}{2} \cdot S(x, 0) \cdot (x - 0)^2 + \frac{F}{2} \cdot S(x, A) \cdot (x - A)^2 - \frac{w}{2} \cdot S(x, L) \cdot (x - L)^2 + \frac{P}{6} \cdot S(x, 0) \right]$$

$$y(x) := \left[ \frac{M}{2} \cdot S(x, 0) \cdot (x - 0)^2 + \frac{R}{6} \cdot S(x, 0) \cdot (x - 0)^3 + \frac{F}{6} \cdot S(x, A) \cdot (x - A)^3 - \frac{w}{6} \cdot S(x, L) \cdot (x - L)^3 + \frac{P}{24} \cdot S(x, 0) \right]$$



## Deflection

$$\text{test} := 1$$

$$y_{\max} := \text{Minimize}(y, \text{test}) = 27.578$$

$$y(y_{\max}) = 1.721 \times 10^{-3}$$

Pole Weight

$\text{Vol} := \text{Area} \cdot L$

$\text{Weight} := \text{Vol} \cdot \text{massdensity} = 4.02$

$$\int (x, 0) \cdot (x - 0)^0$$

$$\int (x - 0)^1$$

$$\int (x - 0)^2$$

$$\int (x - 0)^3 + C_1 \left] \cdot \frac{1}{E \cdot I}$$

$$\int (x - 0)^4 + C_1 \cdot x + C_2 \left] \cdot \frac{1}{E \cdot I}$$

# Appendix K: Quality Inspection Report

## Quality Inspection Report

Part Name	Part Number	Quantity	Material	Date	Order #	P.O #
Top Plate	2	1,000	AL 6062	2021.3.25		

File Specifications				Part Measurement: (Black text = tolerance OK, Red text = Out of Spec)										Tool	Notes	
# of Dimension	Nominal	Tolerance +	Tolerance -	Part Tag #												
				Part 1	Part 2	Part 3	Part 4	Part 5	Part 6	Part 7	Part 8	Part 9	Part 10			
Surface Finish				✓												
Inserts																
Paint/Finish																
X																
Y																
Z																
1	1.888	0.005	0.005	1.890												CP
2	0.211	0.005	0.005	0.216												CP
3	0.158	0.003	0.000	0.168												PG
4	0.98	0.010	0.010	0.993												CP
5	2.35	0.010	0.010	2.350												CP
6	0.375	0.000	0.002	0.374												PG
7	0.180	0.005	0.005	0.178												CP
8																
9																
10																
11																
12																
13																
14																
15																
16																
17																

Coordinate Machine	Projector	Micrometer	Depth Vernier	Callipers	Radius Gauge	Pin Gauge	Vernier
CMM	PJ	MM	DV	CP	RG	PG	VI

FOR-10-000

### Quality Inspection Report

Part Name	Part Number	Quantity	Material	Date	Order #	P.O #
Bottom Plate	1	1.000	AL 5052	2021.3.25		

File Specifications				Part Measurement: (Black text = tolerance OK, Red text = Out of Spec)												
# of Dimension	Nominal	Tolerance +	Tolerance -	Part Tag #										Tool	Notes	
				Part 1	Part 2	Part 3	Part 4	Part 5	Part 6	Part 7	Part 8	Part 9	Part 10			
Surface Finish				√												
Inserts																
Paint/Finish																
X																
Y																
Z																
1	2.35	0.010	0.010	2.349												CP
2	0.984	0.005	0.005	0.982												CP
3	0.188	0.003	0.000	0.189												CP
4	0.375	0.003	0.000	0.377												CP
5	0.211	0.005	0.005	0.214												CP
6																
7																
8																
9																
10																
11																
12																
13																
14																
15																
16																
17																

Coordinate Machine	Projector	Micrometer	Depth Vernier	Calipers	Radius Gauge	Pin Gauge	Vernier
CMM	PJ	MM	DV	CP	RG	PG	VI

FOR-10-000